We thank the referees for their thorough review of the manuscript. Their comments are reproduced below in ***bold italic font***. Our responses are given in regular font. The line numbers in our responses below refer to the version posted on the ACPD web site.

Anonymous Referee #1 Received and published: 12 February 2018

Osthoff et al present a thorough study of NOy composition in the Lower Fraser Valley in British Columbia where air quality episodes can occur, but did not during their study. Notably, despite being a coastal site, low levels of ClNO2 were observed due to limited nocturnal NOx chemistry. A comprehensive description of the results is provided.

My main comments below surround the discussion of the aerosol data and the presentation/formatting of the main text. A full list of detailed comments is provided below.

We thank the reviewer for the constructive and detailed feedback.

It is clear from some of the line numbers that this particular reviewer referred to that she/he occasionally commented on an earlier version of the manuscript (the one subject to the "quick review" process; e.g., section 3.1.5, which the reviewer refers to lines 509-517 which changed to lines 527-536). In the version posted for discussion on the ACPD web site, we had already incorporated changes in response to the reviewer's feedback during the "quick review" phase. Hence, some of the reviewer's concerns raised below (such as concerns about what the ACSM quantifies) were already addressed.

As to the concerns regarding formatting (style of reaction numbering, paragraph breaks etc.): please see our comments in the next section.

Major Comments:

There are numerous places in the manuscript where 1-2 sentence "paragraphs" exist (Section 2.2 and elsewhere throughout); these sentences should be integrated in longer paragraphs for improved flow. Currently, this makes the manuscript difficult to read, and it also makes appears sloppy.

I disagree with the authors that these revisions should wait until "the type setting stage" (authors' response to Quick Review), as I believe that it significantly impacts the presentation of the results and discussion.

We appreciate the author's opinion, though we do not share this sentiment. There are no are set rules that guide the length of paragraphs in scientific papers. Guidelines on how paragraphs should be constructed vary considerably between disciplines, and writing is rightfully referred to as an "art" (Plaxco, 2010).

In our opinion, a paragraph should discuss a single idea and thus should have a single, unifying theme running through it; as a result, we generally started a new paragraph whenever the theme changed or deviated and couldn't be simply be tied to the original one. The paragraphs in section 2.2, for example, focus on properties common to all techniques (paragraph 1), properties only common to gas-phase instruments operated from the U Calgary trailer (paragraph 2), and properties only common to the

aerosol and VOC measurements made by Metro Vancouver and ECCC (paragraph 3). In our opinion, the paragraph/line breaks improve clarity and were, in fact, carefully and intentionally (not sloppily) constructed, though we admit that some paragraphs ended up on the short side. We have tried to the best of our ability to make improvements, for example by removing line breaks where they were perhaps not needed.

Similarly, please refer to reaction numbers in the text when the reactions are presented (e.g. page 4 and elsewhere).

Done.

There are many places in the text that state "(not shown)" with respect to results and ask the reader/reviewer to trust the authors; it would be more helpful for the reader's evaluation of the results for these data to be presented in the supplementary information.

There were four such instances. In all cases, the information not shown are on the periphery of the manuscript, and we felt it unnecessary to needlessly bloat the paper. However, we do not mind adding the information requested to the S.I. and have now done so in most cases.

The first of these instances, on line 424, refers to the average of the NO_x/NO_y ratio for entire campaign:

"The average NO_x/NO_y ratio for the entire campaign was 0.89 (data not shown)."

In the paragraph preceding this sentence, it is noted that the time series of NO_y and of NO and NO_2 are shown in Figures 3B and 3C, respectively. We therefore feel it is unnecessary to also show a time series of the ratio, especially since the ratios carry substantial uncertainties (see Table 1 – NO and NO_y are good to ±30%, NO_2 to ±10%): In the absence of NO, the uncertainty in the ratio of NO_x to NO_y is ±40% (and higher still in the presence of NO).

In response to the reviewer's comment, we have removed the phrase "(data not shown)" since the data are shown Figures 3B and 3C but have inserted the uncertainty.

"The average NO_x/NO_y ratio for the entire campaign was 0.9±0.4."

The second instance refers to the NH_3 data (line 557). As was stated on line 556, we the NH_3 data collected by Metro Vancouver were not quality-assured and hence non-quantitative (in part due to inlet memory effects). Regardless, these are now shown as Figure S-1 in the S.I.:

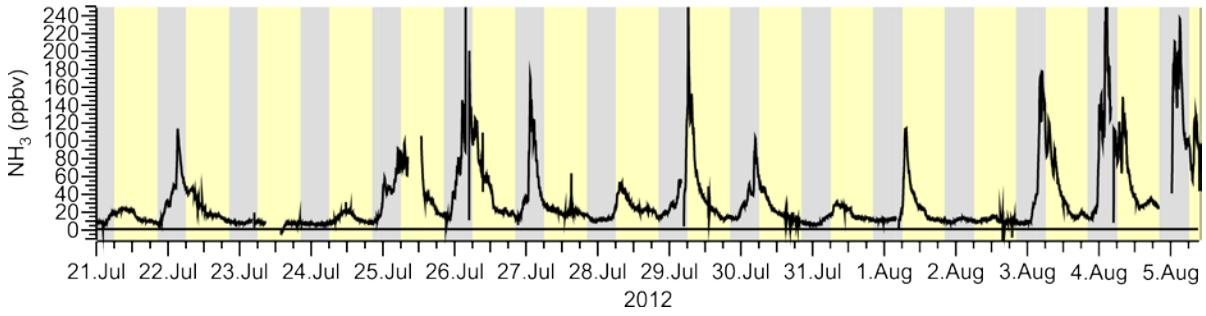

Figure S-1. Time series of gas-phase ammonia data reported by Metro Vancouver. Data were not quality-assured and are non-quantitative.

The third instance (line 630) refers to a box model simulation in which a single reaction was added. We have modified this section as follows

"The addition of this biogenic VOC only had a marginal effect on O_x ~~and resulted in a slightly better reporduction of the faster Ox loss at the beginning of the night (not shown)~~ (Figure S-3)."

and have added the following description of this rather simple model to the S.I.

Box model to rationalize O_x loss by dry deposition

A box model was set up to simulate the median nocturnal decays of O_3 and O_x. These simulations are intended as back-of-the-envelope type estimates of major processes only since an accurate description of the nocturnal boundary layer chemistry would require modeling of horizontal and vertical transport, i.e., altitude-resolved information (Geyer and Stutz, 2004). Such information was not available in this work.

The reactions used in this model are summarized in Table S-2. The mechanism consists of O_3 and NO_2 dry deposition, titration of NO with O_3 (R8) and chemical loss of O_3 to a generic biogenic hydrocarbon. For dry deposition, the velocities of $v_d(O_3)$ = 0.2 cm s^{-1} and $v_d(NO_2) = \alpha \times v_d(O_3)$ with α=0.65 from Lin et al. (2010) were used. The rate constants for reaction with the generic biogenic hydrocarbon was set to that of α-pinene with O_3 (5×10^{-11} cm^3 $molec.^{-1}$ s^{-1} (Seinfeld and Pandis, 2006)).

Model simulations were carried out using a custom differential equation integrator macro in the software package Igor Pro (Wavemetrics) and were initiated with the campaign median NO_2 and O_3 concentrations observed at sunset.

Table S-2. Reactions included in box model to estimate dry deposition velocities

Reaction	Rate constant
$O_3 \rightarrow$ products	$k_{dep}(O_3)$
$NO_2 \rightarrow$ products	$k_{dep}(NO_2)$
$O_3 + NO \rightarrow NO_2 + O_2$	4.8×10^{-4} $ppbv^{-1}$ s^{-1}
O_3 + VOC $\rightarrow$ products	1.25 $ppbv^{-1}$ s^{-1}

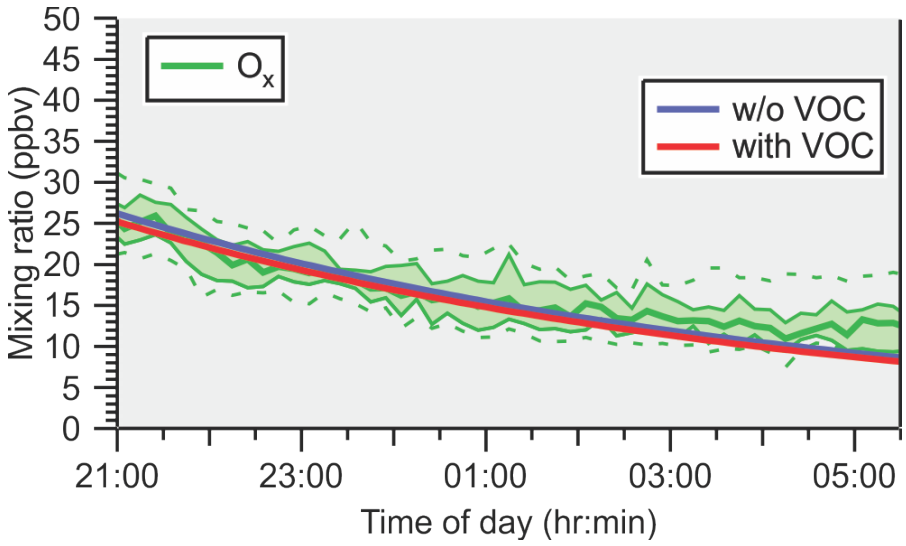

Figure S-3. Effect of biogenic VOC emissions on O_x. The observed and simulated O_x loss in the NBL at Abbotsford assuming an O_3 dry deposition rate of 4×10^{-5} s^{-1} are shown as green and blue traces, respectively. The red trace shows the effect of adding 1 ppbv of reactive biogenic VOC at sunset and continuous biogenic VOC emissions of 3×10^{5} molecules cm^{-3} s^{-1} throughout the night.

The fourth (line 672) is a box model simulation to estimate the time to achieve steady state. The methodology has been described by Brown et al. in J. Geophys. Res., 108, 4539, doi: 4510.1029/2003JD003407, 2003. We have added the following text to the S.I.:

Box model to determine the time necessary for NO_3 and N_2O_5 to achieve a steady state with respect to production and loss

The validity of the steady state assumption was evaluated in a similar fashion as described by Brown et al. (2003) using a simple box model. Reactions and rate coefficients included in these simulations are listed in Table S-3. Model simulations were carried out using a custom differential equation integrator macro in the software package Igor Pro (Wavemetrics). Rate coefficients were calculated for a temperature of 286 K, which is the median nocturnal temperature of this study (Figure 8B). Simulations were initiated with the median nocturnal NO_2 and O_3 mixing ratios of 7.5 ppbv (1.92×10^{11} molecules cm^{-3}) and of either 18 ppbv (4.5×10^{11} molecules cm^{-3}) or 5.0 ppbv (1.3×10^{11} molecules cm^{-3}), respectively. The simulations assume pseudo-first order N_2O_5 and NO_3 loss with frequencies of 1×10^{-3} s^{-1} and between 1×10^{-2} s^{-1} and 0 s^{-1}, respectively.

Simulated temporal profiles of NO_3 and N_2O_5 are show in Figure S-5 (left axis) and those of O_3 and NO_2 on the right axis. The subpanels A, B, and C are simulations with k_{NO3} = 0 s^{-1}, 1×10^{-3} s^{-1} or 1×10^{-2} s^{-1}, respectively. In each case, the rate of change of $[N_2O_5]$ with respect to time, $d[N_2O_5]/dt$, approaches zero after a period of ~70 min, or less, indicating the time to approach steady state.

The simulations also show that the amount of O_3 and NO_2 removed through chemical reactions of NO_3 and N_2O_5 are ~1 ppbv and between ~1.9 and ~1.6 ppbv over a period of 4 hours. These are upper limits as, in this study, much of the NO_3 was titrated by NO. In any case, loss of O_3 through nocturnal gas-phase

is predicted to be rather small compared to the total O_3 loss observed (~26 ppbv over 9 hours, see section 3.1.3 and Figure 4C in the main text).

Brown et al. (2003) show that in these scenarios, NO_3, N_2O_5, and NO_2 remain in equilibrium almost throughout; for completeness, the corresponding plot for these simulations is shown in Figure S-6.

As shown in equation (2) of the manuscript, the steady state lifetime is approximately equal to:

$$\frac{[N_2O_5]}{k_1[NO_2][O_3]} \approx \left(k_{N_2O_5} + \frac{k_{NO_3}}{K_2[NO_2]}\right)^{-1} \quad (2)$$

A comparison of these two expressions is shown in Figure S-7. The time when these two expressions are equal is equal to the time to steady state.

Table S-3. Reactions included in the box model to estimate the time for NO_3 and N_2O_5 to achieve steady state with respect to their production and loss

#	Reaction	Rate coefficient
R1	$NO_2 + O_3 \rightarrow NO_3 + O_2$	2.28×10^{-17} cm^3 molecule^{-1} s^{-1}
$R2_f$	$NO_3 + NO_2 \rightarrow N_2O_5$	1.35×10^{-12} cm^3 molecule^{-1} s^{-1}
$R2_r$	$N_2O_5 \rightarrow NO_3 + NO_2$	0.00923 s^{-1}
(R7)	$NO_3 \rightarrow$ products	$k_x = k_{NO3} = 0$ s^{-1}, 1×10^{-3} s^{-1} or 1×10^{-2} s^{-1}
(R5)	$N_2O_5 \rightarrow$ products	$k_y = k_{N2O5} = 1\times10^{-3}$ s^{-1}

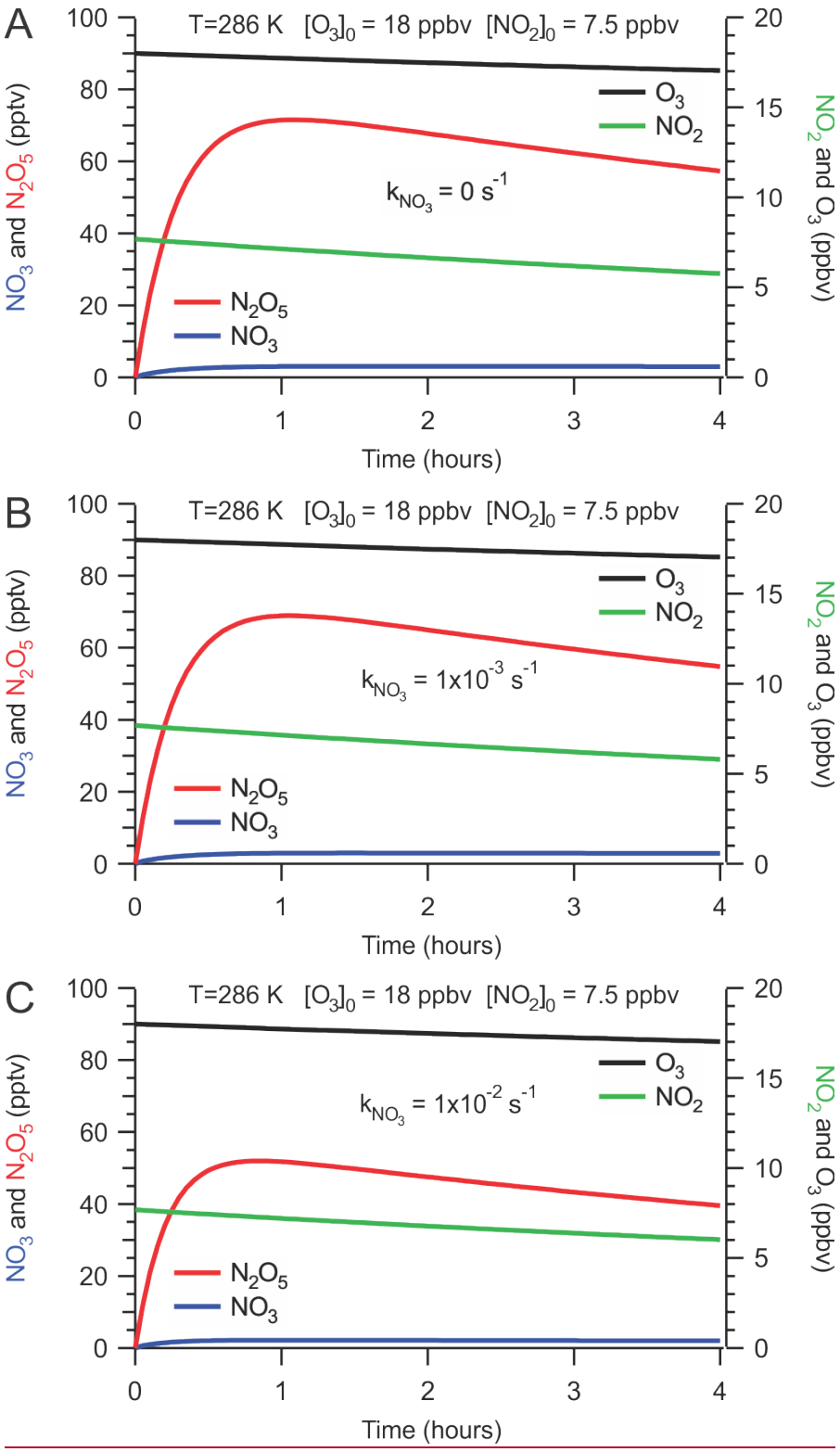

Figure S-5. Simulated temporal profiles of NO_3 and N_2O_5 (left axis) and O_3 and NO_2 (right axis). The subpanels A, B, and C are simulations with k_{NO3} = 0 s^{-1}, 1×10^{-3} s^{-1} or 1×10^{-2} s^{-1}, respectively.

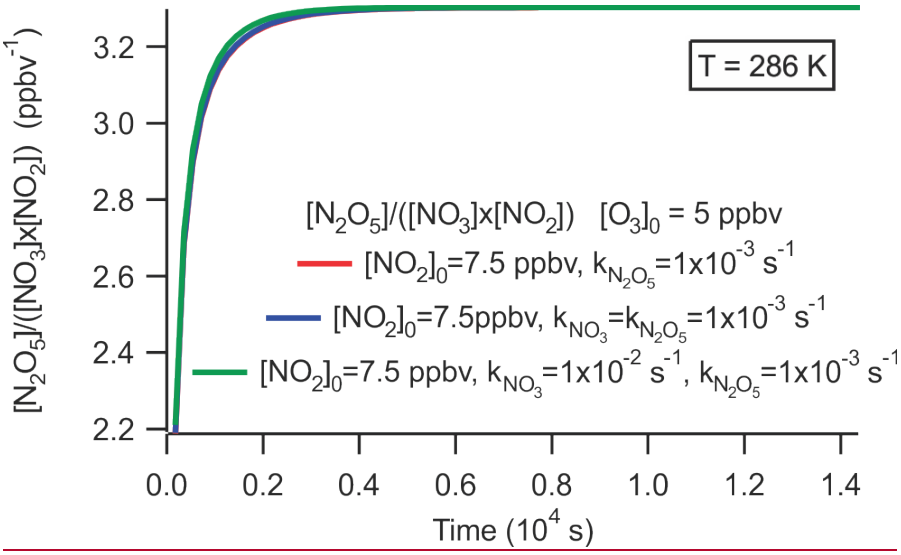

Figure S-6. Equilibrium constants for reaction (2) calculated for the three scenarios shown in Figure S-4.

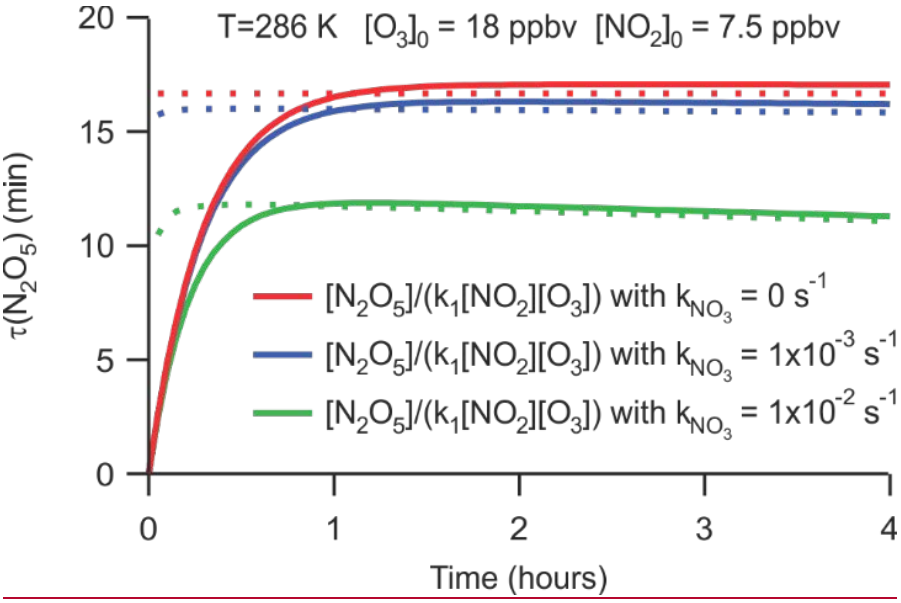

Figure S-7. Comparison of $\tau(N_2O_5)$ calculated using equation (2) of the main manuscript. with the dashed lines calculated using equation (11) of Brown et al. (2003).

Section 2.5: More information is needed for the description of the box model. A list of reactions should be provided in the supplementary information. Is chlorine chemistry included? Are aerosols included?

We have added a list of reactions to the S.I. as requested (see above).

It is stated in section 2.5 that "These simulations are intended as back-of-the-envelope type estimates of major processes only since an accurate description of the nocturnal boundary layer chemistry would require modeling of horizontal and vertical transport, i.e., altitude-resolved information not available in this study (Geyer and Stutz, 2004)." Because of the limited scope of these simulations, chlorine and aerosol chemistry was neglected; more importantly, their impact in this study on O_3 and O_x at night was likely very minor. No further changes were made to the manuscript.

Lines 443-445: This sentence can be strengthened by referring at least to the timing of the ozone maximum for support, and perhaps referring to the next section. Otherwise it sounds like a guess that you cannot support further, which is not true.

We are assuming that the reviewer is referring to the following sentence: "This can be rationalized by a greater abundance of oxidants that oxidize NO to NO_2, i.e., O_3 (see Figures 3 and 4) and organic peroxy radicals in the afternoon, a topic outside the scope of this manuscript."

We have inserted "and section 3.1.3." following Figures 3 and 4 since the timing of the ozone maximum is discussed in that section.

Section 3.1.5: This section needs the most revision, particularly with respect to the presentation and discussion of the ACSM data. The authors quantify fractions of "total aerosol mass" (e.g. line 541); however, only non-refractory submicron aerosol was measured. It is expected at refractory sea salt aerosol contributes significantly to this site, so these calculations are expected to be inaccurate.

The paragraph starts out with "The ACSM submicron aerosol composition data ..." to acknowledge this important point. Furthermore, on line 540 we specifically state "... mass fraction of the non-refractory aerosol". However, we agree that the term "total aerosol mass" could have nevertheless been misunderstood and have qualified "total aerosol mass" by adding "measured by the ACSM" on line 541. We also inserted "PM_1" throughout the manuscript for additional clarity that larger particles were not quantified.

Since we report fractions within the non-refractory submicron aerosol, they are accurate (within the ability of the ACSM to make such measurements), not inaccurate as the reviewer claims.

Similarly, the authors discuss the "inorganic mass fraction" and "most abundant inorganic component", which also are influenced by refractory aerosol, such that the mass fractions are expected to be inaccurate.

We believe it is obvious from the context (especially after the changes already made to the comments above) that we refer to the ACSM data, i.e., non-refractory aerosol. We disagree with the reviewer's assertion of inaccuracy and note that the mass fractions are accurate within the ability of the ACSM to make such measurements. No further modifications were made to the manuscript in response to the above comment.

The discussion of the ACSM data must clearly reflect that only submicron non-refractory mass was measured

This is stated on lines 343-344 ("The chemical composition of non-refractory ~~submicron particulate matter~~PM_1 was monitored using an Aerosol Chemical Speciation Monitor (ACSM, Aerodyne)") in the experimental section.

No further changes were made to the manuscript in response to the above.

and that sea salt aerosol (most relevant for ClNO2 production) was not measured.

This is stated in the abstract on lines 36-37 "unquantified supermicron sized or refractory sea salt derived aerosol" but had not been reiterated in the text. We added the following on line 346:

"The composition of the refractory aerosol (i.e., sea salt) was not quantified."

Lines 509-517: It should be clarified that this only reflects the aerosol <0.5 um in diameter, based on the size range measured by the SMPS. Since aerosol surface area peaks at a higher diameter than aerosol number, it would be expected that this calculation of aerosol surface area may be a significant underestimate. This should be stated, and the implications of this should be discussed where appropriate.

The reviewer is probably referring to the section titled "aerosol size distribution measurements" (section 3.1.5) that appears on lines 527-536.

The size range of the SMPS was already stated on line 348 (10 to 487 nm).

We question the reviewer's assertion that the surface area is significantly underestimated. The aerosol in the LFV is of urban and rural organic nature (see, for example, the title of (Alfarra et al., 2004)). John Seinfeld and Spiros Pandis state in their third and most recent edition of "Atmospheric Chemistry and Physics: From air pollution to climate change" in section 8.2.1 "Urban aerosols" on pages 343-344 that "... most of the surface area is in the 0.1 to 0.5 μm size range".

Below, we have included a graph of median aerosol surface area distribution observed in this study. The graph shows that the bulk of the surface area is captured.

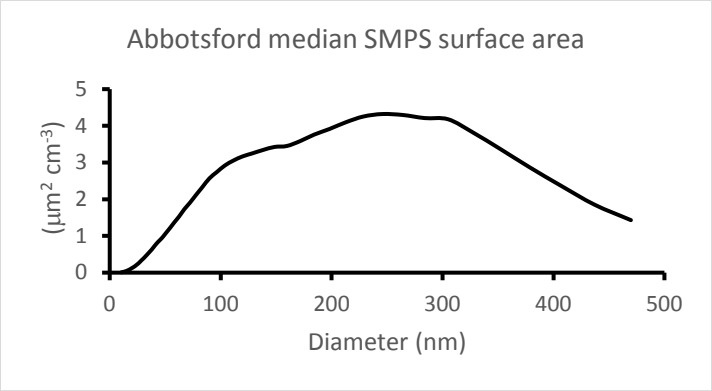

We added the following on line 531:

"The size distribution data show that bulk of the surface area (i.e., the mean diameter ($\overline{D}_s$)) is in the range of 200 to 300 nm, such that most of the area of the accumulation mode was captured. However, the surface area calculations do not include contributions from larger diameter particles which were not quantified."

Lines 554-558: The authors should refer to Zhang et al (2007, Environ. Sci. Technol.) for the proper method for examining aerosol acidity using ACSM data.

Zhang et al. give the following expression for neutralization ratio:

$$NH_4^+{}_{meas}/NH_4^+{}_{neu} = NH_4^+/18/(2 \times SO_4^{2-}/96 + NO_3^-/62 + Cl^-/35.5) \quad (2)$$

In our expression, the square brackets denote molar concentrations, which is now clearly stated in the text. We converted the mass concentrations (micrograms per cubic meter) to molar concentrations (molecules per cubic centimeter) using the appropriate molecular weights (18 g/mol, 96 g/mol, and 62 g/mol etc.). Inclusion of the numbers 18, 96, 62, etc. in the equation is only necessary if one normally works with mass concentrations. We omitted the chloride concentrations because they were negligible.

However, there was a mistake in our equation in that the stoichiometric factor of 2 was left off by mistake. This has been corrected, and the median NR value was recalculated to 1.19. We also added a citation to Zhang et al., 1997 for the NR calculation.

The sentence in question now reads:

"The neutralization ratio, NR ≈ $[NH_4^+]:([NO_3^-]+2[SO_4^{2-}])$ (Zhang et al., 2007), where the square brackets denote molar concentrations (calculated from the mass concentrations reported by the ACSM by dividing by the appropriate molecular weights), was 1.19 (median value)."

We have also updated Figure 6C to reflect the corrected NR values. The changes were sufficiently minor that the text did not require further revision.

Please show the gas-phase NH3 data, at least in the supplementary information.

Done (See page 2 above).

Lines 559-562 and Figure 6 caption: Only non-refractory chloride was monitored by the ACSM, and this should be noted, given the importance for ClNO2 production.

We inserted "non-refractory" prior to "chloride" as per the reviewer's request.

If the signal was below the instrument limit of detection, then the concentration calculated is, by definition, not accurate.

I believe we're in agreement here - we stated on line 560 (relevant text passage underlined):

"The ACSM software also ~~identified~~ reported non-refractory chloride with an average (±1 standard deviation) concentration of 0.01±0.03 µg m^{-3}, though it is unclear if this signal was real as it did not vary over the course of the campaign and was below the stated ACSM detection of limit of 0.2 µg m^{-3} (Ng et al., 2011)."

No further changes were made to the manuscript.

The text should be revised to reflect these two important points.

Done.

Lines 566-570: The time of year is expected to be quite important for these comparisons. Please provide this information in the discussion.

Both studies were conducted in the summer: Pacific 2001 was conducted in August, 2001, which is now stated in the text:
"Previous AMS measurements in Vancouver during the month of August as part of Pacific 2001 ..."

Lines 616 & 621: Do these dry deposition rates make sense in the context of previously published literature?

Yes, they do. For dry deposition of O_3 and NO_2, as stated in section 2.5, we used dry deposition rates from Lin et al. Atmos. Environm., 44, 4364-4371, 10.1016/j.atmosenv.2010.07.053, 2010 and ran several simulations, varying mixing height.

For dry deposition of NO_3 and N_2O_5 it is less clear as there have been few reports let alone measurements of deposition velocities. For example, Kim et al. [PNAS, 2014] reported N_2O_5 exchange velocities of -1.7+/-0.6 cm/s with an ocean surface, and Bill Simpson studied uptake of N_2O_5 on snow in Alaska. The surface of the LFV is covered by vegetation and is obviously quite different from marine and snow covered environments. We are not aware of flux measurements of N_2O_5 or NO_3 on such terrain, but believe the magnitude assumed here to be feasible given the reactive nature of N_2O_5 and NO_3.

Lines 629-630: Why is this data not shown? It is about modeling the "faster Ox loss at the beginning of the night", which seems central to the section header "Box model simulations of the nocturnal O3 and Ox loss in the NBL".

As stated above, we have added this result as Figure S-3 (see pg. 4 above).

Lines 632-634: Why was the model not simply constrained to measured NO?

Any NO emitted will react with O_3 and hence "add" NO_2. Simply constraining NO to measured quantities is unlikely to capture this effect. No changes were made in response to this comment.

Did NO under these modeled conditions match what was measured?

Yes, they do (see figure below). The black line is the amount of NO the model predicts; the purple area is the 75%-25% percentile of observed (solid line is the median).

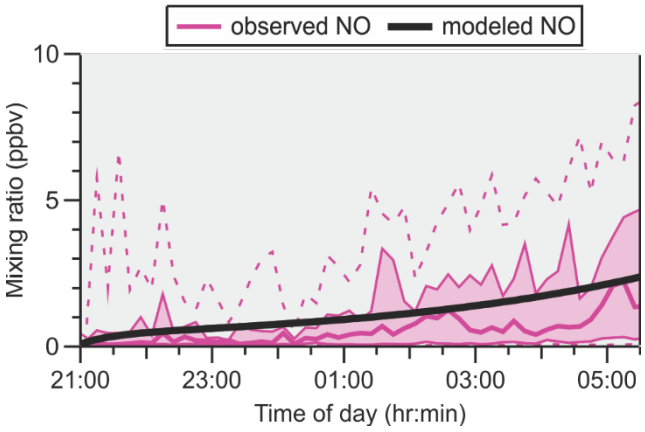

The figure above has been added to the S.I. as Figure S-4.

The main manuscript text was changed as follows:

"There is reasonable agreement between the simulations and observations of O_x and O_3 until ~3:00 (and between simulation and observation of NO, Figure S-4). This~~, which~~ shows that the nocturnal O_3 and O_x loss can be rationalized without active NO_3 and N_2O_5 chemistry and suggests that NO_3, N_2O_5, and $ClNO_2$ did not contribute significantly to O_x and O_3 loss in the NBL."

Lines 692-694: Not including loss of NO3 to hydrocarbons is not justified here. Why not assume a generic BVOC as you did in an earlier section, or use the data that you do have? These options seem better than blindly ignoring this NO3 loss process.

Further, on lines 706-707, you state that reaction between NO3 and isoprene was likely significant, suggesting that that reaction should be included, especially since the authors have at least some measurements of isoprene.

We neglected the reaction of NO_3 with unsaturated VOCs because there simply wasn't sufficient data to include it: As stated in the manuscript "Missing from equation (3) are losses of NO_3 to hydrocarbons (which was omitted because of the poor VOC data coverage)", VOC data were only available for the nights shown in Figure 7. On those nights, unfortunately, mixing ratios of O_3 and hence N_2O_5 and $ClNO_2$ were small, and any isoprene concentrations measured would have been larger than on other nights (due to the difference in the magnitude of chemical sinks) so those VOC data cannot be simply extrapolated to other nights. We clearly stated that the results therefore are upper limits only.

On the other hand, not including reactions of NO_3 with VOCs gave us an important result: Figure 8C shows that the experimental N_2O_5 lifetime from 21:00 to midnight was lower than calculated from the expression given on line 691. Part of this may be due to the time of ~70 min it takes to reach steady state. The remainder is likely due to NO_3 reacting with residual isoprene or terpenes that continue to be emitted (stated on lines 706-707). The effect of these VOCs appears to lessen over the course of the night.

No changes were made in response to the above comment.

Also, not including NO3 and N2O5 deposition is not justified. It seems that dry deposition could be easily included.

This is correct and was an oversight on our part. We have revised the manuscript, added dry deposition ($k_{dep}(NO_3)$ and $k_{dep}(N_2O_5)$) to the lifetime expression and recalculated the upper limit to the N_2O_5 lifetime. Earlier in the text (section 3.2.1), we estimated that $k_{dep}(NO_3)$ and $k_{dep}(N_2O_5)$ were ~4×10^{-4} s^{-1} at night; during the day, these are, of course, much smaller due to higher mixing heights (though this won't matter since the daytime sinks for NO_3 and N_2O_5 are much larger).

The paragraph in question now reads as follows:

" Superimposed on the right-hand side of Figure 8C are upper limits to the steady state lifetime of N_2O_5, calculated using the sum of pseudo first-order rate coefficients for the titration of NO_3 by NO ($k_3[NO]$, R3), NO_3 photolysis ($j(NO_3)$, R4), and NO_3 dry deposition ($k_{dep}(NO_3)$)-, all divided by the N_2O_5 over NO_3 ratio at equilibrium given by K_2NO_2 (Figure 8B), plus the pseudo first-order rate coefficient for N_2O_5 heterogeneous uptake ($k_{het}(N_2O_5)$, equation (1)) plus N_2O_5 dry deposition ($k_{dep}(N_2O_5)$).

$$\tau(N_2O_5) = \left(\frac{k_{NO_3}}{K_2[NO_2]} + k_{N_2O_5}\right)^{-1} < \left(\frac{k_3[NO] + j(NO_3) + k_{dep}(NO_3)}{K_2[NO_2]} + k_{het}(N_2O_5) + k_{dep}(N_2O_5)\right)^{-1} \quad (3)$$

The dry deposition rate constants were set to 4×10^{-4} s^{-1} (see section 3.2.1), which likely overestimates dry deposition during the day due to higher mixing heights; however, the error this introduces is negligible compared to the large daytime sinks such as NO_3 photolysis and its reaction with NO. "

We also updated Figure 8C (see next comment).

Where time periods that fog and rain occurred used? If so, these periods should be removed for these calculations.

Please note the following modifications in response to the above comment:

"Missing from equation (3) are losses of NO_3 to hydrocarbons (which was omitted because of the poor VOC data coverage) and terms for NO_3 and N_2O_5 ~~dry and~~ wet (i.e., on cloud and rain droplets) deposition. Periods affected by precipitation or fog (shown in Figure 3D) were hence excluded from the calculation."

Only a small fraction of the data set was affected by rain or fog. It therefore made little difference to the final result if those data are included or excluded in this data set. Likewise, the inclusion of the dry deposition terms only marginally changed the results of the calculations (the other sinks were just that much larger), such that discussion of these results did not need to be changed.

Lines 721-723: It is assumed that the production of nitrate on refractory aerosol is minimal, but this is not justified and is a poor assumption. Nitric acid displacement of HCl is one of the most common sea salt aerosol aging pathways (Gard et al. 1998, Science).

We agree with the reviewer and have clarified the sentence as follows:

"It is assumed further that production of nitrate from N_2O_5 uptake on refractory aerosol (that the ~~ACMS~~ ACSM does not quantify) is minimal."

Line 757-762: Only non-refractory chloride and nitrate were measured! This should be considered and reflected in this discussion.

This is true, but it is entirely possible that uptake of N_2O_5 on refractory aerosol and non-refractory are different in terms of kinetics and $ClNO_2$ yield (the Bertram and Thornton groups have shown this). We explicitly state this is a condition ("if one assumes that all of the $ClNO_2$ is produced on supermicron or refractory aerosol such that $P(ClNO_2)$ on submicron aerosol equals 0 pptv s^{-1}"). The nocturnal uptake of N_2O_5 (whose mixing ratios were measured) has been shown again and again to be an important source of particle-phase nitrate on non-refractory aerosol (whose concentrations were monitored by the ACSM). In this paper, we can make statements about the processes on non-refractory aerosol.

Line 827: How does this observation of a lack of non-refractory submicron aerosol chloride compare to other similar inland coastal AMS/ACSM studies?

Alfarra et al. and Boudries et al. (Alfarra et al., 2004; Boudries et al., 2004) reported AMS data collected during PACFIC 2001 but did not report aerosol chloride as one of their products.

There were, however, size-resolved MOUDI measurements during PACIFIC 2001 (Anlauf et al., 2006). We have modified the text as follows:

"This in turn implies that the submicron aerosol surface did not significantly participate in the production of $ClNO_2$ from N_2O_5 uptake in the NBL, broadly consistent with the conclusions in section 3.2.3 and consistent with measurements of water-soluble aerosol components in the LFV during Pacific 2001 (Anlauf et al., 2006) that showed no evidence for chloride redistribution to PM_1 from larger particles where aerosol chloride was present."

Lines 913-916: The authors suggest that the lack of particle-phase chloride (should be 'non-refractory' chloride) is in contrast to their previous study, Mielke et al. 2013, in Pasadena, CA. However, in that previous paper, AMS PM1 showed very little nonrefractory chloride, with far higher levels of PM2.5 chloride (refractory + non-refractory measured by PILS-IC) measured. So, this is not a complete comparison, and in fact, in terms of non-refractory PM1 chloride, the studies seem fairly similar. This discussion should be reconsidered and revised.

We disagree. In the 2010 study, a median value of ~0.1 µg m^{-3} aerosol chloride were observed by the AMS on the non-refractory aerosol fraction, ~0.1 µg m^{-3} more than that was observed in this study. So yes, there was a sizeable difference. We do not show how $PM_{2.5}$ chloride compares since we don't have such data for the Abbotsford study; those levels are likely "far higher" at both locations.

We have modified the text on line 830:

"Such a redistribution was observed, for example, during the Calnex-LA campaign, where the AMS measured a median chloride concentration of ~0.1 µg m^{-3} on non-refractory aerosol (Mielke et al., 2013)."

Table 1: Please add the SMPS and ACSM size ranges, as well as note that the ACSM aerosol composition reflects only the "non-refractory" aerosol.

These details are stated in the experimental section. No further changes were made to manuscript.

Minor Comments:

Line 65: Fix typo – "particle" should be "particulate".

Done

Reaction 6 should include chloride as a reactant.

Added

Please add references to the following lines: 77, 99, 108, 426, 431, 887.

Done, with exception of lines 426 and 431 since it is common knowledge in the field that NO is emitted by automobiles.

Lines 135-136, 837: Fix reference formatting in sentence.

Done

Line 337: Fix typo – "day used" should likely be "day were used".

Done

Section 3.4, Table 2, & anywhere else: "down-dwelling" and "up-dwelling" should be "down-welling" and "up-welling".

Done

Line 457 & elsewhere: Error should be given as one significant figure, with the average value provided with the same number of decimal places. For example, line 457 should list 64 +/- 1 ppbv, rather than 64.4 +/- 1.2 ppbv.

Done

Lines 459-461: Provide values in parentheses for context.

We changed the text as follows:

"These levels were well below the CAAQS 8-hr standard of 63 ppbv and the 1 hour National Ambient Air Quality Objective of 82 ppbv, smaller than the pre-2003 data analyzed by Ainslie and Steyn (2007)-, who reported between 10 and 20 O_3 1-hour exceedences of 82 ppbv in the 1980s, and of similar magnitude as observed by a high-density monitoring network in the region in 2012 (Bart et al., 2014) , which observed peak O_3 levels of 74 and 83 ppbv at Abbotsford on July 8 and August 17, respectively."

Line 467: Change ":" to "."

Done

Line 469: Fix typo – "loss of are" should likely be "loss are".

Done

Line 482: Fix typo – "at a median value" should be "at median values".

Done

Lines 483-484: Fix typo – "ratio of this campaign was" should be "ratios of this campaign were".

Done

Figure 5: Please clarify this figure caption. It was not obvious at first what "lhs" and "rhs" stood for, as these acronyms are not defined.

Done

Lines 601-603: Please revise sentence to improve clarity.

Original sentence:

"Loss of NO_3 to isoprene was a small sink compared to its loss to NO via reaction (3) and NO_3 photolysis but is approximately on par with k_{N2O5} $K_2[NO_2]$."

Revised sentence:

"Loss of NO_3 to isoprene was a small sink compared to its loss to NO via R3 and NO_3 photolysis (R4) but was approximately on par with its indirect loss, i.e., the heterogeneous uptake of N_2O_5."

Lines 854-859: Please revise sentence to improve clarity.

Original sentence:

"Their presence is likely responsible for some of the gap between the low "observed" N_2O_5 steady state lifetimes, $\tau(N_2O_5)$, compared to the upper limit set by reactions 3-4."

Revised sentence:

"Their presence is likely responsible for the difference between the "observed" N_2O_5 steady state lifetimes, $\tau(N_2O_5)$, and upper limit calculated using equation (3) before midnight (Figure 8C)."

Line 658: Fix typo - "are" should be "is".

Done

Line 664: Delete sentence as this information is already given on line 660.

Done

Lines 730 & 914: Fix typo – "ACMS" should be "ACSM".

Done

Anonymous Referee #2 Received and published: 23 January 2018

This manuscript reports measurements of ClNO2, N2O5 and other chemicals (ozone, NOx, NOy, aerosol size and composition and VOCs etc) at a surface site near the Lower Fraser Valley during a two-week period in summer 2012. The study was motivated by the need to investigate the role of ClNO2 in ozone exceedance in the region.

However, the relatively short field study did not capture any high ozone events, and low ClNO2 levels were observed due to fresh emissions of NO which suppress the production of N2O5 and ClNO2 at nigjt. The paper investigated some metrics related to production and loss of N2O5/ClNO2 with the aid of a simple box model, and the results show small contribution of ClNO2 to radical production in such an environment, as one would expect.

While the data on ClNO2 and N2O5 add to the global data base of the two important and poorly documented species, the main finding (low N2O5/ClNO2 in high NO condition and resulting small contribution of photolysis of ClNO2 to radical source) gives limited new insight on the processes and impact of N2O5 and ClNO2, as such the significance of this work is unclear.

We thank the reviewer for these comments. The reviewer states that "the study was motivated by the need to investigate the role of $ClNO_2$ in ozone exceedance in the region". While we agree that this is a penultimate goal, the focus of this paper was to provide observational data, as there had been no prior measurements of $ClNO_2$ and N_2O_5 mixing ratios in the LFV; in this work, we presented the first such measurements, which are challenging in their own right, and provided an analysis of nitrogen oxide budgets, nocturnal O_3 loss, and a comparison of photochemical radical sources.

The mixing ratios of $ClNO_2$ at ground level were low, in fact, considerably lower than current literature on $ClNO_2$ suggests (Table 3). However, there is general bias in how measurement sites have been selected (and are reported): They're typically located in highly polluted regions (such as the LFV), and as a consequence, many $ClNO_2$ data sets to date reported fairly large mixing ratios (many ppbv) that

constitute large fractions of NO_y. Not in this work – in spite of the proximity to pollution sources (NO_x from a Megacity) and the Pacific Ocean which provides sea salt aerosol.

Could this have been expected? Perhaps. Though doubtful.

A key aspect of this data set is the lack of redistribution of aerosol chloride from the refractory sea salt derived aerosol to the refractory fraction. This suggests that uptake of H_2SO_4 and HNO_3 on sea salt aerosol and displacement of HCl were less active than at other locations (e.g., Pasadena). This is surprising insofar as acid displacement, chloride deficits, etc. are well documented. Since the aerosol surface in this study is dominated by the smaller, non-refractory size fraction, most of N_2O_5 reacts on that surface. The lack of chloride implies the efficiency of N_2O_5 to $ClNO_2$ conversion on that surface is also much lower.

We believe that this paper adds to the body of work on $ClNO_2$ and nitrogen oxide chemistry in general in that the data allow constraints to be placed on future photochemical models of O_3 production in the region. Currently, we are not aware of any chemical transport model simulations of O_3 production in the LFV that incorporate chlorine chemistry. In addition, this work provides valuable guidance for future field campaigns in the region in that the focus should be on processes happening within the residual layer and measurements of aerosol composition should include refractory aerosol.

Specific questions on methods:

What was the extent of N2O5 loss in the sampling line during the field study?

This information was stated on line 297
" The N_2O_5 response varied between 65% and 100% depending on inlet "age"; the Teflon™ inlet and aerosol inlet filter were changed every 2 – 3 days."

Please note that this response factor also accounts for laser wavelength drifts from the NO_3 absorption line (likely less variable than N_2O_5 losses in the sampling line).

We have modified the sentence slightly to reflect this:

"The N_2O_5 response (which accounted for N_2O_5 loss in the sampling line and slight mismatches of the laser wavelengths with the NO_3 absorption line) varied between 65% and 100% and depended on inlet "age""

For NOy measurements, was the Mo converter placed at the sample inlet outside?

Yes, it was placed outside. The following was inserted into the manuscript (on line 307)

"An NO-O_3 chemiluminescence instrument (Thermo 42i) was used to monitor mixing ratios of NO and NO_y, which was reduced to NO in a Mo converter heated to ~320 °C placed outside a short distance (< 1 m) from the sample inlet."

Was a filter placed before the Mo converter?

Yes, there was a filter. This was stated on line 308:

"This instrument sampled from the main inlet via a Teflon™ filter and filter holder ...."

The aerosol size measurements only covered size 10 nm to 487 nm, were the larger size particles considered when calculating the aerosol surface areas density?

Larger size fraction data were not available, so this was unfortunately not possible. Since the limitations and consequences are already noted in the text, no~~t~~ changes were made to the manuscript in response to this comment.

What was the uncertainty of the simple box model adopted?

Uncertainty in box models are generally difficult to assess accurately. This is typically accomplished by probing the sensitivity to changing inputs. Here, we ran several simulations. The data in Figure S-1 show that changing the dry deposition rate of O_3 by a factor of 2 causes a considerable deviation between model and observation. Thus, the model is at least accurate within that factor.

This, of course, hinges on whether the assumptions in this simple model hold, such as a negligible role of nighttime nitrogen oxide chemistry in O_3 and NO_2 depletion. This particular assumption is quite reasonable as the model simulations to assess the time to steady state (which neglect dry deposition) show that NO_3/N_2O_5 chemistry at most only removes ~3 ppbv of O_x.

Anonymous Referee #3 Received and published: 15 February 2018

General Comments:

This is a well written manuscript describing studies of nocturnal chemistry in the Lower Frasier Valley, a region near a megacity (Vancouver) and with sea salt sources. The combination of these pollution (NOx) sources and sea salt aerosol particles might be expected to produce nitryl chloride. In fact, Pasadena, CA, in the Los Angeles area (also a megacity near the ocean) had much larger nitryl chloride at ground level. The authors argue that shallow boundary layers, titration of ozone by fresh NO emissions at ground level and potentially biogenic VOC inputs often preclude nitryl chloride formation at ground level, which is supported by the data in the manuscript. The work is well written, sufficiently referenced, and appropriate for publication in ACP.

We thank the referee for this positive opinion of the manuscript.

There is a lot of evidence in this manuscript that titration of ozone at ground level was a reason for low NO3 and N2O5 levels. On the nights when there was ozone, N2O5 and ClNO2 were at their largest mixing ratios. Presumably this titration is caused by input of NO at ground level, which does not mix to very high altitude. Therefore, it is likely that aloft there is more active N2O5 chemistry and probably ClNO2 production. For this reason, I think that the manuscript's title should be modified to include "Low levels of nitryl chloride at ground level...".

An excellent suggestion. We have modified the title as suggested by the referee.

The peaking of ClNO2 after sunrise and coincident with breakup of the nocturnal boundary layer would seem to indicate that ClNO2 aloft is likely higher.

Agreed.

The manuscript has discussion about chloride measurements based upon the ACSM, which is not good at detecting chloride in the form of NaCl.

This is correct. Please see our replies to referee #1 (who raised this issue as well).

There should be measurements in the area of PM2.5 chemical composition that could help to better understand the presence of sea salt chloride. The authors should examine available aerosol chloride measurements to expand their analysis and interpretation through consideration of these data.

We agree that lack of refractory aerosol composition measurements is a limitation of this study. This limitation is noted in section 3.2.3 on lines 751-752 "... production of $ClNO_2$ from uptake of N_2O_5 on unquantified supermicron (i.e., > 0.5 μm) or refractory aerosol (which takes place simultaneously) is not accounted for."

There are not many aerosol chloride data sets out there. Anlauf et al. showed that sea salt aerosol is present in the LFV, but mainly in the supermicron size fraction that was not quantified in this work. We are now citing Anlauf et al. (2006) on line 756 (since we showed supermicron aerosol in the LFV to be mainly sea salt derived, so we no longer need to speculate about that). Since we are already concluding that ClNO2 production that does take place happens mainly on unquantified sea salt aerosol, our conclusions do not need to be revised or altered.

We hope that the referees understand that in this line of work, we are sometimes compromised by budgetary constraints, and will not always have every measurement at our disposal, no matter how desirable such measurements might be. In response to the reviewer's comment we have modified the final sentence of the discussion section to express this desire:

"Future studies should therefore target the NRL, for example through missed-approaches by aircraft, a blimp, or from a tall tower, especially during episodes of a developing O_3 exceedance event and also include composition measurements of refractory aerosol."

Specific comments:

Showing population density (in some way) on the Figure 1 map would be nice.

We agree but since we don't have access to such data have chosen to leave Figure 1 as is.

Figure 3 seems to be mentioned before Fig. 2

We don't believe this to be the case. Figure 2 and Figure 3 are first mentioned on lines 234 and 386, respectively. On line 193, we call out Figure 3 of another paper, though. No changes were made to the manuscript.

Line 194: I think the word is "aging"

We agree and have made the change in the text.

Line 199: I don't think ECCC is defined?

This has been fixed.

"~~ECCC~~ Environment and Climate Change Canada (ECCC)"

Line 202: Define THS?

It's a company name (named after Tanner, Huey and Stickel). We have inserted the word "Instruments" following "THS" to make that clearer.

Line 360: Presumably after measuring the upwelling/downwelling actinic ratio, this ratio was used to correct all downwelling actinic flux data to be a total actinic flux. If this was done, it should be noted.

This was noted on lines 359/360

"On several days, the spectrometer was inverted hourly to determine the up-~~d~~welling radiation, which was added to the down-~~d~~welling flux."

No changes were made to the manuscript in response to this comment.

Line 394: I think K2 is first used here but not defined until later. This should probably be done near line 80

We have added "In ambient air, N_2O_5, NO_3 and NO_2 are usually in equilibrium; the equilibrium constant, K_2, is temperature dependent, favoring NO_3 and NO_2 at higher temperatures (Osthoff et al., 2007)." near line 80 as requested.

Line 533: This equation is applicable when diffusion limitations are not important, which might not be true if supermicron particle surface area is involved.

An important point. We have added the sentence "Equation (1) is valid for uptake on small, submicron aerosol as it neglects gas-phase diffusion limitations (Davidovits et al., 2006).

Line 554: Make clear that an equivalent basis (e.g. 2x the molar concentration of sulfate) is being used in this neutralization ratio equation.

Fixed (issue already raised by reviewer #1).

Line 559-562: Does the ACSM detect chloride efficiently? Standard filter samples would show chloride and could be used to verify its presence or absence. Historical data from the area would tell you the ratio of chloride to other inorganic ions (e.g. nitrate and sulfate), so you should be able to tell if the ACSM is not actually detecting chloride efficiently.

This point was already raised by reviewer #1 – please see our responses above.
Briefly, the reviewers are correct in that the ACSM does not quantify "refractory" chloride (i.e., chloride present in sea salt derived aerosol). Unfortunately, no other data are available since filter samples were not collected during this campaign. For historical data, during PACIFIC 2001 there were AMS measurements (Alfarra et al., 2004; Boudries et al., 2004) and measurements of water-soluble aerosol components (Anlauf et al., 2006). All these papers are now cited.

Line 751 area: Presumably some pollution monitoring studies looked at PM2.5 via IC and could address presence of at least 1 to 2.5 micron particles containing Cl-

Correct. Anlauf and coworkers collected MOUDI data during PACIFIC 2001 and showed variable sea salt concentrations in the supermicron size fraction (Anlauf et al., 2006).
We have modified the following sentences in the introduction:

"... sea spray aerosol is a primary source of particulate matter (PM) and hence directly affect particle concentrations and mass loadings (Pryor et al., 2008) and aerosol chloride concentrations (Anlauf et al., 2006) in the LFV, ..."

and

"Previous studies in the LFV have shown high biogenic VOC concentrations (Biesenthal et al., 1997; Gurren et al., 1998; Drewitt et al., 1998) yet there was active nighttime nitrogen oxide chemistry and aerosol chloride present mainly as sea salt derived aerosol in >1 µm diameter aerosol (Anlauf et al., 2006)."

References cited

Alfarra, M. R., Coe, H., Allan, J. D., Bower, K. N., Boudries, H., Canagaratna, M. R., Jimenez, J. L., Jayne, J. T., Garforth, A. A., Li, S.-M., and Worsnop, D. R.: Characterization of urban and rural organic particulate in the Lower Fraser Valley using two Aerodyne Aerosol Mass Spectrometers, Atmos. Environm., 38, 5745-5758, 10.1016/j.atmosenv.2004.01.054, 2004.

Anlauf, K., Li, S.-M., Leaitch, R., Brook, J., Hayden, K., Toom-Sauntry, D., and Wiebe, A.: Ionic composition and size characteristics of particles in the Lower Fraser Valley: Pacific 2001 field study, Atmos. Environm., 40, 2662-2675, 10.1016/j.atmosenv.2005.12.027, 2006.

Biesenthal, T. A., Wu, Q., Shepson, P. B., Wiebe, H. A., Anlauf, K. G., and Mackay, G. I.: A study of relationships between isoprene, its oxidation products, and ozone, in the Lower Fraser Valley, BC, Atmos. Environm., 31, 2049-2058, 10.1016/S1352-2310(96)00318-4, 1997.

Boudries, H., Canagaratna, M. R., Jayne, J. T., Alfarra, M. R., Allan, J., Bower, K. N., Coe, H., Pryor, S. C., Jimenez, J. L., Brook, J. R., Li, S., and Worsnop, D. R.: Chemical and physical processes controlling the distribution of aerosols in the Lower Fraser Valley, Canada, during the Pacific 2001 field campaign, Atmos. Environm., 38, 5759-5774, 10.1016/j.atmosenv.2004.01.057, 2004.

Brown, S. S., Stark, H., and Ravishankara, A. R.: Applicability of the steady state approximation to the interpretation of atmospheric observations of NO_3 and N_2O_5, J. Geophys. Res., 108, 4539, 10.1029/2003JD003407, 2003.

Drewitt, G. B., Curren, K., Steyn, D. G., Gillespie, T. J., and Niki, H.: Measurement of biogenic hydrocarbon emissions from vegetation in the Lower Fraser Valley, British Columbia, Atmos. Environm., 32, 3457-3466, 10.1016/S1352-2310(98)00043-0, 1998.

Geyer, A., and Stutz, J.: Vertical profiles of NO_3, N_2O_5, O_3, and NO_x in the nocturnal boundary layer: 2. Model studies on the altitude dependence of composition and chemistry, J. Geophys. Res., 109, D12307, doi:12310.11029/12003JD004211, 2004.

Gurren, K., Gillespie, T., Steyn, D., Dann, T., and Wang, D.: Biogenic isoprene in the Lower Fraser Valley, British Columbia, J. Geophys. Res.-Atmos., 103, 25467-25477, 10.1029/98jd01214, 1998.

Lin, C. H., Lai, C. H., Wu, Y. L., and Chen, M. J.: Simple model for estimating dry deposition velocity of ozone and its destruction in a polluted nocturnal boundary layer, Atmos. Environm., 44, 4364-4371, 10.1016/j.atmosenv.2010.07.053, 2010.

Ng, N. L., Herndon, S. C., Trimborn, A., Canagaratna, M. R., Croteau, P. L., Onasch, T. B., Sueper, D., Worsnop, D. R., Zhang, Q., Sun, Y. L., and Jayne, J. T.: An Aerosol Chemical Speciation Monitor (ACSM) for Routine Monitoring of the Composition and Mass Concentrations of Ambient Aerosol, Aerosol Sci. Technol., 45, 780-794, 10.1080/02786826.2011.560211, 2011.

Osthoff, H. D., Pilling, M. J., Ravishankara, A. R., and Brown, S. S.: Temperature dependence of the NO_3 absorption cross-section above 298 K and determination of the equilibrium constant for NO_3+NO_2 <-> N_2O_5 at atmospherically relevant conditions, Phys. Chem. Chem. Phys., 9, 5785-5793, 10.1039/b709193a, 2007.

Plaxco, K. W.: The art of writing science, Protein Science : A Publication of the Protein Society, 19, 2261-2266, 10.1002/pro.514, 2010.

Pryor, S. C., Barthelmie, R. J., Schoof, J. T., Binkowski, F. S., Delle Monache, L., and Stull, R.: Modeling the impact of sea-spray on particle concentrations in a coastal city, Sci. Tot. Environm., 391, 132-142, 10.1016/j.scitotenv.2007.10.059, 2008.

Seinfeld, J. H., and Pandis, S. N.: Atmospheric chemistry and physics: from air pollution to climate change, 2nd ed., Wiley, Hoboken, N.J., 2006.

Zhang, Q., Jimenez, J. L., Worsnop, D. R., and Canagaratna, M.: A case study of urban particle acidity and its influence on secondary organic aerosol, Environm. Sci. Technol., 41, 3213-3219, 10.1021/es061812j, 2007.

Low levels of nitryl chloride at ground level: Nocturnal nitrogen oxides in the Lower Fraser Valley of British Columbia

Hans D. Osthoff[1], Charles A. Odame-Ankrah[1], Youssef M. Taha[1], Travis W. Tokarek[1], Corinne L. Schiller[2], Donna Haga[3], Keith Jones[2], and Roxanne Vingarzan[2]

[1] {Department of Chemistry, University of Calgary, Calgary, Alberta T2N 1N4, Canada}

[2] {Applied Science Division, Prediction and Services West, Meteorological Service of Canada, Environment and Climate Change Canada, Vancouver, British Columbia V6C 3S5, Canada}

[3] {British Columbia Ministry of Environment and Climate Change Strategy, Cranbrook, British Columbia V1C 7G5, Canada}

Correspondence to: H. D. Osthoff (hosthoff@ucalgary.ca)

Abstract

The nocturnal nitrogen oxides, which include the nitrate radical (NO_3), dinitrogen pentoxide (N_2O_5), and its uptake product on chloride containing aerosol, nitryl chloride ($ClNO_2$), can have profound impacts on the lifetime of NO_x (= NO + NO_2), radical budgets, and next-day photochemical ozone (O_3) production, yet their abundances and chemistry are only sparsely constrained by ambient air measurements.

Here, we present a measurement data set collected at a routine monitoring site near the Abbotsford International Airport (YXX) located approximately 30 km from the Pacific Ocean in the Lower Fraser Valley (LFV) on the West coast of British Columbia. Measurements were made from July 20 to August 4, 2012, and included mixing ratios of $ClNO_2$, N_2O_5, NO, NO_2, total odd nitrogen (NO_y), O_3, photolysis frequencies, and size distribution and composition of non-refractory submicron aerosol (PM_1).

At night, O_3 was rapidly and often completely removed by dry deposition and by titration with NO of anthropogenic origin and unsaturated biogenic hydrocarbons in a shallow nocturnal inversion surface layer. The low nocturnal O_3 mixing ratios and presence of strong chemical sinks for NO_3 limited the extent of nocturnal nitrogen oxide chemistry at ground level. Consequently, mixing ratios of N_2O_5 and $ClNO_2$ were low (<30 and <100 parts-per-trillion by volume (pptv) and median nocturnal peak values of 7.8 pptv and 7.9 pptv, respectively). Mixing ratios of $ClNO_2$ frequently peaked 1 - 2 hours after sunrise rationalized by more efficient formation of $ClNO_2$ in the nocturnal residual layer aloft than at the surface and the breakup of the nocturnal boundary layer structure in the morning. When quantifiable, production of $ClNO_2$ from N_2O_5 was efficient and likely occurred predominantly on unquantified supermicron sized or refractory sea salt derived aerosol. After sunrise, production of Cl radicals from photolysis of $ClNO_2$ was negligible compared to production of OH from the reaction of $O(^1D) + H_2O$ except for a short period after sunrise.

Keywords

Lower Fraser Valley, $ClNO_2$, surface measurements, nocturnal residual layer, $ClNO_2$ morning peak, vertical entrainment

1 Introduction

The Lower Fraser Valley (LFV) is prone to episodes of poor air quality, in part because of its geography which facilitates stagnation periods and accumulation of airborne pollutants through processes such as the Wake-Induced Stagnation Effect (Brook et al., 2004), and also because of continued growth of human population and associated emissions from urban, suburban, agricultural and marine sources. Of special concern have been repeated exceedances of the Canada-Wide Standard and, as of 2012, the Canadian Ambient Air Quality Standards (CAAQS) for fine particulate matter ($PM_{2.5}$) and ozone (O_3) at Chilliwack and Hope, located in the eastern part of the LFV downwind of Vancouver (Ainslie et al., 2013). These exceedances have occurred in spite of ongoing declines in emissions of both nitrogen oxides (NO_x = NO + NO_2) and volatile organic compounds (VOCs) resulting from the introduction of new vehicle standards and (now discontinued) local vehicle emission testing programs (Ainslie et al., 2013). Previous large-scale studies in the LFV such as Pacific 1993 (Steyn et al., 1997), the Regional Visibility Experimental Assessment in the Lower Fraser Valley (REVEAL) I and II (Pryor et al., 1997; Pryor and Barthelmie, 2000) and Pacific 2001 (Vingarzan and Li, 2006) have added important information regarding atmospheric processes leading to O_3 and aerosol formation and visibility issues. However, the transformation of primary (e.g., NO_x, VOCs, SO_2, NH_3, etc.) to secondary pollutants (i.e.., O_3 and fine particulate matter) is highly complex, and the scientific understanding of these highly non-linear processes remains incomplete.

A complicating factor in the LFV is the interaction of anthropogenic emissions with marine derived sea salt aerosol. While sea spray aerosol is a primary source of ~~particle~~ particulate matter (PM) and hence directly affect~~s~~ particle concentration**s** and mass loadings (Pryor et al., 2008) and aerosol chloride concentrations (Anlauf et al., 2006) in the LFV, there is now considerable evidence from modeling (Knipping and Dabdub, 2003), laboratory (Raff et al., 2009), and field studies (Tanaka et al., 2003; Osthoff et al., 2008) that "active chlorine" species released from sea salt can negatively affect air quality and promote O_3 and secondary aerosol formation in coastal regions.

In an analysis of 20 years of O_3 air quality data in the LFV region, Ainslie and Steyn (2007) concluded that precursor buildup, prior to an exceedance day, plays an important role in the spatial O_3 pattern on exceedance days. Secondary processes involving active chlorine

Formatted: Font: Not Italic

produced from the interaction of marine aerosol with anthropogenic pollution would fit this profile but are not currently constrained by measurements.

One pathway to activate chlorine from sea salt is the reactive uptake of dinitrogen pentoxide (N_2O_5) on chloride containing aerosol to yield nitryl chloride ($ClNO_2$) (Behnke et al., 1997; Finlayson-Pitts et al., 1989). Briefly, N_2O_5 is formed from the reversible reaction of nitrogen dioxide (NO_2) with the photo-labile nitrate radical (NO_3; R1), which in turn is formed from reaction of NO_2 with O_3 (R2).

$$NO_2 + O_3 \rightarrow NO_3 + O_2 \quad (R1)$$

$$NO_3 + NO_2 \rightleftharpoons N_2O_5 \quad (R2)$$

In ambient air, N_2O_5, NO_3 and NO_2 are usually in equilibrium; the equilibrium constant, K_2, is temperature dependent, favoring NO_3 and NO_2 at higher temperatures (Osthoff et al., 2007). During daytime, NO_3 (and, indirectly, N_2O_5) is removed primarily via its reaction (R3) with NO (which is generated from NO_2 photolysis and directly emitted, for example, by automobiles) and by NO_3 photolysis (R4) (Wayne et al., 1991).

$$NO_3 + NO \rightarrow 2NO_2 \quad (R3)$$

$$NO_3 + h\nu \rightarrow 0.9NO_2 + 0.1NO \quad (R4)$$

The heterogeneous hydrolysis of N_2O_5 to nitric acid (HNO_3) is an important nocturnal NO_x and odd oxygen ($O_x = NO_2 + O_3$) removal pathway (Chang et al., 2011; Brown et al., 2006a). On chloride containing aerosol, however, uptake of N_2O_5 yields up to a stoichiometric amount of $ClNO_2$ (R5) (Behnke et al., 1997; Finlayson-Pitts et al., 1989):

$$N_2O_5 + H_2O(het) + \phi Cl^-(het) \rightarrow (2-\phi)HNO_3(het) + \phi ClNO_2,\ 0 \leq \phi \leq 1 \quad (R5)$$

The $ClNO_2$ yield, ϕ, is primarily a function of aerosol chloride and water content (Behnke et al., 1997; Bertram and Thornton, 2009; Roberts et al., 2009; Ryder et al., 2014; Ryder et al., 2015b; Ryder et al., 2015a). Formation of $ClNO_2$ impacts air quality in the following ways: Since $ClNO_2$ is long-lived at night ~~(Osthoff et al., 2008)~~, its primary fate is photo-dissociation (to Cl and NO_2) in the morning hours after sunrise (R6) (Osthoff et al., 2008).

$$ClNO_2 + h\nu \rightarrow NO_2 + Cl \quad (R6)$$

This reaction increases the morning abundance of O_x, leading to greater net photochemical O_3 production throughout the day. The other photo fragment, the Cl atom, is highly reactive towards hydrocarbons and will initiate radical chain reactions that produce O_3 and secondary aerosol (Behnke et al., 1997; Young et al., 2014). The fate and impact of $ClNO_2$ is thus similar to that of nitrous acid (HONO), which also accumulates during the night and photodissociates in the morning to release NO and the hydroxyl radical (OH) that go on to produce O_3 (Alicke et al., 2003).

Data collected during the 2006 Texas Air Quality Study – Gulf of Mexico Atmospheric Composition and Climate Study (TEXAQS-GOMACCS) have shown that $ClNO_2$ production is efficient in the nocturnal polluted marine boundary layer even on primarily non-sea salt aerosol surfaces (Osthoff et al., 2008). As a result, up to 15% of total odd nitrogen (NO_y) was present in the form $ClNO_2$ at night (Osthoff et al., 2008). The high efficiency of $ClNO_2$ formation on aerosol of medium-to-low total chloride content has been confirmed by several laboratory investigations (Bertram and Thornton, 2009; Raff et al., 2009; Roberts et al., 2009) and direct measurements of N_2O_5 uptake on ambient particles (Riedel et al., 2012b). Some ambiguity remains as to the detailed mechanism of ~~the reaction~~R5, but there is agreement that acid displacement of HCl from supermicron (predominantly sea salt aerosol) to submicron (predominantly non-sea salt aerosol) is a key step in the efficient production of $ClNO_2$. These results suggested that this chemistry is active anywhere where pollution in the form of NO_x and O_3 comes in contact with marine air, including the LFV.

However, while the yield of $ClNO_2$ in reaction ~~(~~R5~~)~~ is high in polluted coastal regions, the $ClNO_2$ yield relative to the amount of NO_3 produced ~~from~~ via ~~reaction (~~R1~~)~~ cannot be easily predicted because NO_3 is consumed by reactions with VOCs (R7), e.g., with biogenic VOCs such as isoprene and monoterpenes as well as aldehydes, and dimethyl sulfide (Wayne et al., 1991).

$$NO_3 + VOC \rightarrow \text{products} \qquad (R7)$$

Previous studies in the LFV have shown high biogenic VOC concentrations (Biesenthal et al., 1997; Gurren et al., 1998; Drewitt et al., 1998) yet there was active nighttime nitrogen oxide chemistry and aerosol chloride present mainly as sea salt derived aerosol in >1 μm diameter aerosol (Anlauf et al., 2006). During the Pacific 2001 study, measurements of the mixing ratios of NO, NO_2, peroxyacetic nitric anhydride ($CH_3C(O)O_2NO_2$, PAN), HONO, HNO_3, and NO_y at three ground sites in the LFV indicated deficits of up to 15% in the nocturnal NO_y

budget (Hayden et al., 2004) attributable to unquantified species such as alkyl nitrates, N_2O_5, and $ClNO_2$. McLaren and coworkers quantified mixing ratios of NO_2 and NO_3 by differential optical absorption spectroscopy (DOAS) at the Sumas Eagle Ridge site (~250 m above the floor of the LFV) as part of Pacific 2001 (McLaren et al., 2004) and off-shore on Saturna Island (Figure 1) in the Strait of Georgia in 2005 (McLaren et al., 2010). The LFV data showed occasional episodes of active nocturnal nitrogen oxide chemistry in the residual layer with N_2O_5 contributing up to 9% of NO_y, while the Saturna Island data showed NO_3 mixing ratios of > 20 parts-per-trillion by volume (10^{-12}, pptv) every night of measurement. McLaren et al. estimated that between 0.3 and 1.9 ppbv of $ClNO_2$ would be produced under these conditions (2010). Efficient formation of $ClNO_2$ would be consistent with the unidentified O_3 precursor proposed by Ainslie and Steyn and is also a plausible explanation for part of the deficit in the NO_y budget observed by Hayden et al. (2004).

Another feature of the LFV are somewhat unusual diurnal profiles arising from the vertical structure in pollutant concentrations. Measurements of O_3 and NO_2 using tethered balloons by Pisano et al. (1997) during Pacific 93 at the Harris Road site (located ~38 km NW of Abbotsford International Airport) revealed a highly stratified boundary layer with a shallow, 50 m deep isothermal surface layer (also called a nocturnal boundary layer, or NBL) and low surface O_3 concentrations at night. Nocturnal loss of surface O_3 is known to occur by several pathways, including dry deposition, titration with NO (R8), and reaction with unsaturated biogenic hydrocarbons (Neu et al., 1994; Kleinman et al., 1994; Trainer et al., 1987; Logan, 1989; Talbot et al., 2005). Titration of O_3 with NO is readily quantified as the concentration of a product of ~~this reaction~~R8, NO_2, can be measured directly and conserves O_x.

$$O_3 + NO \rightarrow O_2 + NO_2 \qquad (R8)$$

Usually, the major nocturnal sink of O_x is dry deposition of O_3 and NO_2 (Lin et al., 2010).

The balloon data also showed pools of NO_2 and O_3 in a ~100 m deep nocturnal residual layer (NRL) located 200 to 350 m above ground. Following the break-up of the nocturnal layers in the early morning, vertical down-mixing events of O_3 pollution were observed (McKendry et al., 1997). In this process, pollutants are entrained into the growing mixed layer from the NRL, i.e., the growing mixed layer in the hours after sunrise erodes the somewhat deeper NRL, and pollutants are mixed to the surface (Neu et al., 1994; Kleinman et al., 1994).

Formatted: Font: Not Italic

Formatted: Font: Not Italic

Formatted: Font: Not Italic

Formatted: Font: Not Italic

Formatted: Font: Not Italic

In this manuscript, we present the first measurements of $ClNO_2$ and N_2O_5 mixing ratios in the LFV. The data were collected at a surface site east of the Abbotsford International Airport (International Air Transport Association (IATA) airport code YXX) located approximately 35 km from the Pacific Ocean from July 20 to August 5, 2012. Auxiliary measurements included NO, NO_2, NO_y, O_3, photolysis frequencies, and ~~submicron~~ non-refractory PM_1 aerosol composition and size distributions. An analysis of nocturnal nitrogen oxide chemistry including the formation of $ClNO_2$ and its potential impact on nocturnal O_3 and NO_2 loss and radical budgets in the LFV are presented.

2 Experimental

2.1 Location

The map shown in Figure 1 indicates the location of the study. Ambient air measurements were conducted at the T45 routine monitoring site located to the east YXX at latitude 49.0212 (N) and longitude -122.3267 (W) and ~60 m above sea level (ASL) and ~30 km from the Pacific Ocean. A raspberry field was located immediately to the W between the end of the airport runway and the measurement site. Nearby local sources included agricultural operations (such as poultry farms) and emissions from motor vehicle traffic on secondary roads and highways. YXX is located ~60 km ESE of the Vancouver International Airport (YVR) and the City of Vancouver. Abbotsford is in the heart of the so-called "Lower Mainland", the low-lying region stretching from Pacific Ocean at Vancouver to the NW and the Canada-USA border to the S (north of Bellingham, BLI) to the eastern end of the Fraser Valley with a total population in excess of 2,500,000.

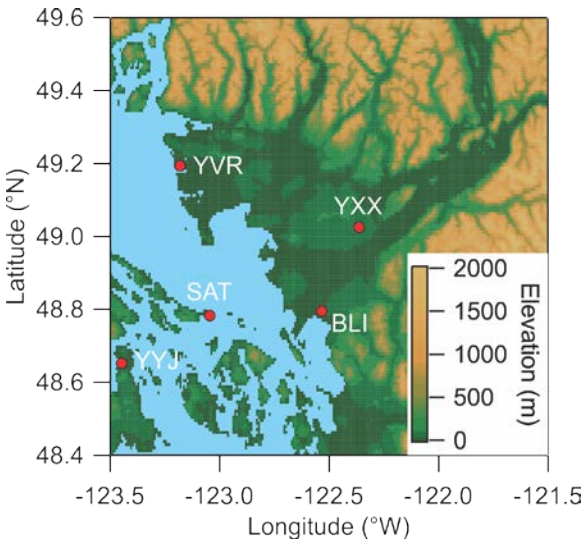

Figure 1. Map of the Lower Fraser Valley. YXX = Abbotsford International Airport (measurement location for this study). YVR = Vancouver Int'l Airport. YYJ = Victoria Int'l Airport. BLI = Bellingham Int'l Airport. SAT = Saturna Island.

2.2 Measurement techniques

The measurement techniques used for this study are listed in Table 1. Data were averaged to 5 min prior to presentation.

The instruments measuring O_3 and nitrogen oxides were housed in an air-conditioned trailer and sampled from a common 0.635 cm (¼") outer diameter (o.d.) and 0.476 cm (3/16") inner diameter (i.d.) Teflon™ inlet at a height of 4 m above ground; the setup is depicted in Figure 3 of Tokarek et al. (2014). A scroll pump whose flow rate was throttled using a 50 standard liters per minute (slpm) capacity mass flow controller was connected to the end of the common inlet to minimize the residence time of the sampled air and to reduce inlet "ageing", i.e., accumulation of aerosol on filters of individual instruments, whose inlets tapped into the main inlet line at 90°. The total inlet flow was in the range of 18 to 20 slpm.

Measurements of PM_1 aerosol composition and size distributions (section 2.3) and of meteorological data were made from the research trailer housing the routine measurements at the site. The Agilent VOC measurements were made from a research trailer owned by Environment and Climate Change Canada (ECCC).

2.2.1 Quantification of $ClNO_2$ by iodide chemical ionization mass spectrometry

Mixing ratios of $ClNO_2$ were quantified as iodide cluster ions at *m/z* 208 using the "THS Instruments" iodide chemical ionization mass spectrometer (iCIMS) described by Mielke et al. (2011) and calibrated using the scheme by Thaler et al. (2011). In this method, a gas stream containing $ClNO_2$ is generated from reaction of Cl_2 (Praxair, 10 ppmv in N_2) with an aqueous slurry saturated with $NaNO_2$ (Sigma-Aldrich) (R9):

$$Cl_2(g) + NO_2^-(aq) \rightleftharpoons ClNO_2(g) + Cl^-(aq) \quad (R9)$$

This gas stream was periodically added to the main inlet with the aid of a normally-open 2-way valve connected to a vacuum pump in a similar fashion as described earlier for N_2O_5 and PAN (Tokarek et al., 2014; Odame-Ankrah and Osthoff, 2011). The $ClNO_2$ content of the calibration gas stream was quantified by thermal dissociation cavity ring-down spectroscopy (TD-CRDS) as described in section 2.2.2. In total, 31 calibrations for $ClNO_2$ were carried out, spread out evenly over the measurement period. The iCIMS response factor at *m/z* 208 was (0.40±0.06) Hz $pptv^{-1}$ (where the error represents the standard deviation of repeated calibrations), normalized to 10^6 counts of reagent ion at *m/z* 127. The $^{37}ClNO_2I^-$ ion at *m/z* 210

Formatted: Font: Not Italic
Formatted: Font: Not Italic
Formatted: Font: Not Italic
Formatted: Font: Not Italic
Formatted: Font: Not Italic
Formatted: Font: Not Italic

was also monitored and found to be (0.298±0.004) times the signal at *m/z* 208 (r^2 = 0.944), slightly lower than Standard Mean Ocean Chloride ^{37}Cl mole fraction in sea water of ~0.319 (Wieser and Berglund, 2009) and our previously observed ratios of 0.315±0.003 in Calgary (Mielke et al., 2011) and 0.3065±0.0002 in Pasadena (Mielke et al., 2013). The reason(s) for these differences are unclear but may be a result of fractionation processes (Koehler and Wassenaar, 2010; Volpe et al., 1998), a topic outside the scope of this manuscript.

The iCIMS was also used to quantify mixing ratios of PAN at *m/z* 59 and PPN at *m/z* 73 (Slusher et al., 2004; Mielke et al., 2011; Mielke and Osthoff, 2012). For this reason, part of the instrument's inlet prior to the ion-molecule reaction region was heated to 190 °C to dissociate PANs into their respective carboxylates. Further, the collisional dissociation chamber (CDC) was operated in declustering mode (-22.7 V) to break up ion clusters. Calibrations and matrix effect correction procedures and a time series of the PAN and PPN data were presented by *Tokarek et al.* (2014).

2.2.2 Quantification of NO_2 and N_2O_5 by cavity ring-down spectroscopy

The CRDS used in this work was an amalgamated version of two instruments described earlier (Paul and Osthoff, 2010; Odame-Ankrah and Osthoff, 2011), called "Improved Detection Instrument for Nitrogen Oxide Species" (iDinos) (Odame-Ankrah, 2015). A schematic of the optical layout is shown in Figure 2. The optical bread board, instrument frame, electronic and data acquisition components were as described by *Paul and Osthoff* (2010). The new instrument was set up with up to six parallel detection channels: four 405 nm "blue" diode laser CRDS cells for quantification at NO_2 via its absorption at 405 nm with a distance between the pairs of high-reflectivity (HR) mirrors (Advanced Thin Films) of 112.5 cm, of which 92.0 cm were filled with sample air, and two newly constructed 662 nm "red" diode laser CRDS cells for quantification at NO_3 via its absorption at 662 nm with a distance between the HR mirrors (Los Gatos) of 93.0 cm of which 73.0 cm were filled with sample air. Light exiting the far ends of the CRDS cells was collected using fixed-focus collimating lenses and multimode optical fibers (Thorlabs) connected to photomultiplier tubes (PMT, Hamamatsu H9433-03MOD) with 10 MHz bandwidth. Bandpass filters (Thorlabs FB405-10 and FB660-10) were placed between the PMTs and the end of the optical fibers.

The two laser diodes were simultaneously square-wave modulated by a function generator (SRS DS335). The PMT voltages were digitized using an 8-channel 14-bit data acquisition

card (National Instruments PCI-6133; 2.5 MS s^{-1} simultaneous sampling sample rate) connected to a laptop computer via a PCMCIA-to-PCI expansion unit (Magma CB4DRQ) and controlled by software written in LABVIEW™ (National Instruments).

Ring-down time constants (τ) were determined from a linear fit to the logarithm of the digitized PMT voltage as described by *Brown et al.* (2002) immediately after acquisition of the ring-down traces (which were co-added to a user-selectable averaging time prior to the fit). The fitting algorithm requires the subtraction of the PMT voltage offset prior to taking the logarithm; this offset was measured between ring-down events after the signal had returned to baseline, which limited the repetition rate of the diode lasers and the number of traces averaged per second to a frequency of 300 Hz.

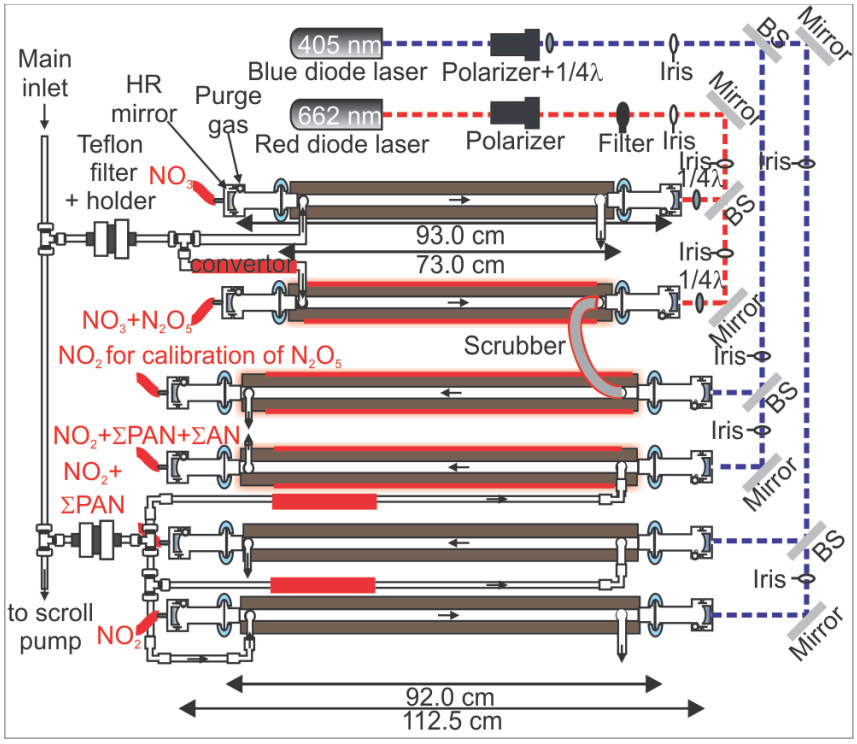

Figure 2. Optical layout of the cavity ring-down spectrometer. ¼λ = quarter wave plate. BS = beam splitter. HR mirror = high reflectivity mirror. Drawing is not to scale.

Ring-down time constants in the absence of the target absorber (τ_0) were determined by flooding the inlet (each once per hour) with ultra-pure, or "zero", air (Praxair) for the 405 nm channels and by titration with NO for the 662 nm channel (Brown et al., 2001; Simpson, 2003) Typical values of τ_0 were in the range of 63 to 67 μs and between 198 and 210 μs for the blue and red channels, respectively. The baseline precision (i.e., standard deviation, σ) of the NO_2 and NO_3 measurements were ±80 pptv and ±3 pptv (1 s data), respectively. For the NO_3 channels, additional noise was introduced by variable background absorption of NO_2, O_3, and water vapor which produce small, spurious structure in the 662 nm absorption signal (Dubé et al., 2006) and were not tracked well by the interpolation of the baseline from the hourly τ_0 determinations.

During the Abbotsford campaign, only five (four blue and one red) CRDS channels were operated because of delays in the fabrication of the final set of CRDS mirror holders. The 662 nm CRDS cell sampled from a Teflon™ inlet heated to 130 °C for quantification of NO_3 plus the NO_3 generated from thermal dissociation N_2O_5 (Brown et al., 2001; Simpson, 2003; Dubé et al., 2006). Under the high-NO_x conditions of this study, equilibrium (2) was sufficiently far to the right (see section 3.3) such that $[NO_3] + [N_2O_5] \approx [N_2O_5]$, i.e., the concentration measured could be equated with $[N_2O_5]$ without introducing a large error (i.e., <5%). The four 405 nm CRDS cells were operated as follows: The first sampled from an ambient temperature inlet and was used to quantify NO_2. The second sampled from a quartz inlet heated to 250 °C and was used to quantify NO_2 plus total peroxyacyl nitrate (ΣPAN) (Paul et al., 2009; Paul and Osthoff, 2010). Data from this channel will be presented in a future manuscript. The third was operated with a quartz inlet heated to 450 °C to enable $ClNO_2$ calibrations (Thaler et al., 2011). Quantification of total alkyl nitrates (ΣAN) in ambient air was not attempted because of the high NO_x levels and resulting large subtraction errors (Thieser et al., 2016). The fourth 405 nm CRDS cell was connected with polycarbonate tubing (⅜" o.d. and ¼" i.d.) in series to the 662 nm channel and was used to calibrate the response of the N_2O_5 channel, which is a function of the transmission efficiency of N_2O_5 through the inlet and the overlap of the diode laser spectrum with the NO_3 absorption line (Odame-Ankrah and Osthoff, 2011). The role of the polycarbonate tube was to scrub NO_3 exiting the N_2O_5 channel, allowing detection of only the NO_2 generated from thermal

dissociation of N_2O_5 and to prevent recombination of NO_3 and NO_2 in the blue calibration channel (Wagner et al., 2011).

N_2O_5 was generated in situ by adding an excess of O_3 (generated by passing O_2 past a 254 nm Hg lamp) to nitric oxide (NO) in a 0.635 cm (¼") o.d. and 0.476 cm (3/16") i.d. Teflon™ calibration line and allowed to equilibrate (i.e., until the output was constant) offline before being switched inline on demand. The N_2O_5 response (which accounted for N_2O_5 loss in the sampling line and slight mismatches of the laser wavelengths with the NO_3 absorption line) varied between 65% and 100% and depended~~ing~~ on inlet "age"; the Teflon™ inlet and aerosol inlet filter were changed every 2 – 3 days. The accuracy of the NO_2 and N_2O_5 data were ±10% and ±25%, respectively, driven mainly by the systematic uncertainty of the NO_2 absorption cross-section and of the N_2O_5 inlet transmission efficiency (Odame-Ankrah, 2015).

2.2.3 Measurements of O_3, NO and NO_y,

Mixing ratios of O_3 were monitored by UV absorption in a commercial instrument (Thermo 49) and were accurate within ±2% and ±1 ppbv. An NO-O_3 chemiluminescence instrument (Thermo 42i) was used to monitor mixing ratios of NO and NO_y, which was reduced to NO in a Mo converter heated to ~320 °C placed outside ~~next to~~a short distance (~ 1 m) from the sample inlet. This instrument sampled from the main inlet via a Teflon™ filter and filter holder and was calibrated daily against CRDS as described by Tokarek et al. (2014). The slope uncertainty for each multipoint calibration was ±15%. Interpolation between calibration runs gave an overall uncertainty of ±30%. The NO zero offset uncertainty (needed for calculating the NO_3 loss rate with respect to reaction with NO, R9) was ±10 pptv.

Formatted: Font: Not Italic

Formatted: Font: Not Italic

2.2.4 VOC measurements

Volatile organic compounds were monitored with a commercial gas chromatograph - mass spectrometer (GC-MS; Agilent model 7890A and 5975C) equipped with an FID detector and a Markes Unity 2 pre-concentrator with an ozone precursor trap cooled to -25 °C.

In a typical sampling sequence, a 500 mL air sample was collected at a flow rate of 25 mL min^{-1}, taken from the center flow of a 1.27 cm (½") stainless steel inlet line which was continuously sampling ambient air at 5 L min^{-1}. The sampled air flowed through a 0.318 cm

(1/8") stainless steel line and particles were removed using a 1 µm pore size fritted filter. Once 500 mL of air were collected, the pre-concentrator was flushed with helium to remove air while awaiting injection. At the start of a GC run, the sample in the pre-concentrator was flash heated to 300 °C and held for 3 min. The sample was separated on 2 columns with the entire sample going through the Agilent VRX column with a Dean switch directing the first gases emitted to a second GasPro column and then to the FID detector (~<C4) while the heavier compounds were detected using the MS detector in scan mode.

The cycle time for the GC analysis was 1 hour with the sample being collected during the previous runs analyses. The 20 min sample was taken at the start of a 1 hour time period.

Due to the low temperature of the trap, the air was dried using a trap at -30 °C. The trap was heated and dried between each sample and reconditioned for 10 min prior to sample collection. All sample lines were stainless steel with a Restek Sulfinert^{TM} coating to minimize sample loss on the lines. Calibrations were performed once per day for 105 species using a 100 ppbv U.S. Environmental Protection Agency (EPA) photochemical assessment monitoring system (PAMS) and a 100 ppb EPA air method, toxic organics – 15 (TO15) standard tanks (Linde Specialty Gases) at an approximately concentration of 2 ppbv. The terpenes were semi-quantitatively measured as a calibration source was not available at the time and only the changes in concentration strength with time of day were used. The accuracy of the measurements varied depending on the species but was better than ±30% throughout. Peaks were manually reintegrated using Chemstation software from Agilent. Table S-1 summarizes the VOCs quantified.

2.3 Aerosol measurements

The chemical composition of non-refractory ~~submicron particulate matter~~PM_1 was monitored using an Aerosol Chemical Speciation Monitor (ACSM, Aerodyne), which reported concentrations of NO_3-, SO_4^{2-}, Cl^-, NH_4^+, and total organics. A general description of this instrument designed for routine monitoring has been given by Ng et al. (2011). The composition of the refractory aerosol (i.e., sea salt) was not quantified.

Submicron aerosol size distributions were quantified by a scanning mobility particle sizer (SMPS, TSI 3034). This instrument measured aerosol particles in the range from 10 to 487 nm using 54 size channels (32 channels per decade). Both of these instruments were housed in

a trailer operated by Metro Vancouver. The ACSM and the SMPS sampled air off a shared stainless steel inlet that had a total flow of 5 L min^{-1} and contained a $PM_{2.5}$ sharpcut filter at the inlet and was operated at ambient relative humidity.

2.4 Photolysis frequencies

Photolysis frequencies were determined by solar actinic flux spectroradiometry (Hofzumahaus et al., 1999) using a commercial radiometer with 2π receptor optics and photo diode array (PDA) detector (Metcon; 512 pixels, wavelength range 285 nm - 690 nm) calibrated by the manufacturer. The spectrometer was mounted facing up (zenith view) and hence measured the down-~~dwelling~~welling radiation. On several days, the spectrometer was inverted hourly to determine the up-~~dwelling~~welling radiation, which was added to the down-~~dwelling~~welling flux. Photolysis frequencies including $j(NO_3)$, $j(NO_2)$, $j(O^1D)$, and $j(ClNO_2)$ were calculated using reference spectra and quantum yields from (Sander et al., 2010) and (Ghosh et al., 2012). Table 2 gives the ratio of observed up-~~dwelling~~welling to down-~~dwelling~~welling for selected photolysis frequencies. For August 3 (a cloud-free day), the measurements were compared to (hourly) predictions with the online "Tropospheric Ultraviolet and Visible (TUV) Radiation Model" V5.0 (Madronich and Flocke, 1997); with default settings, the model reproduced the measured $j(NO_2)$ and $j(O^1D)$ quite well: a scatter plot of observed against TUV rate constants had correlation coefficients (r) of 0.997 and 0.998, slopes of 1.06±0.02 and 1.10±0.02, and offsets of $(3\pm1)\times10^{-4}$ s^{-1} and $(5\pm3)\times10^{-7}$ s^{-1}.

2.5 Box model simulations of the nocturnal O_3 and O_x loss in the NBL

A box model was set up to reconcile the median nocturnal decays of O_3 and O_x. These simulations are intended as back-of-the-envelope type estimates of major processes only since an accurate description of the nocturnal boundary layer chemistry would require modeling of horizontal and vertical transport, i.e., altitude-resolved information not available in this study (Geyer and Stutz, 2004). The model's assumptions are a well-mixed NBL that is decoupled from the NRL above it as observed by earlier balloon vertical profiling (Pisano et al., 1997), O_3 and NO_2 dry deposition velocities of $v_d(O_3)$ = 0.2 cm s^{-1} and $v_d(NO_2) = \alpha \times v_d(O_3)$ with α=0.65 (Lin et al., 2010), and negligible chemical O_3 and O_x losses other than titration of O_3 by NO (~~reaction~~ R8) and by reaction with a generic biogenic hydrocarbon (assumed to react

394 with O_3 with a rate coefficient of 5×10^{-11} cm^3 $molec.^{-1}$ s^{-1}, i.e., the rate coefficient for reaction
395 of α-pinene with O_3 (Seinfeld and Pandis, 2006)). Simulations were initiated with the median
396 NO_2 and O_3 concentrations observed at sunset. More details are given in the S.I.
397

3 Results

3.1 Overview of data set

3.1.1 Meteorology

A time series of local wind direction and speed are displayed in Figure 3D. During the two-week long measurement period, the air flow to the site was from the Pacific Ocean to the SW and WSW with a moderate wind speed of 8.7 km hr^{-1} (median value). On most nights, local wind speeds were calm, i.e., < 5 km hr^{-1} (median speed 3.6 km hr^{-1}) and from variable directions, though predominantly from the W and N. The two exceptions were the nights of July 22/23 and August 1/2 when stronger winds (> 5 km hr^{-1}) from the W and SW persisted. These nights saw relatively high $ClNO_2$ mixing ratios (see section 3.1.4).

The air temperatures were quite mild and ranged from a minimum of 11.0 °C to a maximum of 31.9 °C. The warm temperatures shifted equilibrium K_2 from N_2O_5 towards NO_3 and NO_2 (further analyzed in section 3.2.2). At night, temperatures frequently dropped to the dew point, resulting in occasional fog formation (shown as grey rectangles in Figure 3D), sometimes after sunrise. Fog droplets are strong sinks for N_2O_5 (Osthoff et al., 2006). In total, the impact of fog was minor, affecting 5% of the data. In addition, there were two periods with precipitation: The first occurred intermittently on July 20 until the morning of July 21. The second rainfall event was a 24-hour period from mid-day July 22 to the afternoon of July 23 (shown as blue dots in Figure 3D). July 23 also exhibited the highest wind speeds of the campaign (Figure 3C) and lowest daytime photolysis frequencies. The time series of $j(ClNO_2)$ is shown as a representative example in Figure 3A. The photolysis data indicates that it was sunny on 6 days (July 25, 26, 29, Aug 1, 4 and 5) and that the remaining days had variable cloud cover, consistent with hourly meteorological logs that showed 10% of the measurement period affected by precipitation.

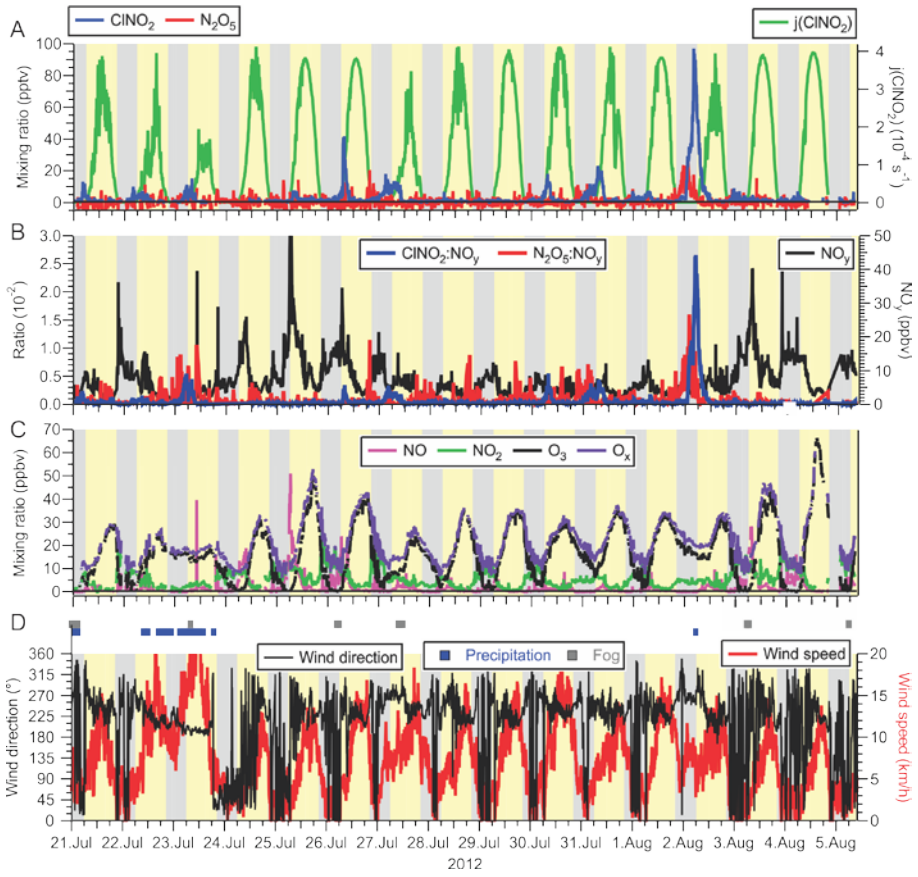

Figure 3. (**A**) Time series of N_2O_5 and $ClNO_2$ mixing ratios (left axis) and $ClNO_2$ photolysis frequency (right axis) observed at T45 near the Abbotsford International Airport. (**B**) Time series of the ratios of $ClNO_2$ and N_2O_5 to NO_y (left axis) and of NO_y (right axis). (**C**) Time series of NO, NO_2, O_3, and O_x (= NO_2 + O_3) mixing ratios. (**D**) Time series of local wind direction (left axis) and speed (right axis). The blue and grey dots above the time series indicates periods of precipitation (drizzle or rain) and fog, respectively, as identified in hourly meteorological logs.

3.1.2 NO and NO_2

The rates of N_2O_5 and $ClNO_2$ formation depend on the rate of NO_3 production, $P(NO_3)=k_1[NO_2][O_3]$ (analyzed further in section 3.2.2); therefore, it is informative to first examine the mixing ratios of NO_2 and O_3 (see section 3.1.3). The time series of NO, NO_2, O_3, and O_x (= O_3 + NO_2) mixing ratios are shown in Figure 3C, and their diurnal averages are shown as 10^{th}, 25^{th}, 50^{th}, 75^{th} and 90^{th} percentiles in Figures 4B and 4C.

The median NO and NO_2 mixing ratios for the entire campaign were 0.9 and 5.9 ppbv, respectively. The average NO_x/NO_y ratio for the entire campaign was ~~0.89~~0.9±0.4 ~~(data not shown)~~. These concentration levels are characteristic of an urban air mass impacted by relatively fresh emissions from combustion engines in automobiles.

At night, mixing ratios of NO were generally lower than during the day though not negligible (median 0.3 ppbv, Figure 4B) as NO was oxidized by O_3 to NO_2 (~~reaction~~ R8) and was not replenished by NO_2 photolysis. However, mixing ratios of NO increased throughout the night, often coinciding with complete nocturnal removal of O_3 (see section 3.1.3), which indicates the presence of nearby combustion sources of NO_x (most likely automobile exhaust). The presence of NO titrates NO_3 (~~via reaction~~ R3) and effectively shut down N_2O_5 and $ClNO_2$ production for most of the study: 68% of the measurement period had NO mixing ratios > 100 pptv and NO_3 lifetimes (with respect to its reaction with NO) of < 15 s. In contrast, NO_2 mixing ratios were highest at night (median 7.3 ppbv), amplified further by NO_x emissions that continued throughout the night and likely by low nocturnal mixing heights (see discussion).

Mixing ratios of NO and NO_x were highest in the morning hours. Concentration changes at this time of day are difficult to interpret since the NBL breaks up during this time, resulting in vertical mixing of air masses, photolabile species (e.g., $ClNO_2$, HONO, N_2O_5, etc.) that accumulated overnight begin to photodissociate, and local emissions change with the onset of rush hour.

In contrast to the morning increase in NO, an afternoon/early evening maximum in NO was absent. This can be rationalized by a greater abundance of oxidants that oxidize NO to NO_2, i.e., O_3 (see Figures 3 and 4 and section 3.1.3) and organic peroxy radicals in the afternoon, a topic outside the scope of this manuscript.

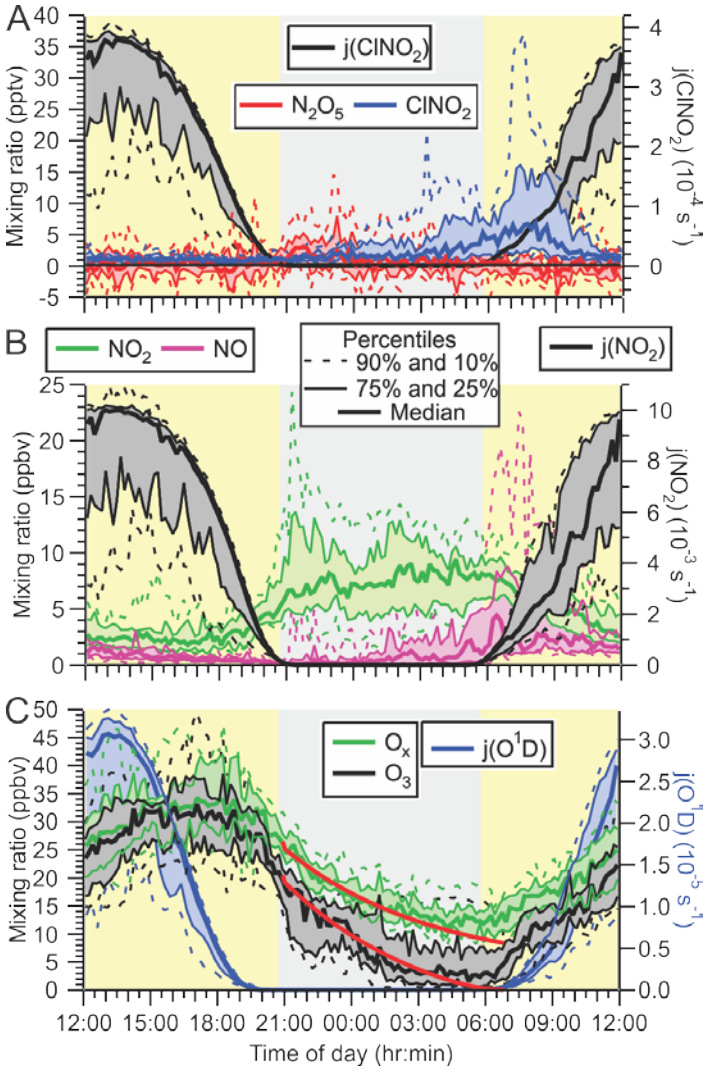

463

464 **Figure 4**. (**A**) Diurnal variation of $ClNO_2$ and N_2O_5 mixing ratios (left axis) and $ClNO_2$
465 photolysis frequencies (right axis). (**B**) Diurnal profiles of NO and NO_2 (left axis) and NO_2
466 photolysis frequency (right axis). (**C**) Diurnal profiles of O_3 and $O_x = O_3 + NO_2$ (left axis) and
467 $O_3 \rightarrow O(^1D)$ photolysis frequency (right axis). The superimposed lines shown in red are results
468 from a simple box model (see text).

469

3.1.3 O_3 and O_x

The time series of O_3 mixing ratios and its diurnal profile are shown in Figure 3C and 4C, respectively. O_3 mixing ratios were small (average ± 1 standard deviation of 16±12 ppbv) and peaked at ~17:00 in the afternoon. The highest concentrations were observed on August 4 from 13:55 to 15:30, when mixing ratios were 64~~.4~~±1~~.2~~ ppbv (the 8-hour running average was 52 ppbv). These levels were well below the CAAQS 8-hr standard of 63 ppbv and the 1 hour National Ambient Air Quality Objective of 82 ppbv, smaller than the pre-2003 data analyzed by Ainslie and Steyn (2007), who reported between 10 and 20 O_3 1-hour exceedences of 82 ppbv in the 1980s, and of similar magnitude as observed by a high-density monitoring network in the region in 2012 (Bart et al., 2014), which observed peak O_3 levels of 74 and 83 ppbv at Abbotsford on July 8 and August 17, respectively.

Formatted: Font: Not Italic

A recurring feature of this data set was the rapid and often complete loss of O_3 at night (Figure 4C). This was accompanied by an increase in the NO_2 mixing ratios, though by less (+6 ppbv on average) than the amount of O_3 that was lost (-26 ppbv on average), showing that NO to NO_2 conversion (~~reaction~~ R8) was a contributor, though minor (~25%) to the nocturnal O_3 loss.

The diurnal profile of O_x was similar to that of O_3, in that the highest concentrations occurred in the afternoon (at ~18:00) and a considerable fraction of O_x was removed at night~~:~~. At sunset, a median amount of 26 ppbv of O_x were present, which decreased to 12 ppbv at sunrise (Figure 4C). The pathways contributing to nocturnal O_3 and O_x loss ~~of~~ are probed using box model simulations in section 3.2.1.

There were two (out of 16 total) nights when O_3 was not completely removed. ~~: o~~On July 22-23 and August 1-2, O_3 mixing ratios dropped from a daytime maxima of ~33 ppbv to non-zero nocturnal minima of ~16 ppbv. On both of these nights, $ClNO_2$ and N_2O_5 mixing ratios were elevated (Figure 3A), and the two largest $ClNO_2$ to NO_y ratios were observed (Figure 3B). The local wind speeds were > 6 km hr^{-1}, whereas on other nights, local winds were calmer (Figure 3C). The greater local wind speeds likely induced more turbulence and a higher vertical mixing height.

3.1.4 N_2O_5 and $ClNO_2$

Time series of $ClNO_2$ and N_2O_5 mixing ratios and $ClNO_2$ photolysis frequencies are shown in Figure 3A. Mixing ratios of $ClNO_2$ and N_2O_5 were small (campaign averages at night of 4.0 pptv and 1.4 pptv, respectively). The mixing ratios peaked prior to sunrise at ~~a~~ median value~~s~~ of 7.9 and 7.8 pptv for $ClNO_2$ and N_2O_5, respectively. The highest mixing ratio~~s~~ of this campaign ~~was~~ were 97 pptv for $ClNO_2$ and 23 pptv for N_2O_5, both observed on the night of August 1-2. This night was also the only time when nocturnal $ClNO_2$ mixing ratios exceeded 20 pptv and is analyzed in greater detail in section 3.2.3.

Consistent with their low mixing ratios, neither $ClNO_2$ nor N_2O_5 were significant components of NO_y (Figure 3B): on average, they contributed 0.1% to the nocturnal NO_y budget, though NO_y mixing ratios were large (median 6.3 ppbv at night), typical for a site impacted by urban emissions. The only exception was the night of August 1-2, when $ClNO_2$ and N_2O_5 constituted 2.6% and 1.6% of NO_y, respectively, and NO_y mixing ratios were 4.4 ppbv on average (Figure 3B).

The $ClNO_2$ and N_2O_5 mixing ratios are displayed as functions of time of day in Figure 4A. Before midnight local time, N_2O_5 mixing ratios were slightly larger (median value of 1.8 pptv on average) than those of $ClNO_2$ (median value of 1.4 pptv on average), whereas after midnight, $ClNO_2$ mixing ratios were larger than those of N_2O_5 (2.0 pptv vs. 0.6 pptv). The latter is consistent with observations at other ground sites, which generally showed higher concentrations of the longer-lived $ClNO_2$ prior to sunset (Thornton et al., 2010; Mielke et al., 2013). The higher N_2O_5 than $ClNO_2$ abundances at the beginning of the nights suggests that the N_2O_5 production rate at that time exceeded its ability to react heterogeneously and convert to $ClNO_2$, potentially due to a lack of available aerosol chloride or otherwise reduced N_2O_5 heterogeneous uptake parameters (Thornton et al., 2010).

Production of $ClNO_2$ from N_2O_5 uptake on aerosol ceases after sunrise because of the rapid removal of N_2O_5 and NO_3 as the latter is titrated by NO and destroyed by photolysis (~~reactions~~ R3 and R4) (Wayne et al., 1991). In spite of this, $ClNO_2$ mixing ratios frequently (on 12 out of 15 measurement days) continued to increase after sunrise (Figures 3A and 4), peaking on average at ~07:45 in the morning approximately 2 hours after sunrise. The median mixing ratio at that time was 6.7 pptv larger than the median value of 5.3 pptv observed at sunrise. The most prominent example of this phenomenon occurred on the morning of July 26. For a two hour period leading up to sunrise, there was fog (virtually ensuring the absence

of N_2O_5), and $ClNO_2$ mixing ratios were < 5 pptv. The fog then dissipated at sunrise. One hour later, $ClNO_2$ mixing ratios increased to > 40 pptv. Similar events (though with more modest $ClNO_2$ increases) were observed on the mornings of July 22, 23, 25, 27, 28, 30, 31, and Aug 1. Two of these (July 23 and 27) overlapped with brief fog events.

Qualitatively similar $ClNO_2$ morning peaks have been observed at other ground sites and were rationalized by vertical mixing (Tham et al., 2016; Bannan et al., 2015; Faxon et al., 2015).

In the period after the $ClNO_2$ morning peak after ~09:00, $ClNO_2$ mixing ratios decreased, coinciding with the increasing $ClNO_2$ photolysis rate. Box model simulations (see S.I.) indicate that the decay of $ClNO_2$ (after 09:00) was consistent with its destruction by photolysis.

There were two exceptions: the mornings of July 27 and Aug 2, when the decay of $ClNO_2$ concentration occurred at a rate faster than its photolysis. On July 27, fog was not observed until 8:00, at which time the $ClNO_2$ mixing ratio rapidly decreased because of dissolution and/or an air mass shift to one with a different chemical history. On Aug 2, the campaign maximum of 97 pptv was observed at 04:40 prior to sunrise, followed by a sharp decline. Hourly logs indicated scattered showers at 06:00.

3.1.5 ~~Aerosol~~ PM_1 size distribution and composition measurements

The time series of ~~submicron~~ PM_1 surface area density (S_A) observed by the SMPS is shown in Figure 5A. The aerosol loadings were modest: the average (median) surface area density was 128 (104) $\mu m^2\ cm^{-3}$ and ranged from extremes of 26 to 618 $\mu m^2\ cm^{-3}$. The size distribution data show that bulk of the surface area (i.e., the mean diameter ($\bar{D}_s$)) is in the range of 200 to 300 nm, such that most of the area of the accumulation mode was captured. However, the surface area calculations do not include contributions from larger diameter particles which were not quantified. Shown on the right hand side of Figure 5A is the rate coefficient for heterogeneous uptake of N_2O_5, $k_{N_2O_5}$ calculated using equation (1~~0~~).

$$k_{N_2O_5} = \frac{1}{4}\gamma \bar{c} S_A \qquad (1~~0~~)$$

Here, γ and $\bar{c}$ are the uptake probability and the mean molecular speed of N_2O_5, respectively. Equation (1) is valid for uptake on small, submicron aerosol as it neglects gas-phase diffusion

limitations (Davidovits et al., 2006). For this calculation, a γ value of 0.025 was assumed. The average (±1 standard deviation) of $k_{N_2O_5}$ was (1.82±1.1)×10^{-4} s^{-1}.

The ACSM submicron aerosol composition data are shown as a time series in Figure 5B and as a function of time of day in Figure 6. Consistent with the size distributions, mass loadings were also modest overall (average 2.3 μg m^{-3}). The ACSM factor analysis identified oxygenated organic aerosol (OOA) as the largest mass fraction of the non-refractory aerosol (average ± standard deviation 1.4±1.2 μg m^{-3}, 63.3% of the total aerosol mass measured by the ACSM). Hydrocarbon-like organic aerosol (HOA) associated with primary emissions was a minor component (average 0.03 μg m^{-3}, 1.1%) but occasionally enhanced in plumes (maximum 8.3 μg m^{-3}).

The oxygenated aerosol fraction (OOA) did not exhibit a discernible diurnal profile (Figure 6A), which is consistent with the modest photochemistry at this site as judged from the modest peak O_3 levels observed.

The inorganic mass fraction was dominated by nitrate (0.47±0.40 μg m^{-3}, 20.7%). The second most abundant inorganic component was ammonium (0.2±1.4 μg m^{-3}, (8.8%) followed by sulfate (0.15±0.15 μg m^{-3}, 6.8%). The data are of similar magnitude as aerosol mass spectrometry (AMS) data collected at nearby Langley as part of Pacific 2001 (Boudries et al., 2004); then, organics had also been the largest component (average of 1.6 μg m^{-3}, 49%), though sulfate and ammonium mass loadings had been larger (0.88 and 0.44 μg m^{-3}, 25% and 14%, respectively) and nitrate mass loadings smaller (0.38 μg m^{-3}, 12%).

The ~~aerosol was frequently neutralized; the~~ neutralization ratio, NR ~~≈~~= $[NH_4^+]$:($[NO_3^-]$+2$[SO_4^{2-}]$) (Zhang et al., 2007), where the square brackets denote molar concentrations (calculated from the mass concentrations reported by the ACSM by dividing by the appropriate molecular weights), was ~~1.38~~ 1.19 (median value). The high NH_3 content is qualitatively consistent with the non-quantitative data collected by Metro Vancouver (using a Thermo Scientific 17i NH_3/NO/NO_2/NO_x analyzer), which showed large concentrations of gas-phase NH_3 (~~data not shown~~Figure S-1).

The ACSM software also ~~identified~~ reported non-refractory chloride with an average (±1 standard deviation) concentration of 0.01±0.03 μg m^{-3}, though it is unclear if this signal was real as it did not vary over the course of the campaign and was below the stated ACSM detection of limit of 0.2 μg m^{-3} (Ng et al., 2011).

Aerosol nitrate exhibited a clear diurnal profile with higher concentrations at night (Figure 6B). In particular, the amount of aerosol nitrate increased at the beginning of the night, when the nocturnal NO_3 production rates were greatest.

Previous AMS measurements in Vancouver during the month of August as part of Pacific 2001 reported a slightly higher total mass loadings of 7.0 μg m^{-3} that included a greater HOA component (2.4 μg m^{-3}, 34%) and a smaller nitrate fraction (0.6 μg m^{-3}, 8.5%) (Alfarra et al., 2004; Jimenez et al., 2009) than observed here. The lower HOA in this data set are likely a result of tighter emission controls implemented since the earlier study, a topic outside the scope of this paper.

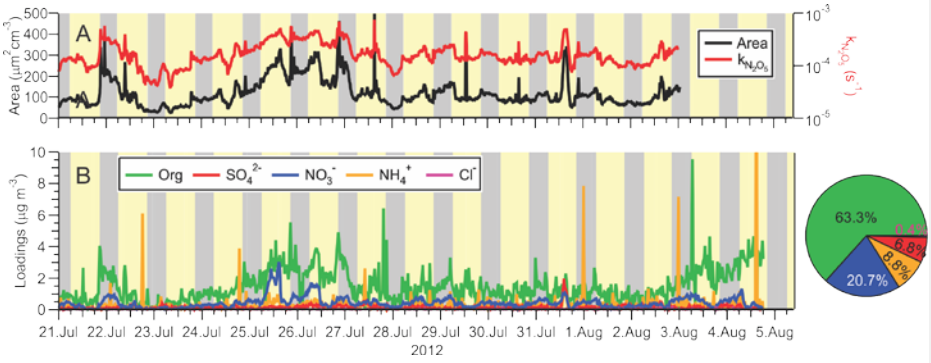

Figure 5. Time series of (A) submicron surface area density measured by the TSI 3034 scanning mobility particle sizer (~~lhs~~left-hand side) and calculate heterogeneous N_2O_5 uptake rate coefficient assuming γ=0.025 (~~rhs~~right-hand side), and (B) non-refractory submicron aerosol species measured by ACSM. The average total loading was 2.3 μg m^{-3}. The pie chart shows the average campaign composition.

609

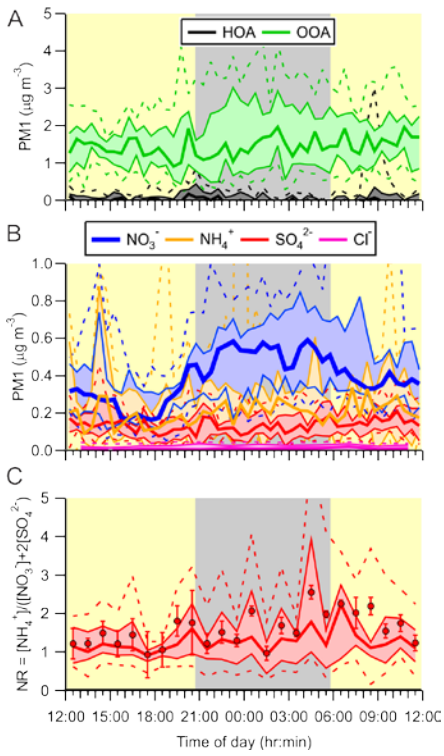

610

611 **Figure 6**. Diurnal averages of submicron (PM1) ~~ACMS~~ACSM data. (**A**). Organic aerosol
612 displayed as hydrocarbon-like organic aerosol (HOA) and oxygenated organic aerosol (OOA)
613 factors. (**B**) Inorganic aerosol fractions. (C) Neutralization ratio (NR).

3.1.6 Hydrocarbon measurements

Mixing ratios of hydrocarbons were quantified during daytime and during the nights of August 2-3 and 3-4. A portion of the hydrocarbon data is shown in Figure 7A.

Mixing ratios were generally smaller during the day than during night, due to the larger daytime mixing heights. On the nights of August 2/3 and 3/4, N_2O_5 was not detected, consistent with low $P(NO_3)$ values as O_3 mixing ratios approached zero (Figure 3). At the same time, there were strong NO_3 sinks present: Mixing ratios of α-pinene and limonene (left-hand axis) increased throughout the night, as thermal emissions continued into the shallow NBL. In contrast, mixing ratios of isoprene, whose emissions are driven by photosynthesis (Hewitt et al., 2011; Guenther et al., 1995), increased at the beginning of the nights and then decreased as isoprene was removed by oxidation with O_3 and NO_3 and by transport. Throughout both nights, the site was also influenced by anthropogenic hydrocarbons (e.g., isooctane and toluene, right-hand axis). Because synoptic conditions as judged from local wind speed and direction (Figure 3D) were similar on most of the other nights when hydrocarbons were not quantified, the data shown in Figure 7A were likely representative for much of the campaign.

The VOC data were not sufficiently comprehensive to allow an accurate determination of the NO_3 loss frequency to hydrocarbons, given by $\Sigma k_{NO3+VOC,i}[VOC]_i$. Shown in Figure 7B is the loss frequency of NO_3 to isoprene, calculated by multiplying its concentration with the NO_3 rate coefficient taken from Seinfeld and Pandis (2006). Loss of NO_3 to isoprene was a small sink compared to its loss to NO via ~~reaction (~~R3~~)~~ and NO_3 photolysis (R4) but ~~is~~ was approximately on par with its indirect loss, i.e., the heterogeneous uptake of N_2O_5 ~~$k_{N_2O_5}$ $K_2[NO_2]$~~.

Formatted: Font: Not Italic

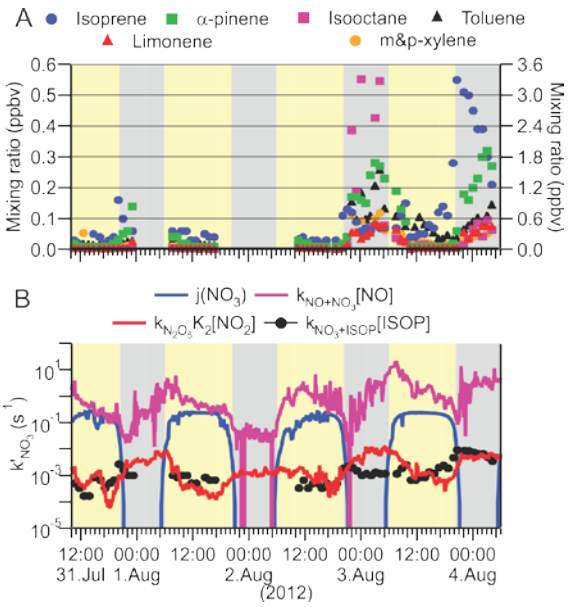

Figure 7. (A) Time series of selected VOC mixing ratios observed on the nights of August 2/3 and August 3/4, 2012. Biogenic VOCs (isoprene, α-pinene and limonene) are shown on the left-hand axis, and anthropogenic VOCs (isooctane, toluene and m&p-xylene) on the right-hand axis. The α-pinene and limonene measurements are semiquantitative. (B) Time series of NO_3 loss rate coefficients. ISOP = isoprene.

3.2 Analysis

3.2.1 Box model simulations of the nocturnal O_3 and O_x loss in the NBL

In initial simulations, the O_3 and NO_2 deposition rates were tuned until the median nocturnal O_x loss was reproduced. An O_3 dry deposition rate of 4×10^{-5} s^{-1} produced a simulation that reasonably matched the observations (Figure S-~~1~~2). The magnitude of this rate corresponds to a NBL height of 50 m, the same mixing height that was frequently observed in balloon vertical profiles reported by Pisano et al. (1997). Modeling studies have assumed N_2O_5 and NO_3 deposition velocities of up to 2 cm s^{-1} in urban areas (Sander and Crutzen, 1996); adopting this value allows the dry deposition rate constants of N_2O_5 and NO_3 to be estimated at ~4×10^{-4} s^{-1}, which is on par with the estimated heterogeneous uptake rate constant of N_2O_5 on submicron aerosol.

Next, the generic biogenic VOC was added. For this, a biogenic hydrocarbon abundance of 1 ppbv at sunset (mostly isoprene – see Figure 7) and a (monoterpene) emission rate of 3×10^5 molecules cm^{-3} s^{-1} based on the crop emission factor given by Guenther et al. (2012) into a 50 m deep NBL were assumed. This assumed flux gives a similar emission rate as the 0.3 ppbv increase over a 6 hour period observed on Aug 3-4 (Figure 7).

The addition of this biogenic VOC only had a marginal effect on O_x ~~and resulted in a slightly better reproduction of the faster O_x loss at the beginning of the night~~ (~~not shown~~Figure S-3).

The simulations presented in Figures S-~~1~~2 underpredict the observed loss of O_3, necessitating the addition of an NO source that results in selective removal of O_3 while preserving O_x. Since automobiles are the largest NO_x source in the region, a constant emission source of 95% NO and 5% NO_2 (Wild et al., 2017) was added and its magnitude varied. The NO_x source strength necessary to reproduce the median O_3 loss was ~1.1 ppbv hr^{-1}. The simulation results using these parameters are superimposed (in red) in Figure 4C. There is reasonable agreement between the simulations and observations of O_x and O_3 until ~3:00 (and between simulation and observation of NO, Figure S-4). ~~, which~~This shows that the nocturnal O_3 and O_x loss can be rationalized without active NO_3 and N_2O_5 chemistry and suggests that NO_3, N_2O_5, and $ClNO_2$ did not contribute significantly to O_x and O_3 loss in the NBL.

3.2.2 Metrics of nocturnal nitrogen oxide chemistry: $P(NO_3)$, $\phi'(ClNO_2)$ and $\tau(N_2O_5)$

Nocturnal N_2O_5 chemistry was analyzed using several common metrics: the rate of NO_3 production by ~~reaction (~~R1~~)~~, $P(NO_3)=k_1[NO_2][O_3]$, the yield of $ClNO_2$ relative to the total amount of NO_3 formed at night, $\phi'(ClNO_2)$, and the steady state lifetime of N_2O_5, $\tau(N_2O_5)$.

The time of day dependence of $P(NO_3)$ is shown in Figure 8A. The NO_3 production rates were small (median values < 0.3 ppbv hr^{-1}) and were larger during the day than at night due to the low O_3 mixing ratios. After midnight, for example, the median $P(NO_3)$ was (55±23) pptv hr^{-1}. These are very modest NO_3 production rates for a site influenced by urban emissions. In a recent study on a mountain top in Hong Kong, for instance, $P(NO_3)$ in excess of 1 ppbv hr^{-1} was observed in polluted air (Brown et al., 2016).

The median integrated nocturnal NO_3 production over the course of the night was 940 pptv (Figure 8A, right hand axis), of which 600 pptv were produced before midnight.

The amount of $ClNO_2$ produced relative to this amount, $\phi'(ClNO_2)$, was very small (median 0.17%, maximum 5.4% on the morning of August 2) and considerably less than reported by our group for Calgary (median 1.0%) (Mielke et al., 2016) and Pasadena, CA (median 12%) (Mielke et al., 2013).

A frequently calculated metric of nighttime nitrogen oxide chemistry ~~are~~ is the steady state lifetimes of NO_3 and N_2O_5, $\tau(NO_3)$ and $\tau(N_2O_5)$ (Aldener et al., 2006; Heintz et al., 1996). The latter is calculated from (Brown et al., 2003; Brown and Stutz, 2012):

$$\tau(N_2O_5) = \frac{[N_2O_5]}{P(NO_3)} = \frac{[N_2O_5]}{k_1[NO_2][O_3]} \approx \left(k_{N_2O_5} + \frac{k_{NO_3}}{K_2[NO_2]} \right)^{-1} \quad (~~11~~2)$$

Here, $k_{N_2O_5}$ and k_{NO_3} are the pseudo-first order loss-rate coefficients of N_2O_5 and NO_3 respectively, and K_2 is the equilibrium constant for equilibrium (R2).

~~The derivation of equation (11~~2~~) is given by *Brown et al.* (2003).~~ A central assumption in this derivation is that NO_3, NO_2, and N_2O_5 more rapidly equilibrate than NO_3 is formed and either NO_3 or N_2O_5 are destroyed, i.e., NO_3+N_2O_5 are assumed to be in steady state with respect to production and loss. Brown et al. (2003) outlined potential pitfalls concerning the validity of the steady state approximation and recommended that box model simulations are carried out

Formatted: Font: Not Italic

to evaluate if a steady state in N_2O_5 can be assumed. Using the median nocturnal NO_2 and O_3 mixing ratios of 7.5 ppbv and 18 to 5.0 ppbv, respectively, a temperature of 286 K, and assumed N_2O_5 and NO_3 pseudo-first order loss frequencies of 1×10^{-3} s^{-1} and between 1×10^{-2} s^{-1} and 0 s^{-1}, the time to achieve steady state in N_2O_5 is 70 min or less (~~data not shown~~see S.I.). Thus, the steady state assumption is reasonable for this data set.

A key parameter in equation ~~11~~ (2) is the strongly temperature dependent equilibrium constant K_2 (Osthoff et al., 2007). At night, the air temperatures during this study were quite warm (median nocturnal minimum of +13 °C) and did not vary a lot between nights (Figure 8B). The warm temperatures shift equilibrium R2 away from N_2O_5 and towards NO_3 and NO_2, making losses via NO_3 (~~reactions~~ R3-R4 and R7) more competitive with the losses of N_2O_5 (that produce $ClNO_2$; R), i.e., the $\frac{k_{NO_3}}{K_2[NO_2]}$ term in equation 11 becomes large relative to $k_{N_2O_5}$. On the other hand, the relatively high NO_2 mixing ratios (median value 7.5±0.8 ppbv) shift the equilibrium towards N_2O_5. Thus, in spite of the relatively warm temperatures, the N_2O_5:NO_3 equilibrium ratios were large on aggregate (>15; Figure 8B), enabling $ClNO_2$ formation via ~~reaction~~ R~~7~~5.

The steady state lifetime of N_2O_5, $\tau(N_2O_5)$, is shown as a diurnal average in Figure 8C. The median $\tau(N_2O_5)$ at night was short (~1 min), and the 90th percentile peaked at a modest 7.6 min at sunrise, considerably shorter than observed above the NBL (Brown et al., 2006b) and at other ground sites (Wood et al., 2005; Crowley et al., 2010; Brown et al., 2016)

Superimposed on the right-hand side of Figure 8C are upper limits to the steady state lifetime of N_2O_5, calculated using the sum of pseudo first-order rate coefficients for the titration of NO_3 by NO ($k_3[NO]$, ~~reaction~~ R3), NO_3 photolysis ($j(NO_3)$, ~~reaction~~ R4), and NO_3 dry deposition ($k_{dep}(NO_3)$), all divided by the N_2O_5 over NO_3 ratio at equilibrium given by K_2NO_2 (Figure 8B), plus the pseudo first-order rate coefficient for N_2O_5 heterogeneous uptake ~~calculated using~~ ($k_{het}(N_2O_5)$, equation (1))~~0, all divided by the N_2O_5 over NO_3 ratio at equilibrium, given by K_2NO_2~~ plus N_2O_5 dry deposition ($k_{dep}(N_2O_5)$)~~(Figure 8B)~~.

$$\tau(N_2O_5) = \left(\frac{k_{NO_3}}{K_2[NO_2]} + k_{N_2O_5}\right)^{-1}$$

$$< \left(\frac{k_3[NO] + j(NO_3) + k_{dep}(NO_3)}{K_2[NO_2]} + k_{het}(N_2O_5) + k_{dep}(N_2O_5)\right)^{-1}$$

$$\tau(N_2O_5) = \left(\frac{k_{NO_3}}{K_2[NO_2]} + k_{N_2O_5}\right)^{-1} < \left(\frac{k_3[NO] + j(NO_3)}{K_2[NO_2]} + k_{N_2O_5}\right)^{-1} \quad (123)$$

The dry deposition rate constants were set to 4×10^{-4} s^{-1} (see section 3.2.1), which likely overestimates dry deposition during the day due to higher mixing heights; however, the error this introduces is negligible compared to the large daytime sinks such as NO_3 photolysis and its reaction with NO. Missing from equation (123) are losses of NO_3 to hydrocarbons (which was omitted because of the poor VOC data coverage) and terms for NO_3 and N_2O_5 dry and wet (i.e., on cloud and rain droplets) deposition. Periods affected by precipitation or fog (shown in Figure 3D) were hence excluded from the calculation.

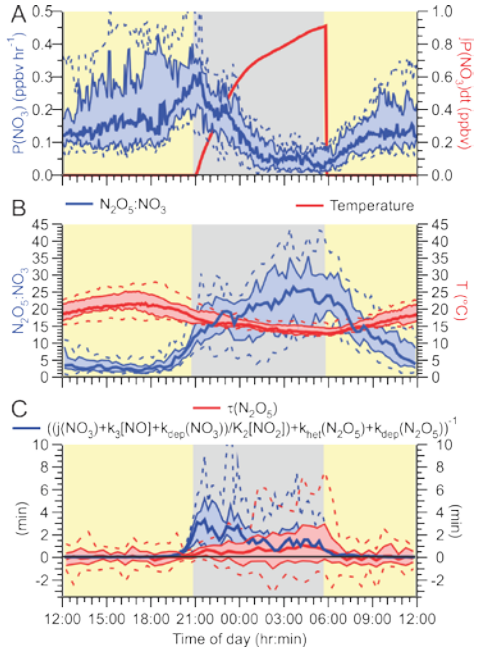

Figure 8. (**A**) NO_3 production rate $P(NO_3) = k_1[NO_2][O_3]$ as a function of time of day. The red line is the total amount NO_3 generated since sunset, $\int P(NO_3)dt$. (**B**) Equilibrium ratio of N_2O_5 to NO_3 calculated by multiplying the temperature-dependent equilibrium constant, K_2, with the NO_2 concentration, $[NO_2]$ (left axis), and air temperature (right axis). (**C**) Steady state lifetime of N_2O_5 (left axis) and upper limits calculated using equation (123) (right axis) as functions of time of day.

The median "observed" $\tau(N_2O_5)$ is below or equal to the upper limit calculation with equation ~~12~~ (3) during both night and day. The largest discrepancy is observed at the beginning of the night, when oxidation of (unsaturated) hydrocarbons by NO_3 (~~reaction~~ R7~~6~~) was likely most significant due to the presence of isoprene. It is also the time when the steady state approximation is most likely invalid.

3.2.3 Heterogeneous conversion of N_2O_5 to $ClNO_2$ on the night of August 1/2

Phillips et al. (2016) recently applied several methods to estimate the N_2O_5 uptake parameter (γ) and yield of $ClNO_2$ (ϕ) from ambient measurements of NO_3, N_2O_5, $ClNO_2$, and aerosol nitrate. One of these methods uses the covariance of $ClNO_2$ and aerosol nitrate production rates, $P(NO_3^-)$ and $P(ClNO_2)$:

$$\phi = 2(P(NO_3^-)/P(ClNO_2) +1)^{-1} \quad (\text{~~15~~}4)$$

$$\gamma = 2(P(NO_3^-)+P(ClNO_2))/(c\ S_A\ [N_2O_5]) \quad (\text{~~16~~}5)$$

In the above equation, c is the mean molecular speed of N_2O_5 ($\approx$ 237 m s^{-1}). The use of equations (~~15-16~~4-5) assumes that the relevant properties of the air mass are conserved (i.e., identical upwind of and at the measurement location and affected identically by air masses mixing), that losses of measured species are not significant, that the efficiency of N_2O_5 uptake and production of $ClNO_2$ and NO_3^- is independent of particle size, and the absence of partitioning of $HNO_{3(g)}$ and aerosol nitrate between the gas and particle phases (Phillips et al., 2016). It is assumed further that production of nitrate from N_2O_5 uptake on refractory aerosol (that the ~~ACMS~~ACSM does not quantify) is minimal.

In this data set, $ClNO_2$ and ~~submicron aerosol~~PM_1 nitrate rarely covaried (Figure 9); the only instance showing a modest correlation (r=0.66) is the time period prior to sunrise of August 2 (shown as red dots in Figure 9).

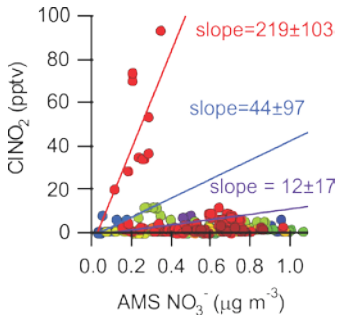

Figure 9. Scatter plot of $ClNO_2$ mixing ratios with submicron (PM_1) ~~ACMS~~ACSM NO_3^- data. The slopes were calculated for three periods: Aug 2, 01:25 – 04:55 (red dots; slope = 219±103; ϕ = 0.72), July 23, 03:00 – 04:25 (blue dots slope = 44±97; ϕ = 0.21), and July 21, 02:25 – 05:20 (purple dots slope = 12±17; ϕ = 0.06).

The night of August 1-2 exhibited the highest nocturnal nitrogen oxide concentrations for the entire campaign. Winds were initially from the NW and relatively light (4.8±0.7 km hr^{-1}) and after 01:00 picked up in speed (to 8~~.2~~±1~~.3~~ km hr^{-1}) and shifted to the W. Judging from the HYbrid Single-Particle Lagrangian Integrated Trajectory (HYSPLIT) back trajectories (Draxler and Rolph, 2013), the upwind air had moved in from the coast, roughly from the direction of the city of Victoria, BC (Odame-Ankrah, 2015).

After sunset at ~21:00 local time, N_2O_5 levels started increasing and continued to increase until about 01:30 (Figure 3A). The steady state N_2O_5 lifetime at this time was the highest of the campaign, ~10 min. At 01:20, $ClNO_2$ mixing ratio increased from 20.4 pptv at 01:25 to 93.7 pptv at 04:55 and the aerosol nitrate content from 0.10 to 0.34 µg m^{-3} (40 to 127 pptv). During this time, N_2O_5 mixing ratios and PM_1 surface area density were relatively constant, 11~~.1~~±6~~.4~~ pptv and 67±4 µg m^{-3} (average ± standard deviation), respectively. The combined amount of N_2O_5, $ClNO_2$ and NO_3^- produced (172 pptv) is less than the amount of NO_3 produced from ~~reaction (~~R1~~)~~ which was 519 pptv during this period.

From equations (~~15~~4) and (~~16~~5), a $ClNO_2$ yield of $\phi = 0.7$~~2~~±0.3~~4~~ and an N_2O_5 uptake probability of γ = 0.15±0.07 were calculated for this period. Both of these values are upper

limits because production of $ClNO_2$ from uptake of N_2O_5 on unquantified supermicron (i.e., > 0.5 μm) or refractory aerosol (which takes place simultaneously) is not accounted for.

A γ value of > 0.05 is greater than can be rationalized from laboratory and field studies (Chang et al., 2011) and is hence unrealistic. This suggests that $ClNO_2$ production took place predominantly on supermicron or refractory aerosol, which likely was comprised of mainly sea salt derived aerosol ~~on this night~~(Anlauf et al., 2006).

On the other hand, if one assumes that all of the $ClNO_2$ is produced on supermicron or refractory aerosol such that P($ClNO_2$) on submicron aerosol equals 0 pptv s^{-1} (which is not unreasonable considering the absence of measurable amounts of aerosol chloride in this size fraction, see section 3.1.5), a γ value of 0.08±0.04 is calculated. This large value suggests very efficient N_2O_5 uptake (and conversion to aerosol nitrate) on the non-refractory submicron aerosol that night.

3.3 Impacts of $ClNO_2$ on radical production

Photolysis of $ClNO_2$ increases the rates of photochemical O_3 production (and hence worsen air quality) by producing NO_2 and reactive Cl atoms (reaction 6). The amounts of $ClNO_2$ available for photolysis in the morning (median 3.5 pptv at sunrise and 6.8 pptv at 08:00 local time) were too small to have had a measurable impact on local NO_2 concentrations (Figure 3C) but were sufficiently large to, at least occasionally, impact radical budgets.

Figure 10 shows the instantaneous radical production rates of Cl and OH, P(Cl)=j($ClNO_2$)×[$ClNO_2$] and P(OH) from reaction of $O(^1D)+H_2O$. The latter was calculated from an assumed steady state in $O(^1D)$ with respect to its production from O_3 photolysis and reactions with N_2, O_2, and H_2O as described by Mielke et al. (2016). This analysis does not account for OH radical production from photolysis of nitrous acid or aldehydes and, hence, overestimates the importance of Cl radicals.

Formatted: Font: Not Italic

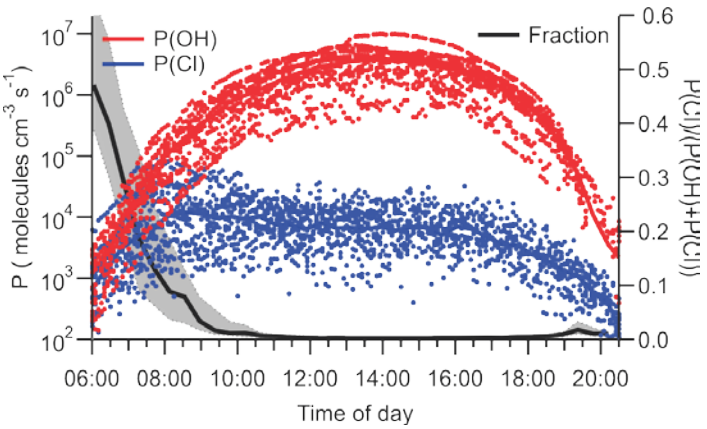

Figure 10. Plots of instantaneous rates of Cl (blue) and OH (red) radical production from $ClNO_2$ photolysis and reaction of O^1D, generated from O_3 photolysis, with H_2O and as a function of time of day. The fraction of radicals produced from $ClNO_2$ photolysis is shown in black. The solid line indicates median values, and shaded areas the 75th and 25th percentiles.

The largest P(Cl) values were observed on July 26, 07:45 local time (9.5×10^4 atoms cm^{-3} s^{-1}), accounting for 40% of the total radical production. The largest fraction of radicals produced from $ClNO_2$ photolysis was observed on the same day at 6:35 local time (74%, 7.8×10^3 atoms cm^{-3} s^{-1}). The photolysis of $ClNO_2$ produces a median value of 6.5×10^3 atoms cm^{-3} s^{-1} during daytime, which is negligibly small compared to the median P(OH) of 3.8×10^6 molecules cm^{-3} s^{-1} at noon.

4 Discussion

It is now well-established that $ClNO_2$ is an abundant nitrogen oxide in many regions of the troposphere (Table 3). The results presented in this paper are atypical in that they show consistently small $ClNO_2$ mixing ratios in spite of close proximity to sources, i.e., in a region where nearby oceanic emissions of sea salt aerosol and NO_x emissions from a megacity combine. In the following, factors contributing to the low $ClNO_2$ mixing ratios observed in this study and broader implications of $ClNO_2$ in the LFV are discussed.

The main reason for the low $ClNO_2$ mixing ratios observed in this work are the low nocturnal mixing ratios of O_3 and small NO_3 production rate, $P(NO_3)$, resulting from the stratification of the boundary layer at night and decoupling of the shallow NBL from the NRL. In the following, it is assumed that a boundary layer structure similar to those observed during PACIFIC 93 (Pisano et al., 1997; McKendry et al., 1997; Hayden et al., 1997) also existed on most measurement nights of this study. Once the nocturnal boundary layer formed at sunset, O_3 and O_x in the NBL were rapidly (lifetime of ~ 4 hours) removed. The box model simulations presented in section 3.2.1 show that this removal can be rationalized by dry deposition and titration of O_3 with NO and biogenic VOCs alone, leaving little room for nitrogen oxide chemistry to destroy O_3 or NO_2, for example, via heterogeneous formation of HONO which destroys NO_2 (Bröske et al., 2003; Stutz et al., 2004a; Indarto, 2012) or formation of N_2O_5 and subsequent heterogeneous hydrolysis which consumes 2 molecules of NO_2 and 1 molecule of O_3 (Brown et al., 2006a). It is the often complete absence of O_3 at night which distinguishes this data set from the other measurement locations for which $ClNO_2$ data have been reported, including continental sites where aerosol chloride is likely less abundant (Table 3).

A compounding factor in this study was the occasional formation of fog and occasional precipitation events. Fog droplets act as a very rapid sink for NO_3 and N_2O_5 (Osthoff et al., 2006), which shuts down $ClNO_2$ production, and may have also directly contributed episodically to $ClNO_2$ losses, for example on the morning of July 27. Overall, though, the contribution of fog to $ClNO_2$ losses in this data set was minor, as only 5% of the measurement period was impacted by fog. However, this potential $ClNO_2$ loss mechanism should be investigated further in future lab studies.

The rapid drop of $ClNO_2$ mixing ratio at around 06:00 of Aug 2 is interesting in that it coincided with a very brief precipitation event. Though an air mass shift cannot be ruled out,

this coincidence suggests the possibility that scavenging of $ClNO_2$ by rain droplets followed by hydrolysis may be a possible loss pathway. Scavenging of NO_3, N_2O_5, and $ClNO_2$ by rain droplets is currently not constrained by laboratory investigations (unlike other gases, such as SO_2 or NH_3 (Hannemann et al., 1995)). Similarly to fog, precipitation was not a major factor in this data set as it affected only 10% but may be in other locations or seasons that experience higher rainfall amounts.

An important observation is the lack of non-refractory ~~submicron aerosol~~PM_1 chloride (Figure 5B). This suggests that there was limited redistribution of chloride from acidification of sea salt aerosol onto other aerosol surfaces in this data set. Such a redistribution was observed, for example, during the Calnex-LA campaign, where the AMS measured a median chloride concentration of ~0.1 µg m^{-3} on non-refractory aerosol (Mielke et al., 2013). This in turn implies that the submicron aerosol surface did not significantly participate in the production of $ClNO_2$ from N_2O_5 uptake in the NBL, broadly consistent with the conclusions in section 3.2.3 and consistent with measurements of water-soluble aerosol components in the LFV during Pacific 2001 (Anlauf et al., 2006) that showed no evidence for chloride redistribution to PM_1 from larger particles where aerosol chloride was present.

The low observed $\tau(N_2O_5)$ levels are consistent with earlier studies that reported strong vertical gradients in $\tau(N_2O_5)$ due to elevated near-surface sinks from emissions by plants (i.e., monoterpenes) and automobiles (i.e., NO and butadiene (Curren et al., 2006)) that titrate NO_3 (Stutz et al., 2004b; Wang et al., 2006; Brown et al., 2007; Young et al., 2012). An emblematic example is the study by Wood et al. (2005) at a ground site east of the San Francisco Bay Area in January 2004: They observed relatively modest N_2O_5 mixing ratios of up to 200 pptv, corresponding to $\tau(N_2O_5) < 5$ min for the entire study period ~~(Wood et al., 2005)~~. Studies for which vertically resolved data were available (e.g., (Stutz et al., 2004b; Wang et al., 2006; Brown et al., 2007; Young et al., 2012; Tsai et al., 2014) generally showed higher N_2O_5 concentrations and hence larger $\tau(N_2O_5)$ aloft in the NRL than at the surface.

A different scenario likely played out aloft in the NRL, which would exhibit higher NO_3 production rates (via reactions 1) than the surface layer. Assuming levels of 20 ppbv of O_3 and NO_2 in the NRL (Pisano et al., 1997; McKendry et al., 1997), the NO_3 production rate would equal ~1.1 ppbv hr^{-1} in the NRL, roughly on par with values recently reported for Hong Kong, the current record holder for $ClNO_2$ mixing ratios (Brown et al., 2016; Wang et al.,

Formatted: Superscript

Formatted: Font: Not Italic

2016). Recent aircraft and tower studies have shown high rates of production of $ClNO_2$ aloft (Riedel et al., 2013; Young et al., 2012), which likely also occurred in this work.

In contrast, the low mixing height of the NBL is conducive to high levels of biogenic hydrocarbons (section 3.1.6). The nocturnal temperatures during this study were quite warm and did not vary a lot between nights (Figure 8B). Emissions of monoterpenes, which are reactive towards NO_3, are driven by a temperature-dependent process from storage tissue within the plants at night (Guenther et al., 1995) and, hence, were likely substantial. Their presence is likely responsible for ~~some of~~ the ~~gap~~ difference between the ~~low~~ "observed" N_2O_5 steady lifetimes, $\tau(N_2O_5)$, ~~compared to the upper limit set by reactions 3-4~~ and upper limit calculated using equation (3) before midnight (Figure 8C). Even if one assumes a relatively large uptake probability of γ=0.025 and accounts for the large ratios of N_2O_5:NO_3, the loss rate of N_2O_5 on submicron aerosol was likely small in comparison to losses via NO_3 for most of this data set (Figure 7B). Hence, only a small fraction of the integrated nocturnal NO_3 production of 940 pptv resulted in $ClNO_2$ formation at the surface.

Because of the relatively long lifetime of $ClNO_2$, the breakdown of the surface layer and merging of the surface air with the NRL constituted itself as a $ClNO_2$ "morning peak" in a similar manner as what has recently been reported at other locations (Tham et al., 2016; Bannan et al., 2015; Faxon et al., 2015). This morning peak is rationalized by higher net $ClNO_2$ production in the NRL; the break-up of this layer ~2 hours after sunrise then mixes $ClNO_2$ down to the surface. Such a vertical mixing process was not seen during Calnex-LA (Young et al., 2012; Tsai et al., 2014) where the NBL was sufficiently deep to prevent complete O_3 removal and the $ClNO_2$ produced mixed down to the surface at night.

Assuming a 100 m deep NRL where $ClNO_2$ production takes place, a mixed layer height of 500 m by 08:00 (Pisano et al., 1997) and negligible destruction of $ClNO_2$ by photolysis (which is reasonable as the lifetime of $ClNO_2$ with respect to photolysis is >4.6 hours at that time of day), a morning increase in $ClNO_2$ mixing ratio by 40 pptv at the surface as seen on the morning of July 26 suggests a pool of $ClNO_2$ in the NRL at sunrise of ~200 pptv, likely a modest value considering that the (assumed) NO_3 production rate may have integrated to ~9 ppbv over the course of the night.

The largest nocturnal $ClNO_2$ mixing ratios were observed on July 22/23 and August 1/2. Both of these nights exhibited high wind speeds and are counterexamples to what was observed on other nights. We speculate that the higher levels of wind shear and turbulence altered the

nocturnal boundary layer structure which exhibited a greater degree of vertical mixing and higher O_3 concentrations at the surface. Consistent with this interpretation and the notion that an isolated NRL with higher net $ClNO_2$ production was absent on those nights, the mornings of July 23 and Aug 2 did not show a "morning peak". In contrast, low surface wind speeds were observed on the other nights, facilitating a stable and shallow nocturnal surface layer.

It is conceivable that a land-sea breeze effect transported air from a region closer to the coast that saw higher $ClNO_2$ production than at Abbotsford, i.e., that the $ClNO_2$ morning peaks are generated by horizontal as opposed to vertical transport. Large NO_3 mixing ratios have been reported at Saturna Island (McLaren et al., 2010), which strongly suggest that sizeable reservoirs of $ClNO_2$ form offshore at night. However, it is known how far inland these reservoirs extend. Considering the average wind speed in the morning (6 km hr^{-1}), distance to the coast (35 km), and close proximity (200 m) of the site to the bottom of the polluted NRL with documented high nocturnal pollution levels and early morning down mixing events, the vertical transport explanation is much more likely correct. Nevertheless, measurements of $ClNO_2$ at a site closer to the coast (e.g., at White Rock) would be beneficial.

Formation of $ClNO_2$ affects air quality through its photolysis which generates O_x, NO_x, and reactive Cl radicals in the morning, leading to higher net photochemical O_3 production (Sarwar et al., 2014). In spite of the low levels of $ClNO_2$ observed in this work, the production of radicals from its photodissociation was not always negligible (Figure 10). Conditions leading to O_3 exceedances did not develop during this study. If such conditions had developed, it is highly likely that this radical generation would have played a much greater role.

The data presented here suggest that higher rates of $ClNO_2$ and subsequent radical generation take place routinely in layers aloft, processes that are not directly observable at the surface but whose implications are felt as the ultimate product, O_3, is sufficiently long-lived to mix down to the surface (McKendry et al., 1997). Future studies should therefore target the NRL, for example through missed-approaches by aircraft, a blimp, or from a tall tower, especially during episodes of a developing O_3 exceedance event and also include composition measurements of refractory aerosol.

5 Summary and conclusions

In this paper, we have presented the first measurements of $ClNO_2$ and N_2O_5 mixing ratios in the LFV. In spite of the close proximity to NO_x (megacity of Vancouver) and sea salt aerosol (the Pacific Ocean) sources, $ClNO_2$ and N_2O_5 mixing ratios were small (maximum of 97 and 27 pptv, respectively) and smaller than observed at other measurement locations for which $ClNO_2$ abundances were reported. The low mixing ratios are explained through the removal of O_3 by deposition and titration with NO in a shallow nocturnal surface layer. Measurements of submicron aerosol composition by ~~ACMS~~ACSM showed no enhancements of particle-phase chloride, which is in contrast to locations where high $ClNO_2$ mixing ratios were observed (such as Pasadena (Mielke et al., 2013)) and indicates that there was little processing and redistribution of sea salt derived chloride at this location. There is indirect evidence that higher production of $ClNO_2$ took place above the measurement site in the NRL, observed via downmixing after the break-up of the NBL in the morning, and highlights the need for future vertically resolved measurements (e.g., from an aircraft platform) of $ClNO_2$ and N_2O_5 mixing ratios in the LFV. Conditions leading to O_3 exceedences did not develop during the relatively short measurement period of 2 weeks, such that the full impact that nocturnal formation of $ClNO_2$ could have on radical production and NO_2 recycling remains unquantified.

Data availability

The data used in this study are available from the corresponding author upon request (hosthoff@ucalgary.ca).

Acknowledgments

This project was undertaken with the financial support of the Government of Canada through the Federal Department of the Environment. Ce projet a été réalisé avec l'appui financier du Gouvernement du Canada agissant par l'entremise du ministère fédéral de l'Environnement. Partial funding for this work was provided by the Natural Sciences and Engineering Research Council of Canada (NSERC) in the form of operating ("Discovery") and Research Tools and Instruments (RTI) grants. The Abbotsford field study was financially supported by a BC Clear research grant from the Fraser Basin Council of British Columbia and by Metro Vancouver.

References

Ainslie, B., and Steyn, D. G.: Spatiotemporal Trends in Episodic Ozone Pollution in the Lower Fraser Valley, British Columbia, in Relation to Mesoscale Atmospheric Circulation Patterns and Emissions, J. Appl. Met. Climatol., 46, 1631-1644, 10.1175/JAM2547.1, 2007.

Ainslie, B., Steyn, D. G., Reuten, C., and Jackson, P. L.: A Retrospective Analysis of Ozone Formation in the Lower Fraser Valley, British Columbia, Canada. Part II: Influence of Emissions Reductions on Ozone Formation, Atmosphere-Ocean, 51, 170-186, 10.1080/07055900.2013.782264, 2013.

Aldener, M., Brown, S. S., Stark, H., Williams, E. J., Lerner, B. M., Kuster, W. C., Goldan, P. D., Quinn, P. K., Bates, T. S., Fehsenfeld, F. C., and Ravishankara, A. R.: Reactivity and loss mechanisms of NO_3 and N_2O_5 in a polluted marine environment: Results from in situ measurements during New England Air Quality Study 2002, J. Geophys. Res., 111, D23S73, doi:10.1029/2006JD007252, 2006.

Alfarra, M. R., Coe, H., Allan, J. D., Bower, K. N., Boudries, H., Canagaratna, M. R., Jimenez, J. L., Jayne, J. T., Garforth, A. A., Li, S.-M., and Worsnop, D. R.: Characterization of urban and rural organic particulate in the Lower Fraser Valley using two Aerodyne Aerosol Mass Spectrometers, Atmos. Environm., 38, 5745-5758, 10.1016/j.atmosenv.2004.01.054, 2004.

Alicke, B., Geyer, A., Hofzumahaus, A., Holland, F., Konrad, S., Patz, H. W., Schafer, J., Stutz, J., Volz-Thomas, A., and Platt, U.: OH formation by HONO photolysis during the BERLIOZ experiment, J. Geophys. Res., 108, 8247, 10.1029/2001JD000579, 2003.

Anlauf, K., Li, S.-M., Leaitch, R., Brook, J., Hayden, K., Toom-Sauntry, D., and Wiebe, A.: Ionic composition and size characteristics of particles in the Lower Fraser Valley: Pacific 2001 field study, Atmos. Environm., 40, 2662-2675, 10.1016/j.atmosenv.2005.12.027, 2006.

Bannan, T. J., Booth, A. M., Bacak, A., Muller, J. B. A., Leather, K. E., Le Breton, M., Jones, B., Young, D., Coe, H., Allan, J., Visser, S., Slowik, J. G., Furger, M., Prévôt, A. S. H., Lee, J., Dunmore, R. E., Hopkins, J. R., Hamilton, J. F., Lewis, A. C., Whalley, L. K., Sharp, T., Stone, D., Heard, D. E., Fleming, Z. L., Leigh, R., Shallcross, D. E., and Percival, C. J.: The first UK measurements of nitryl chloride using a chemical ionization mass spectrometer in central London in the summer of 2012, and an investigation of the role of Cl atom oxidation, J. Geophys. Res., 120, 5638-5657, 10.1002/2014jd022629, 2015.

Bart, M., Williams, D. E., Ainslie, B., McKendry, I., Salmond, J., Grange, S. K., Alavi-Shoshtari, M., Steyn, D., and Henshaw, G. S.: High Density Ozone Monitoring Using Gas Sensitive Semi-Conductor Sensors in the Lower Fraser Valley, British Columbia, Environm. Sci. Technol., 48, 3970-3977, 10.1021/es404610t, 2014.

Behnke, W., George, C., Scheer, V., and Zetzsch, C.: Production and decay of $ClNO_2$, from the reaction of gaseous N_2O_5 with NaCl solution: Bulk and aerosol experiments, J. Geophys. Res., 102, 3795-3804, 10.1029/96JD03057 1997.

Bertram, T. H., and Thornton, J. A.: Toward a general parameterization of N_2O_5 reactivity on aqueous particles: the competing effects of particle liquid water, nitrate and chloride, Atmos. Chem. Phys., 9, 8351-8363, 10.5194/acp-9-8351-2009, 2009.

Biesenthal, T. A., Wu, Q., Shepson, P. B., Wiebe, H. A., Anlauf, K. G., and Mackay, G. I.: A study of relationships between isoprene, its oxidation products, and ozone, in the Lower Fraser Valley, BC, Atmos. Environm., 31, 2049-2058, 10.1016/S1352-2310(96)00318-4, 1997.

Boudries, H., Canagaratna, M. R., Jayne, J. T., Alfarra, M. R., Allan, J., Bower, K. N., Coe, H., Pryor, S. C., Jimenez, J. L., Brook, J. R., Li, S., and Worsnop, D. R.: Chemical and physical processes controlling the distribution of aerosols in the Lower Fraser Valley, Canada,

1040 during the Pacific 2001 field campaign, Atmos. Environm., 38, 5759-5774,
1041 10.1016/j.atmosenv.2004.01.057, 2004.

1042 Brook, J. R., Strawbridge, K. B., Snyder, B. J., Boudries, H., Worsnop, D., Sharma, S.,
1043 Anlauf, K., Lu, G., and Hayden, K.: Towards an understanding of the fine particle variations
1044 in the LFV: integration of chemical, physical and meteorological observations, Atmos.
1045 Environm., 38, 5775-5788, 10.1016/j.atmosenv.2004.01.056, 2004.

1046 Bröske, R., Kleffmann, J., and Wiesen, P.: Heterogeneous conversion of NO_2 on secondary
1047 organic aerosol surfaces: A possible source of nitrous acid (HONO) in the atmosphere?,
1048 Atmos. Chem. Phys., 3, 469-474, 10.5194/acp-3-469-2003, 2003.

1049 Brown, S. S., Stark, H., Ciciora, S. J., and Ravishankara, A. R.: In-situ measurement of
1050 atmospheric NO_3 and N_2O_5 via cavity ring-down spectroscopy, Geophys. Res. Lett., 28, 3227-
1051 3230, 10.1029/2001GL013303, 2001.

1052 Brown, S. S., Stark, H., Ciciora, S. J., McLaughlin, R. J., and Ravishankara, A. R.:
1053 Simultaneous in situ detection of atmospheric NO_3 and N_2O_5 via cavity ring-down
1054 spectroscopy, Rev. Sci. Instrum., 73, 3291-3301, 10.1063/1.1499214, 2002.

1055 Brown, S. S., Stark, H., and Ravishankara, A. R.: Applicability of the steady state
1056 approximation to the interpretation of atmospheric observations of NO_3 and N_2O_5, J.
1057 Geophys. Res., 108, 4539, 10.1029/2003JD003407, 2003.

1058 Brown, S. S., Neuman, J. A., Ryerson, T. B., Trainer, M., Dube, W. P., Holloway, J. S.,
1059 Warneke, C., de Gouw, J. A., Donnelly, S. G., Atlas, E., Matthew, B., Middlebrook, A. M.,
1060 Peltier, R., Weber, R. J., Stohl, A., Meagher, J. F., Fehsenfeld, F. C., and Ravishankara, A. R.:
1061 Nocturnal odd-oxygen budget and its implications for ozone loss in the lower troposphere,
1062 Geophys. Res. Lett., 33, L08801, 10.1029/2006GL025900, 2006a.

1063 Brown, S. S., Ryerson, T. B., Wollny, A. G., Brock, C. A., Peltier, R., Sullivan, A. P., Weber,
1064 R. J., Dube, W. P., Trainer, M., Meagher, J. F., Fehsenfeld, F. C., and Ravishankara, A. R.:
1065 Variability in nocturnal nitrogen oxide processing and its role in regional air quality, Science,
1066 311, 67-70, 10.1126/science.1120120 2006b.

1067 Brown, S. S., Dube, W. P., Osthoff, H. D., Stutz, J., Ryerson, T. B., Wollny, A. G., Brock, C.
1068 A., Warneke, C., De Gouw, J. A., Atlas, E., Neuman, J. A., Holloway, J. S., Lerner, B. M.,
1069 Williams, E. J., Kuster, W. C., Goldan, P. D., Angevine, W. M., Trainer, M., Fehsenfeld, F.
1070 C., and Ravishankara, A. R.: Vertical profiles in NO_3 and N_2O_5 measured from an aircraft:
1071 Results from the NOAA P-3 and surface platforms during the New England Air Quality Study
1072 2004, J. Geophys. Res., 112, D22304, 10.1029/2007JD008883, 2007.

1073 Brown, S. S., and Stutz, J.: Nighttime radical observations and chemistry, Chem. Soc. Rev.,
1074 41, 6405-6447, 10.1039/c2cs35181a, 2012.

1075 Brown, S. S., Thornton, J. A., Keene, W. C., Pszenny, A. A. P., Sive, B. C., Dubé, W. P.,
1076 Wagner, N. L., Young, C. J., Riedel, T. P., Roberts, J. M., VandenBoer, T. C., Bahreini, R.,
1077 Öztürk, F., Middlebrook, A. M., Kim, S., Hübler, G., and Wolfe, D. E.: Nitrogen, Aerosol
1078 Composition, and Halogens on a Tall Tower (NACHTT): Overview of a wintertime air
1079 chemistry field study in the front range urban corridor of Colorado, J. Geophys. Res., 118,
1080 8067-8085, 10.1002/jgrd.50537, 2013.

1081 Brown, S. S., Dubé, W. P., Tham, Y. J., Zha, Q., Xue, L., Poon, S., Wang, Z., Blake, D. R.,
1082 Tsui, W., Parrish, D. D., and Wang, T.: Nighttime chemistry at a high altitude site above
1083 Hong Kong, J. Geophys. Res.-Atmos., 121, 2457-2475, 10.1002/2015jd024566, 2016.

1084 Chang, W. L., Bhave, P. V., Brown, S. S., Riemer, N., Stutz, J., and Dabdub, D.:
1085 Heterogeneous Atmospheric Chemistry, Ambient Measurements, and Model Calculations of

N_2O_5: A Review, Aerosol Sci. Technol., 45, 655 - 685, 10.1080/02786826.2010.551672, 2011.

Crowley, J. N., Schuster, G., Pouvesle, N., Parchatka, U., Fischer, H., Bonn, B., Bingemer, H., and Lelieveld, J.: Nocturnal nitrogen oxides at a rural mountain-site in south-western Germany, Atmos. Chem. Phys., 10, 2795-2812, 10.5194/acp-10-2795-2010, 2010.

Curren, K. C., Dann, T. F., and Wang, D. K.: Ambient air 1,3-butadiene concentrations in Canada (1995–2003): seasonal, day of week variations, trends, and source influences, Atmos. Environm., 40, 170-181, 10.1016/j.atmosenv.2005.09.025, 2006.

Davidovits, P., Kolb, C. E., Williams, L. R., Jayne, J. T., and Worsnop, D. R.: Mass accommodation and chemical reactions at gas-liquid interfaces, Chem. Rev., 106, 1323-1354, 2006.

HYSPLIT (HYbrid Single-Particle Lagrangian Integrated Trajectory) Model access via NOAA ARL READY Website http://ready.arl.noaa.gov/HYSPLIT.php, 2013.

Drewitt, G. B., Curren, K., Steyn, D. G., Gillespie, T. J., and Niki, H.: Measurement of biogenic hydrocarbon emissions from vegetation in the Lower Fraser Valley, British Columbia, Atmos. Environm., 32, 3457-3466, 10.1016/S1352-2310(98)00043-0, 1998.

Dubé, W. P., Brown, S. S., Osthoff, H. D., Nunley, M. R., Ciciora, S. J., Paris, M. W., McLaughlin, R. J., and Ravishankara, A. R.: Aircraft instrument for simultaneous, in situ measurement of NO_3 and N_2O_5 via pulsed cavity ring-down spectroscopy, Rev. Sci. Instrum., 77, 034101, 10.1063/1.2176058, 2006.

Edwards, P. M., Brown, S. S., Roberts, J. M., Ahmadov, R., Banta, R. M., deGouw, J. A., Dube, W. P., Field, R. A., Flynn, J. H., Gilman, J. B., Graus, M., Helmig, D., Koss, A., Langford, A. O., Lefer, B. L., Lerner, B. M., Li, R., Li, S.-M., McKeen, S. A., Murphy, S. M.,

1109 Parrish, D. D., Senff, C. J., Soltis, J., Stutz, J., Sweeney, C., Thompson, C. R., Trainer, M. K.,
1110 Tsai, C., Veres, P. R., Washenfelder, R. A., Warneke, C., Wild, R. J., Young, C. J., Yuan, B.,
1111 and Zamora, R.: High winter ozone pollution from carbonyl photolysis in an oil and gas basin,
1112 Nature, 514, 351-354, 10.1038/nature13767, 2014.

1113 Faxon, C., Bean, J., and Ruiz, L.: Inland Concentrations of Cl_2 and $ClNO_2$ in Southeast Texas
1114 Suggest Chlorine Chemistry Significantly Contributes to Atmospheric Reactivity,
1115 Atmosphere, 6, 1487, 10.3390/atmos6101487, 2015.

1116 Finlayson-Pitts, B. J., Ezell, M. J., and Pitts, J. N.: Formation Of Chemically Active Chlorine
1117 Compounds By Reactions Of Atmospheric NaCl Particles With Gaseous N_2O_5 And $ClONO_2$,
1118 Nature, 337, 241-244, 10.1038/337241a0 1989.

1119 Geyer, A., and Stutz, J.: Vertical profiles of NO_3, N_2O_5, O_3, and NO_x in the nocturnal
1120 boundary layer: 2. Model studies on the altitude dependence of composition and chemistry, J.
1121 Geophys. Res., 109, D12307, doi:12310.11029/12003JD004211, 2004.

1122 Ghosh, B., Papanastasiou, D. K., Talukdar, R. K., Roberts, J. M., and Burkholder, J. B.: Nitryl
1123 Chloride ($ClNO_2$): UV/Vis Absorption Spectrum between 210 and 296 K and $O(^3P)$ Quantum
1124 Yield at 193 and 248 nm, J. Phys. Chem. A, 116, 5796-5805, 10.1021/jp207389y, 2012.

1125 Guenther, A., Hewitt, C. N., Erickson, D., Fall, R., Geron, C., Graedel, T., Harley, P.,
1126 Klinger, L., Lerdau, M., McKay, W. A., Pierce, T., Scholes, B., Steinbrecher, R., Tallamraju,
1127 R., Taylor, J., and Zimmerman, P.: A Global-Model Of Natural Volatile Organic-Compound
1128 Emissions, J. Geophys. Res., 100, 8873-8892, 10.1029/94JD02950, 1995.

1129 Guenther, A. B., Jiang, X., Heald, C. L., Sakulyanontvittaya, T., Duhl, T., Emmons, L. K.,
1130 and Wang, X.: The Model of Emissions of Gases and Aerosols from Nature version 2.1
1131 (MEGAN2.1): an extended and updated framework for modeling biogenic emissions, Geosci.
1132 Model Dev., 5, 1471-1492, 10.5194/gmd-5-1471-2012, 2012.

1133 Gurren, K., Gillespie, T., Steyn, D., Dann, T., and Wang, D.: Biogenic isoprene in the Lower
1134 Fraser Valley, British Columbia, J. Geophys. Res.-Atmos., 103, 25467-25477,
1135 10.1029/98jd01214, 1998.

1136 Hannemann, A. U., Mitra, S. K., and Pruppacher, H. R.: On the scavenging of gaseous
1137 nitrogen compounds by large and small rain drops 1. A wind tunnel and theoretical study of
1138 the uptake and desorption of NH_3 in the presence of CO_2, J. Atmos. Chem., 21, 293-307,
1139 10.1007/bf00696760, 1995.

1140 Hayden, K. L., Anlauf, K. G., Hoff, R. M., Strapp, J. W., Bottenheim, J. W., Wiebe, H. A.,
1141 Froude, F. A., Martin, J. B., Steyn, D. G., and McKendry, I. G.: The vertical chemical and
1142 meteorological structure of the boundary layer in the Lower Fraser Valley during Pacific '93,
1143 Atmos. Environm., 31, 2089-2105, 10.1016/S1352-2310(96)00300-7, 1997.

1144 Hayden, K. L., Anlauf, K. G., Li, S. M., Macdonald, A. M., Bottenheim, J. W., Brook, J. R.,
1145 and Wiebe, H. A.: Characterization of gaseous nitrogen oxides in the Lower Fraser Valley
1146 during Pacific 2001, Atmos. Environm., 38, 5811-5823, 10.1016/j.atmosenv.2003.12.048,
1147 2004.

1148 Heintz, F., Platt, U., Flentje, H., and Dubois, R.: Long-term observation of nitrate radicals at
1149 the Tor station, Kap Arkona (Rugen), J. Geophys. Res., 101, 22891-22910,
1150 10.1029/96JD01549, 1996.

1151 Hewitt, C. N., Ashworth, K., Boynard, A., Guenther, A., Langford, B., MacKenzie, A. R.,
1152 Misztal, P. K., Nemitz, E., Owen, S. M., Possell, M., Pugh, T. A. M., Ryan, A. C., and Wild,
1153 O.: Ground-level ozone influenced by circadian control of isoprene emissions, Nat. Geosci.,
1154 4, 671-674, 10.1038/ngeo1271, 2011.

1155 Hofzumahaus, A., Kraus, A., and Muller, M.: Solar actinic flux spectroradiometry: a
1156 technique for measuring photolysis frequencies in the atmosphere, Appl. Optics, 38, 4443-
1157 4460, 10.1364/AO.38.004443, 1999.

1158 Indarto, A.: Heterogeneous reactions of HONO formation from NO_2 and HNO_3: a review,
1159 Res. Chem. Intermed., 38, 1029-1041, 10.1007/s11164-011-0439-z, 2012.

1160 Jimenez, J. L., Canagaratna, M. R., Donahue, N. M., Prevot, A. S. H., Zhang, Q., Kroll, J. H.,
1161 DeCarlo, P. F., Allan, J. D., Coe, H., Ng, N. L., Aiken, A. C., Docherty, K. S., Ulbrich, I. M.,
1162 Grieshop, A. P., Robinson, A. L., Duplissy, J., Smith, J. D., Wilson, K. R., Lanz, V. A.,
1163 Hueglin, C., Sun, Y. L., Tian, J., Laaksonen, A., Raatikainen, T., Rautiainen, J., Vaattovaara,
1164 P., Ehn, M., Kulmala, M., Tomlinson, J. M., Collins, D. R., Cubison, M. J., E., Dunlea, J.,
1165 Huffman, J. A., Onasch, T. B., Alfarra, M. R., Williams, P. I., Bower, K., Kondo, Y.,
1166 Schneider, J., Drewnick, F., Borrmann, S., Weimer, S., Demerjian, K., Salcedo, D., Cottrell,
1167 L., Griffin, R., Takami, A., Miyoshi, T., Hatakeyama, S., Shimono, A., Sun, J. Y., Zhang, Y.
1168 M., Dzepina, K., Kimmel, J. R., Sueper, D., Jayne, J. T., Herndon, S. C., Trimborn, A. M.,
1169 Williams, L. R., Wood, E. C., Middlebrook, A. M., Kolb, C. E., Baltensperger, U., and
1170 Worsnop, D. R.: Evolution of Organic Aerosols in the Atmosphere, Science, 326, 1525-1529,
1171 10.1126/science.1180353, 2009.

1172 Kercher, J. P., Riedel, T. P., and Thornton, J. A.: Chlorine activation by N_2O_5: simultaneous,
1173 in situ detection of $ClNO_2$ and N_2O_5 by chemical ionization mass spectrometry, Atmospheric
1174 Measurement Techniques, 2, 193-204, 10.5194/amt-2-193-2009, 2009.

1175 Kim, M. J., Farmer, D. K., and Bertram, T. H.: A controlling role for the air-sea interface in
1176 the chemical processing of reactive nitrogen in the coastal marine boundary layer, Proc. Natl.
1177 Acad. Sci. U.S.A., 111, 3943-3948, 10.1073/pnas.1318694111, 2014.

Kleinman, L., Lee, Y.-N., Springston, S. R., Nunnermacker, L., Zhou, X., Brown, R., Hallock, K., Klotz, P., Leahy, D., Lee, J. H., and Newman, L.: Ozone formation at a rural site in the southeastern United States, J. Geophys. Res.-Atmos., 99, 3469-3482, 10.1029/93jd02991, 1994.

Knipping, E. M., and Dabdub, D.: Impact of chlorine emissions from sea-salt aerosol on coastal urban ozone, Environm. Sci. Technol., 37, 275-284, 10.1021/es025793z 2003.

Koehler, G., and Wassenaar, L. I.: The stable isotopic composition ($^{37}Cl/^{35}Cl$) of dissolved chloride in rainwater, Applied Geochemistry, 25, 91-96, 10.1016/j.apgeochem.2009.10.004, 2010.

Lin, C. H., Lai, C. H., Wu, Y. L., and Chen, M. J.: Simple model for estimating dry deposition velocity of ozone and its destruction in a polluted nocturnal boundary layer, Atmos. Environm., 44, 4364-4371, 10.1016/j.atmosenv.2010.07.053, 2010.

Logan, J. A.: Ozone in rural areas of the United States, J. Geophys. Res.-Atmos., 94, 8511-8532, 10.1029/JD094iD06p08511, 1989.

Madronich, S., and Flocke, S.: Theoretical Estimation of Biologically Effective UV Radiation at the Earth's Surface, in: Solar Ultraviolet Radiation, edited by: Zerefos, C., and Bais, A., NATO ASI Series, Springer Berlin Heidelberg, 23-48, 1997.

McKendry, I. G., Steyn, D. G., Lundgren, J., Hoff, R. M., Strapp, W., Anlauf, K., Froude, F., Martin, J. B., Banta, R. M., and Olivier, L. D.: Elevated ozone layers and vertical down-mixing over the Lower Fraser Valley, BC, Atmos. Environm., 31, 2135-2146, 10.1016/S1352-2310(96)00127-6, 1997.

McLaren, R., Salmon, R. A., Liggio, J., Hayden, K. L., Anlauf, K. G., and Leaitch, W. R.: Nighttime chemistry at a rural site in the Lower Fraser Valley, Atmos. Environm., 38, 5837-5848, 10.1016/j.atmosenv.2004.03.074, 2004.

McLaren, R., Wojtal, P., Majonis, D., McCourt, J., Halla, J. D., and Brook, J.: NO_3 radical measurements in a polluted marine environment: links to ozone formation, Atmos. Chem. Phys., 10, 4187-4206, 10.5194/acp-10-4187-2010, 2010.

Mielke, L. H., Furgeson, A., and Osthoff, H. D.: Observation of $ClNO_2$ in a mid-continental urban environment, Environm. Sci. Technol., 45, 8889-8896, 10.1021/es201955u, 2011.

Mielke, L. H., and Osthoff, H. D.: On quantitative measurements of peroxycarboxylic nitric anhydride mixing ratios by thermal dissociation chemical ionization mass spectrometry, Int. J. Mass Spectrom., 310, 1-9, 10.1016/j.ijms.2011.10.005, 2012.

Mielke, L. H., Stutz, J., Tsai, C., Hurlock, S. C., Roberts, J. M., Veres, P. R., Froyd, K. D., Hayes, P. L., Cubison, M. J., Jimenez, J. L., Washenfelder, R. A., Young, C. J., Gilman, J. B., de Gouw, J. A., Flynn, J. H., Grossberg, N., Lefer, B. L., Liu, J., Weber, R. J., and Osthoff, H. D.: Heterogeneous formation of nitryl chloride and its role as a nocturnal NO_x reservoir species during CalNex-LA 2010, J. Geophys. Res., 118, 10638-10652, 10.1002/jgrd.50783, 2013.

Mielke, L. H., Furgeson, A., Odame-Ankrah, C. A., and Osthoff, H. D.: Ubiquity of $ClNO_2$ in the nocturnal boundary layer of Calgary, AB, Canada, Canadian Journal of Chemistry, 94, 414-423, 10.1139/cjc-2015-0426, 2016.

Neu, U., Kunzle, T., and Wanner, H.: On the relation between ozone storage in the residual layer and daily variation in near-surface ozone concentration — A case study, Bound.-Layer Meteor., 69, 221-247, 10.1007/bf00708857, 1994.

Ng, N. L., Herndon, S. C., Trimborn, A., Canagaratna, M. R., Croteau, P. L., Onasch, T. B., Sueper, D., Worsnop, D. R., Zhang, Q., Sun, Y. L., and Jayne, J. T.: An Aerosol Chemical Speciation Monitor (ACSM) for Routine Monitoring of the Composition and Mass Concentrations of Ambient Aerosol, Aerosol Sci. Technol., 45, 780-794, 10.1080/02786826.2011.560211, 2011.

Odame-Ankrah, C. A., and Osthoff, H. D.: A compact diode laser cavity ring-down spectrometer for atmospheric measurements of NO_3 and N_2O_5 with automated zeroing and calibration, Appl. Spectrosc., 65, 1260-1268, 10.1366/11-06384, 2011.

Odame-Ankrah, C. A.: Improved detection instrument for nitrogen oxide species, Ph.D., Chemistry, University of Calgary, http://hdl.handle.net/11023/2006, Calgary, 2015.

Osthoff, H. D., Sommariva, R., Baynard, T., Pettersson, A., Williams, E. J., Lerner, B. M., Roberts, J. M., Stark, H., Goldan, P. D., Kuster, W. C., Bates, T. S., Coffman, D., Ravishankara, A. R., and Brown, S. S.: Observation of daytime N_2O_5 in the marine boundary layer during New England Air Quality Study - Intercontinental Transport and Chemical Transformation 2004, J. Geophys. Res., 111, D23S14, doi:10.1029/2006JD007593., 2006.

Osthoff, H. D., Pilling, M. J., Ravishankara, A. R., and Brown, S. S.: Temperature dependence of the NO_3 absorption cross-section above 298 K and determination of the equilibrium constant for NO_3+NO_2 <-> N_2O_5 at atmospherically relevant conditions, Phys. Chem. Chem. Phys., 9, 5785-5793, 10.1039/b709193a, 2007.

Osthoff, H. D., Roberts, J. M., Ravishankara, A. R., Williams, E. J., Lerner, B. M., Sommariva, R., Bates, T. S., Coffman, D., Quinn, P. K., Stark, H., Burkholder, J. B., Talukdar, R. K., Meagher, J., Fehsenfeld, F. C., and Brown, S. S.: High levels of nitryl chloride in the polluted subtropical marine boundary layer, Nat. Geosci., 1, 324-328, 10.1038/ngeo177, 2008.

1246 Paul, D., Furgeson, A., and Osthoff, H. D.: Measurement of total alkyl and peroxy nitrates by
1247 thermal decomposition cavity ring-down spectroscopy, Rev. Sci. Instrum., 80, 114101,
1248 10.1063/1.3258204 2009.

1249 Paul, D., and Osthoff, H. D.: Absolute Measurements of Total Peroxy Nitrate Mixing Ratios
1250 by Thermal Dissociation Blue Diode Laser Cavity Ring-Down Spectroscopy, Anal. Chem.,
1251 82, 6695-6703, 10.1021/ac101441z, 2010.

1252 Phillips, G. J., Tang, M. J., Thieser, J., Brickwedde, B., Schuster, G., Bohn, B., Lelieveld, J.,
1253 and Crowley, J. N.: Significant concentrations of nitryl chloride observed in rural continental
1254 Europe associated with the influence of sea salt chloride and anthropogenic emissions,
1255 Geophys. Res. Lett., 39, L10811, 10.1029/2012gl051912, 2012.

1256 Phillips, G. J., Thieser, J., Tang, M. J., Sobanski, N., Schuster, G., Fachinger, J., Drewnick,
1257 F., Borrmann, S., Bingemer, H., Lelieveld, J., and Crowley, J. N.: Estimating N_2O_5 uptake
1258 coefficients using ambient measurements of NO_3, N_2O_5, $ClNO_2$ and particle-phase nitrate,
1259 Atmos. Chem. Phys., 16, 13231-13249, 10.5194/acp-16-13231-2016, 2016.

1260 Pisano, J. T., McKendry, I., Steyn, D. G., and Hastie, D. R.: Vertical nitrogen dioxide and
1261 ozone concentrations measured from a tethered balloon in the Lower Fraser Valley, Atmos.
1262 Environm., 31, 2071-2078, 10.1016/S1352-2310(96)00146-X, 1997.

1263 Pryor, S. C., Barthelmie, R. J., Hoff, R. M., Sakiyama, S., Simpson, R., and Steyn, D.:
1264 REVEAL: Characterizing fine aerosols in the Fraser Valley, BC, Atmosphere-Ocean, 35,
1265 209-227, 10.1080/07055900.1997.9649592, 1997.

1266 Pryor, S. C., and Barthelmie, R. J.: REVEAL II: Seasonality and spatial variability of particle
1267 and visibility conditions in the Fraser Valley, Sci. Tot. Environm., 257, 95-110,
1268 10.1016/S0048-9697(00)00490-3, 2000.

1269 Pryor, S. C., Barthelmie, R. J., Schoof, J. T., Binkowski, F. S., Delle Monache, L., and Stull,
1270 R.: Modeling the impact of sea-spray on particle concentrations in a coastal city, Sci. Tot.
1271 Environm., 391, 132-142, 10.1016/j.scitotenv.2007.10.059, 2008.

1272 Raff, J. D., Njegic, B., Chang, W. L., Gordon, M. S., Dabdub, D., Gerber, R. B., and
1273 Finlayson-Pitts, B. J.: Chlorine activation indoors and outdoors via surface-mediated reactions
1274 of nitrogen oxides with hydrogen chloride, Proc. Natl. Acad. Sci. U.S.A., 106, 13647-13654,
1275 10.1073/pnas.0904195106, 2009.

1276 Riedel, T. P., Bertram, T. H., Crisp, T. A., Williams, E. J., Lerner, B. M., Vlasenko, A., Li,
1277 S.-M., Gilman, J. B., de Gouw, J., Bon, D. M., Wagner, N. L., Brown, S. S., and Thornton, J.
1278 A.: Nitryl Chloride and Molecular Chlorine in the Coastal Marine Boundary Layer,
1279 Environm. Sci. Technol., 46, 10463-10470, 10.1021/es204632r, 2012a.

1280 Riedel, T. P., Bertram, T. H., Ryder, O. S., Liu, S., Day, D. A., Russell, L. M., Gaston, C. J.,
1281 Prather, K. A., and Thornton, J. A.: Direct N_2O_5 reactivity measurements at a polluted coastal
1282 site, Atmos. Chem. Phys., 12, 2959-2968, 10.5194/acp-12-2959-2012, 2012b.

1283 Riedel, T. P., Wagner, N. L., Dubé, W. P., Middlebrook, A. M., Young, C. J., Öztürk, F.,
1284 Bahreini, R., VandenBoer, T. C., Wolfe, D. E., Williams, E. J., Roberts, J. M., Brown, S. S.,
1285 and Thornton, J. A.: Chlorine activation within urban or power plant plumes: Vertically
1286 resolved $ClNO_2$ and Cl_2 measurements from a tall tower in a polluted continental setting, J.
1287 Geophys. Res., 118, 8702-8715, 10.1002/jgrd.50637, 2013.

1288 Roberts, J. M., Osthoff, H. D., Brown, S. S., Ravishankara, A. R., Coffman, D., Quinn, P. K.,
1289 and Bates, T. S.: Laboratory Studies of Products of N_2O_5 Uptake on Cl^- Containing
1290 Substrates, Geophys. Res. Lett., 36, L20808, 10.1029/2009GL040448, 2009.

1291 Ryder, O. S., Ault, A. P., Cahill, J. F., Guasco, T. L., Riedel, T. P., Cuadra-Rodriguez, L. A.,
1292 Gaston, C. J., Fitzgerald, E., Lee, C., Prather, K. A., and Bertram, T. H.: On the Role of

Particle Inorganic Mixing State in the Reactive Uptake of N_2O_5 to Ambient Aerosol Particles, Environm. Sci. Technol., 48, 1618-1627, 10.1021/es4042622, 2014.

Ryder, O. S., Campbell, N. R., Morris, H., Forestieri, S., Ruppel, M. J., Cappa, C., Tivanski, A., Prather, K., and Bertram, T. H.: Role of Organic Coatings in Regulating N_2O_5 Reactive Uptake to Sea Spray Aerosol, J. Phys. Chem. A, 119, 11683-11692, 10.1021/acs.jpca.5b08892, 2015a.

Ryder, O. S., Campbell, N. R., Shaloski, M., Al-Mashat, H., Nathanson, G. M., and Bertram, T. H.: Role of Organics in Regulating $ClNO_2$ Production at the Air–Sea Interface, J. Phys. Chem. A, 119, 8519-8526, 10.1021/jp5129673, 2015b.

Sander, R., and Crutzen, P. J.: Model study indicating halogen activation and ozone destruction in polluted air masses transported to the sea, J. Geophys. Res., 101, 9121-9138, 10.1029/95JD03793, 1996.

Sander, S. P., Abbatt, J. P. D., Barker, J. R., Burkholder, J. B., Friedl, R. R., Golden, D. M., Huie, R. E., Kolb, C. E., Kurylo, M. J., Moortgat, G. K., Orkin, V. L., and Wine, P. H.: Chemical Kinetics and Photochemical Data for Use in Atmospheric Studies, Evaluation No. 17, JPL Publication 10-6, Jet Propulsion Laboratory, Pasadena, CA, 2010.

Sarwar, G., Simon, H., Xing, J., and Mathur, R.: Importance of tropospheric $ClNO_2$ chemistry across the Northern Hemisphere, Geophys. Res. Lett., 41, 4050-4058, 10.1002/2014gl059962, 2014.

Seinfeld, J. H., and Pandis, S. N.: Atmospheric chemistry and physics: from air pollution to climate change, 2nd ed., Wiley, Hoboken, N.J., 2006.

Simpson, W. R.: Continuous wave cavity ring-down spectroscopy applied to in situ detection of dinitrogen pentoxide (N_2O_5), Rev. Sci. Instrum., 74, 3442-3452, 10.1063/1.1578705, 2003.

1316 Slusher, D. L., Huey, L. G., Tanner, D. J., Flocke, F. M., and Roberts, J. M.: A thermal
1317 dissociation-chemical ionization mass spectrometry (TD-CIMS) technique for the
1318 simultaneous measurement of peroxyacyl nitrates and dinitrogen pentoxide, J. Geophys. Res.,
1319 109, D19315, 10.1029/2004JD004670, 2004.

1320 Steyn, D. G., Bottenheim, J. W., and Thomson, R. B.: Overview of tropospheric ozone in the
1321 Lower Fraser Valley, and the Pacific '93 field study, Atmos. Environm., 31, 2025-2035,
1322 10.1016/S1352-2310(97)00018-6, 1997.

1323 Stutz, J., Alicke, B., Ackermann, R., Geyer, A., Wang, S. H., White, A. B., Williams, E. J.,
1324 Spicer, C. W., and Fast, J. D.: Relative humidity dependence of HONO chemistry in urban
1325 areas, J. Geophys. Res., 109, D03307, 10.1029/2003JD004135, 2004a.

1326 Stutz, J., Alicke, B., Ackermann, R., Geyer, A., White, A., and Williams, E.: Vertical profiles
1327 of NO_3, N_2O_5, O_3, and NO_x in the nocturnal boundary layer: 1. Observations during the Texas
1328 Air Quality Study 2000, J. Geophys. Res., 109, D12306, doi:12310.11029/12003JD004209,
1329 2004b.

1330 Talbot, R., Mao, H. T., and Sive, B.: Diurnal characteristics of surface level O_3 and other
1331 important trace gases in New England, J. Geophys. Res., 110, D09307,
1332 doi:09310.01029/02004JD005449, 2005.

1333 Tanaka, P. L., Riemer, D. D., Chang, S. H., Yarwood, G., McDonald-Buller, E. C., Apel, E.
1334 C., Orlando, J. J., Silva, P. J., Jimenez, J. L., Canagaratna, M. R., Neece, J. D., Mullins, C. B.,
1335 and Allen, D. T.: Direct evidence for chlorine-enhanced urban ozone formation in Houston,
1336 Texas, Atmos. Environm., 37, 1393-1400, 10.1016/S1352-2310(02)01007-5 2003.

1337 Thaler, R. D., Mielke, L. H., and Osthoff, H. D.: Quantification of Nitryl Chloride at Part Per
1338 Trillion Mixing Ratios by Thermal Dissociation Cavity Ring-Down Spectroscopy, Anal.
1339 Chem., 83, 2761-2766, 10.1021/ac200055z, 2011.

1340 Tham, Y., Yan, C., Xue, L., Zha, Q., Wang, X., and Wang, T.: Presence of high nitryl
1341 chloride in Asian coastal environment and its impact on atmospheric photochemistry, Chin.
1342 Sci. Bull., 59, 356-359, 10.1007/s11434-013-0063-y, 2014.

1343 Tham, Y. J., Wang, Z., Li, Q., Yun, H., Wang, W., Wang, X., Xue, L., Lu, K., Ma, N., Bohn,
1344 B., Li, X., Kecorius, S., Größ, J., Shao, M., Wiedensohler, A., Zhang, Y., and Wang, T.:
1345 Significant concentrations of nitryl chloride sustained in the morning: investigations of the
1346 causes and impacts on ozone production in a polluted region of northern China, Atmos.
1347 Chem. Phys., 16, 14959-14977, 10.5194/acp-16-14959-2016, 2016.

1348 Thieser, J., Schuster, G., Schuladen, J., Phillips, G. J., Reiffs, A., Parchatka, U., Pöhler, D.,
1349 Lelieveld, J., and Crowley, J. N.: A two-channel thermal dissociation cavity ring-down
1350 spectrometer for the detection of ambient NO2, RO2NO2 and RONO2, Atmos. Meas. Tech.,
1351 9, 553-576, 10.5194/amt-9-553-2016, 2016.

1352 Thornton, J. A., Kercher, J. P., Riedel, T. P., Wagner, N. L., Cozic, J., Holloway, J. S., Dube,
1353 W. P., Wolfe, G. M., Quinn, P. K., Middlebrook, A. M., Alexander, B., and Brown, S. S.: A
1354 large atomic chlorine source inferred from mid-continental reactive nitrogen chemistry,
1355 Nature, 464, 271-274, 10.1038/nature08905, 2010.

1356 Tokarek, T. W., Huo, J. A., Odame-Ankrah, C. A., Hammoud, D., Taha, Y. M., and Osthoff,
1357 H. D.: A gas chromatograph for quantification of peroxycarboxylic nitric anhydrides
1358 calibrated by thermal dissociation cavity ring-down spectroscopy, Atmos. Meas. Tech., 7,
1359 3263-3283, 10.5194/amt-7-3263-2014, 2014.

1360 Trainer, M., Williams, E. J., Parrish, D. D., Buhr, M. P., Allwine, E. J., Westberg, H. H.,
1361 Fehsenfeld, F. C., and Liu, S. C.: Models and observations of the impact of natural
1362 hydrocarbons on rural ozone, Nature, 329, 705-707, 10.1038/329705a0, 1987.

Tsai, C., Wong, C., Hurlock, S., Pikelnaya, O., Mielke, L. H., Osthoff, H. D., Flynn, J. H., Haman, C., Lefer, B., Gilman, J., de Gouw, J., and Stutz, J.: Nocturnal loss of NO_x during the 2010 CalNex-LA study in the Los Angeles Basin, J. Geophys. Res., 119, 13004–13025 10.1002/2014jd022171, 2014.

Vingarzan, R., and Li, S. M.: The Pacific 2001 Air Quality Study - synthesis of findings and policy implications, Atmos. Environm., 40, 2637-2649, 10.1016/j.atmosenv.2005.09.083, 2006.

Volpe, C., Wahlen, M., Pszenny, A. A. P., and Spivack, A. J.: Chlorine isotopic composition of marine aerosols: Implications for the release of reactive chlorine and HCl cycling rates, Geophys. Res. Lett., 25, 3831-3834, 10.1029/1998gl900038, 1998.

Wagner, N. L., Dube, W. P., Washenfelder, R. A., Young, C. J., Pollack, I. B., Ryerson, T. B., and Brown, S. S.: Diode laser-based cavity ring-down instrument for NO_3, N_2O_5, NO, NO_2 and O_3 from aircraft, Atmospheric Measurement Techniques, 4, 1227-1240, 10.5194/amt-4-1227-2011, 2011.

Wang, S., Ackermann, R., and Stutz, J.: Vertical profiles of O_3 and NO_x chemistry in the polluted nocturnal boundary layer in Phoenix, AZ: I. Field observations by long-path DOAS, Atmos. Chem. Phys., 6, 2671-2693, 10.5194/acp-6-2671-2006, 2006.

Wang, T., Tham, Y. J., Xue, L., Li, Q., Zha, Q., Wang, Z., Poon, S. C. N., Dubé, W. P., Blake, D. R., Louie, P. K. K., Luk, C. W. Y., Tsui, W., and Brown, S. S.: Observations of nitryl chloride and modeling its source and effect on ozone in the planetary boundary layer of southern China, J. Geophys. Res.-Atmos., 121, 2476-2489, 10.1002/2015jd024556, 2016.

Wang, X., Wang, H., Xue, L., Wang, T., Wang, L., Gu, R., Wang, W., Tham, Y. J., Wang, Z., Yang, L., Chen, J., and Wang, W.: Observations of N_2O_5 and $ClNO_2$ at a polluted urban

surface site in North China: High N_2O_5 uptake coefficients and low $ClNO_2$ product yields, Atmos. Environm., 156, 125-134, 10.1016/j.atmosenv.2017.02.035, 2017.

Wayne, R. P., Barnes, I., Biggs, P., Burrows, J. P., Canosamas, C. E., Hjorth, J., Lebras, G., Moortgat, G. K., Perner, D., Poulet, G., Restelli, G., and Sidebottom, H.: The Nitrate Radical - Physics, Chemistry, and the Atmosphere, Atmos. Environm. A, 25, 1-203, 10.1016/0960-1686(91)90192-A, 1991.

Wieser, M. E., and Berglund, M.: Atomic weights of the elements 2007 (IUPAC Technical Report), Pure Appl. Chem., 81, 2131-2156, 10.1351/pac-rep-09-08-03, 2009.

Wild, R. J., Dubé, W. P., Aikin, K. C., Eilerman, S. J., Neuman, J. A., Peischl, J., Ryerson, T. B., and Brown, S. S.: On-road measurements of vehicle NO_2/NO_x emission ratios in Denver, Colorado, USA, Atmos. Environm., 148, 182-189, 10.1016/j.atmosenv.2016.10.039, 2017.

Wood, E. C., Bertram, T. H., Wooldridge, P. J., and Cohen, R. C.: Measurements of N_2O_5, NO_2, and O_3 east of the San Francisco Bay, Atmos. Chem. Phys., 5, 483-491, 10.5194/acp-5-483-2005, 2005.

Young, C. J., Washenfelder, R. A., Roberts, J. M., Mielke, L. H., Osthoff, H. D., Tsai, C., Pikelnaya, O., Stutz, J., Veres, P. R., Cochran, A. K., VandenBoer, T. C., Flynn, J., Grossberg, N., Haman, C. L., Lefer, B., Stark, H., Graus, M., de Gouw, J., Gilman, J. B., Kuster, W. C., and Brown, S. S.: Vertically Resolved Measurements of Nighttime Radical Reservoirs in Los Angeles and Their Contribution to the Urban Radical Budget, Environm. Sci. Technol., 46, 10965-10973, 10.1021/es302206a, 2012.

Young, C. J., Washenfelder, R. A., Edwards, P. M., Parrish, D. D., Gilman, J. B., Kuster, W. C., Mielke, L. H., Osthoff, H. D., Tsai, C., Pikelnaya, O., Stutz, J., Veres, P. R., Roberts, J. M., Griffith, S., Dusanter, S., Stevens, P. S., Flynn, J., Grossberg, N., Lefer, B., Holloway, J. S., Peischl, J., Ryerson, T. B., Atlas, E. L., Blake, D. R., and Brown, S. S.: Chlorine as a

primary radical: evaluation of methods to understand its role in initiation of oxidative cycles, Atmos. Chem. Phys., 14, 3427-3440, 10.5194/acp-14-3427-2014, 2014.

Zhang, Q., Jimenez, J. L., Worsnop, D. R., and Canagaratna, M.: A case study of urban particle acidity and its influence on secondary organic aerosol, Environm. Sci. Technol., 41, 3213-3219, 10.1021/es061812j, 2007.

Formatted: Justified, Indent: Left: 0 cm, Hanging: 0.5 cm, Space Before: 6 pt, Line spacing: 1.5 lines

Table 1. Summary of measurement techniques deployed at T45 during the study.

Species or parameter	Method	Uncer-tainty	Time resolution
$ClNO_2$, PAN, PPN	Chemical ionization mass spectrometry (Mielke et al., 2011)	±25% ±10%	30 s
N_2O_5	Red diode laser cavity ring-down spectroscopy (Odame-Ankrah and Osthoff, 2011)	±25%	1 s
O_3	UV absorption (Thermo 49i)	±10%	10 s
NO/NO_y	O_3-Chemiluminescence (Thermo 42i-Y) with heated Mo converter; operated with inlet filter	±30%	10 s
NO_2	Blue diode laser cavity ring-down spectroscopy (Paul and Osthoff, 2010)	±10%	1 s
PAN, PPN	Gas chromatography with electron capture detection (Tokarek et al., 2014)	±10%	6 min
Photolysis frequencies	Spectral radiometry (Metcon)	±20%	10 s
Aerosol size distribution	Scanning mobility particle sizer (SMPS)		nd
Aerosol composition	Aerosol Chemical Speciation Monitor (ACSM)	±20%	30 min
VOCs	Agilent	±30%	20 min (1 hr*)
Meteorological data	Various		

* Sampled for 20 min within a 1 hour time period

Table 2. Ratios of up- to down-~~dwelling~~welling photolysis frequencies.

Frequency	Ratio
$j(NO_3)$	0.27±0.04
$j(NO_2)$	0.15±0.03
$j(ClNO_2)$	0.14±0.02
$j(O_3 \rightarrow O(^1D))$	0.11±0.02

1421 **Table 3**. Maximum $ClNO_2$ mixing ratios observed to date.

Location	Type	Maximum mixing ratio	Reference(s)
Houston, TX	Off-shore, costal, and inland	1.2 ppbv	(Osthoff et al., 2008)
New England	Off-shore	90 pptv	(Kercher et al., 2009)
Pasadena, CA	Off-shore	2.15 ppbv	(Riedel et al., 2012a)
La Jolla, CA	Coastal	30 pptv	(Kim et al., 2014)
Boulder, CO	Continental	425 pptv	(Thornton et al., 2010)
Calgary, AB	Continental	330 pptv	(Mielke et al., 2016; Mielke et al., 2011)
Erie, CO	Continental	1.3 ppbv	(Riedel et al., 2013; Brown et al., 2013)
Feldberg, GER	Continental	800 pptv	(Phillips et al., 2012; Phillips et al., 2016)
Horsepool, UT	Continental	500 pptv	(Edwards et al., 2014)
Pasadena, CA	Coastal, inland	3.5 ppbv	(Mielke et al., 2013)
London, UK	Coastal, inland	724 pptv	(Bannan et al., 2015)
Hongkong, PRC	Coastal, inland	2.0 ppbv	(Tham et al., 2014)
Southeast TX	Coastal, inland	280 pptv	(Faxon et al., 2015)
Hongkong, PRC	Coastal, inland	4.7 ppbv	(Wang et al., 2016)
North China Plain	Continental	2.1 ppbv	(Tham et al., 2016)
North China Plain	Continental	776 pptv	(Wang et al., 2017)
Abbotsford, BC	Coastal, inland	97 pptv	This work

1422

Supplemental information for

Low levels of nitryl chloride at ground level: Nocturnal nitrogen oxides in the Lower Fraser Valley of British Columbia

H. D. Osthoff[1], C. A. Odame-Ankrah[1], Y. M. Taha[1], T. W. Tokarek[1], C. L. Schiller[2], D. Haga[3], K. Jones[2], and R. Vingarzan[2]

[1] {Department of Chemistry, University of Calgary, Calgary, Alberta T2N 1N4, Canada}

[2] {Science Division, Meteorological Service of Canada, Environment and Climate Change Canada, Vancouver, British Columbia V6C 3S5, Canada}

[3] {British Columbia Ministry of Environment and Climate Change Strategy, Cranbrook, British Columbia V1C 7G5, Canada}

Correspondence to: H. D. Osthoff (hosthoff@ucalgary.ca)

Table of contents

Table S-1. Volatile organic compounds quantified by GC-MS

Butane, 2-methyl-	Pentane, 2,3,4-trimethyl-	Undecane
1-Pentene	Heptane, 2-methyl-	Dodecane
Pentane	Heptane, 3-methyl-	Ethylene
2-Pentene (Z) (cis)	Toluene	Acetylene
Isoprene (1,3-Butadiene, 2-methyl-)	Octane	Ethane
2-Pentene (E) (trans)	Ethylbenzene	Propane
Butane, 2,2-dimethyl-	m & p-Xylene	Propylene
Cyclopentane	Nonane	Isobutane
2,3-Dimethylbutane	Styrene	1-Butene
Pentane, 2-methyl-	o-Xylene	Butane
Pentane, 3-methyl-	Isopropyl Benzene (Benzene, (1-methyleth	2-Butene (trans)
1-Hexene	Benzene, propyl-	2-Butene (cis)
Hexane	Benzene, 1-ethyl-3-methyl-	Freon 11 (Trichloromonofluoromethane)
Cyclopentane, methyl-	Benzene, 1-ethyl-4-methyl-	Isopropyl Alcohol
Pentane, 2,4-dimethyl-	Benzene, 1,3,5-trimethyl-	Acetone
Cyclohexane	Decane	Ethene, 1,1-dichloro-
Hexane, 2-methyl-	Benzene, 1-ethyl-2-methyl-	Methylene Chloride
Benzene	Benzene, 1,2,4-trimethyl-	Freon 113 (Ethane, 1,1,2-trichloro-1,2,2
2,3-Dimethylpentane	Benzene, 1,2,3-trimethyl-	Carbon disulfide
Hexane, 3-methyl-	Benzene, 1,3-diethyl-	Ethene, 1,2-dichloro-, (E)-
Pentane, 2,2,4-trimethyl-	Benzene, 1,4-diethyl-	Methyl tertbutylether
Heptane		
Cyclohexane, methyl-		

(Propane, 2-methox
Ethane, 1,1-dichloro-
Vinyl Acetate (Acetic acid ethenyl ester
2-Butanone
Chloroform (Trichloromethane)
Ethyl Acetate
Furan, tetrahydro-
Ethane, 1,2-dichloro-
Ethane, 1,1,1-trichloro-
Carbon Tetrachloride
Trichloroethylene
Methane, bromodichloro-
1,4-Dioxane
Methyl Methacrylate
1-Propene, 1,3-dichloro-, (Z)-

Methyl Isobutyl Ketone
1-Propene, 1,3-dichloro-, (E)-
Ethane, 1,1,2-trichloro-
2-Hexanone
Methane, dibromochloro-
Ethane, 1,2-dibromo-
Tetrachloroethylene
Benzene, chloro-
Bromoform (Methane, tribromo-)
Ethane, 1,1,2,2-tetrachloro-
Ethane, pentachloro-
Benzyl Chloride
Benzene, 1,3-dichloro-
Benzene, 1,4-dichloro-
Benzene, 1,2-dichloro-

Benzene, 1,2,4-trichloro-
1,3-Butadiene, 1,1,2,3,4,4-hexachloro-
Naphthalene
Freon 12
Chloromethane
Freon 114
Vinyl chloride
1,3 Butadiene
Bromomethane
Chloroethane
Ethanol
1R-alpha-Pinene
Camphene
beta-Pinene
D-Limonene

34

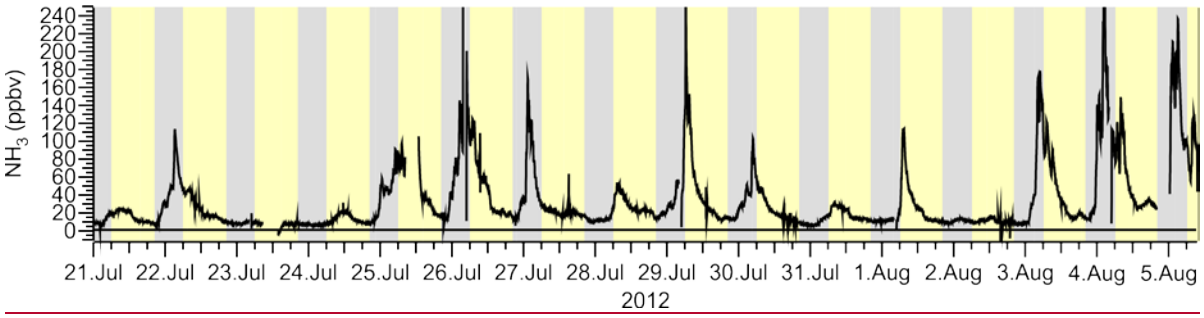

Figure S-1. Time series of gas-phase ammonia data reported by Metro Vancouver. Data were not quality-assured and are non-quantitative.

Box model to rationalize O_x loss by dry deposition

A box model was set up to simulate the median nocturnal decays of O_3 and O_x. These simulations are intended as back-of-the-envelope type estimates of major processes only since an accurate description of the nocturnal boundary layer chemistry would require modeling of horizontal and vertical transport, i.e., altitude-resolved information (Geyer and Stutz, 2004). Such information was not available in this work.

The reactions used in this model are summarized in Table S-2. The mechanism consists of O_3 and NO_2 dry deposition, titration of NO with O_3 (R8) and chemical loss of O_3 to a generic biogenic hydrocarbon. For dry deposition, the velocities of $v_d(O_3)$ = 0.2 cm s^{-1} and $v_d(NO_2) = \alpha \times v_d(O_3)$ with α=0.65 from Lin et al. (2010) were used. The rate constants for reaction with the generic biogenic hydrocarbon was set to that of α-pinene with O_3 (5×10^{-11} cm^3 $molec.^{-1}$ s^{-1}, (Seinfeld and Pandis, 2006)).

Model simulations were carried out using a custom differential equation integrator macro in the software package Igor Pro (Wavemetrics) and were initiated with the campaign median NO_2 and O_3 concentrations observed at sunset.

Table S-2. Reactions included in box model to estimate dry deposition velocities

Reaction	Rate constant
$O_3 \rightarrow$ products	$k_{dep}(O_3)$
$NO_2 \rightarrow$ products	$k_{dep}(NO_2)$
$O_3 + NO \rightarrow NO_2 + O_2$	4.8×10^{-4} $ppbv^{-1}$ s^{-1}
O_3 + VOC $\rightarrow$ products	1.25 $ppbv^{-1}$ s^{-1}

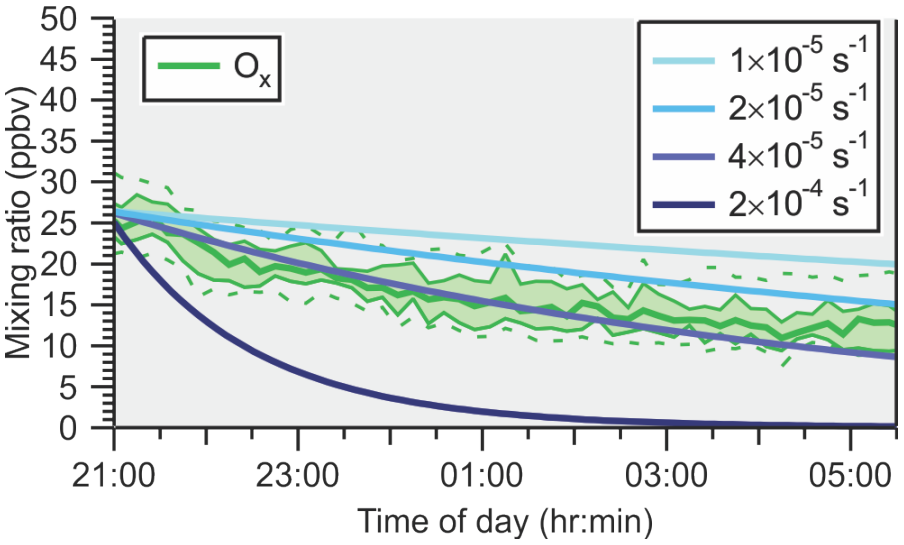

Figure S-~~1~~2. Observed and simulated O_x loss in the NBL at Abbotsford assuming O_3 dry deposition rates of 2×10^{-4} s^{-1}, 4×10^{-5} s^{-1}, 2×10^{-5} s^{-1} and 1×10^{-5} s^{-1}, corresponding to approximate mixing heights of 10 m, 50 m, 100 m, and 200 m.

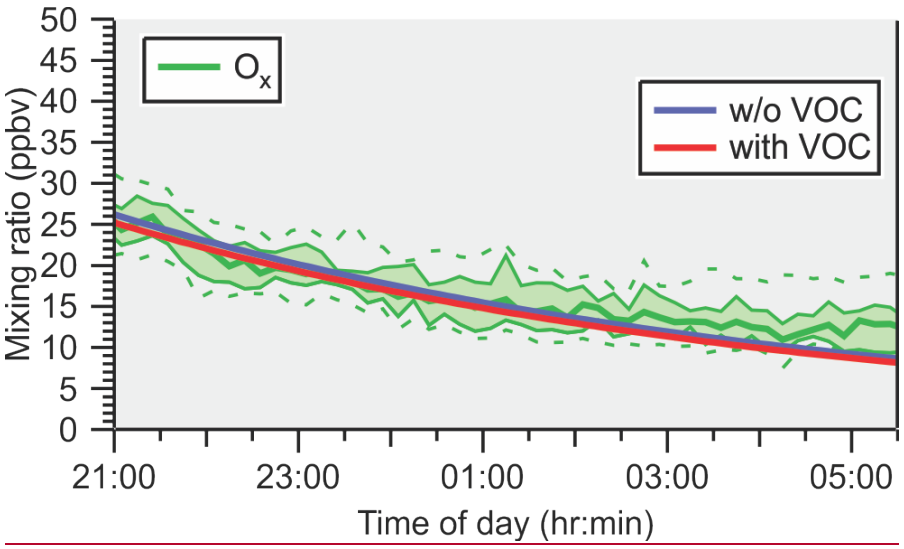

Figure S-3. Effect of biogenic VOC emissions on O_x. The observed and simulated O_x loss in the NBL at Abbotsford assuming an O_3 dry deposition rate of 4×10^{-5} s^{-1} are shown as green and blue traces, respectively. The red trace shows the effect of adding 1 –ppbv of reactive biogenic VOC at sunset and continuous biogenic VOC emissions of 3×10^{5} molecules cm^{-3} s^{-1} throughout the night.

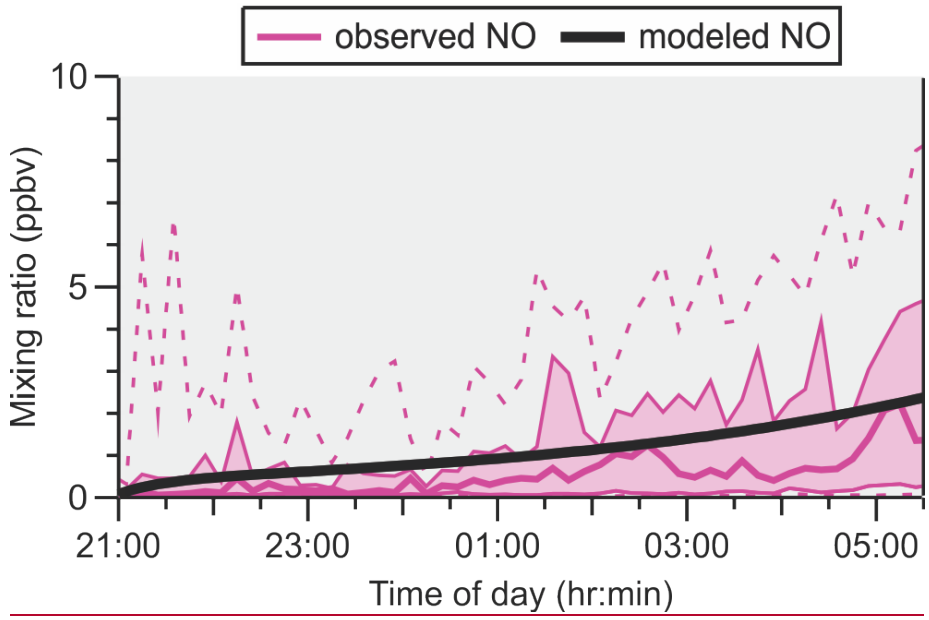

Figure S-4. Comparison of observed and simulated NO mixing ratios after constant emissions of 2.9×10^{-4} ppbv s^{-1} (~1.05 ppbv hr^{-1}) of NO and 3×10^{-5} ppbv s^{-1} (~0.05 ppbv hr^{-1}) of NO_2 were added.

Box model to determine the time necessary for NO_3 and N_2O_5 to achieve a steady state with respect to production and loss~~ss~~

The validity of the steady state assumption was evaluated in a similar fashion as described by Brown et al. (2003) using a simple box model. Reactions and rate coefficients included in these simulations are listed in Table S-3. Model simulations were carried out using a custom differential equation integrator macro in the software package Igor Pro (Wavemetrics). Rate coefficients were calculated for a temperature of 286 K, which is the median nocturnal temperature of this study (Figure 8B). Simulations were initiated with the median nocturnal NO_2 and O_3 mixing ratios of 7.5 ppbv (1.92×10^{11} molecules cm^{-3}) and of either 18 ppbv (4.5×10^{11} molecules cm^{-3}) or 5.0 ppbv (1.3×10^{11} molecules cm^{-3}), respectively. The simulations assume pseudo-first order N_2O_5 and NO_3 loss with frequencies of 1×10^{-3} s^{-1} and between 1×10^{-2} s^{-1} and 0 s^{-1}, respectively.

S~~s~~imulated temporal profiles of NO_3 and N_2O_5 are show in Figure S-5 (left axis) and those of O_3 and NO2 on the ~~(~~right axis~~)~~. The subpanels A, B, and C are simulations with k_{NO3} = 0 s^{-1}, 1×10^{-3} s^{-1} or 1×10^{-2} s^{-1}, respectively. In each case, the rate of change of $[N_2O_5]$ with respect to time, $d[N_2O_5]/dt$, approaches zero after a period of ~70 min, or less, indicating the time to approach steady state.

The simulations also show that the amount of O_3 and NO_2 removed through chemical reactions of NO_3 and N_2O_5 are ~1 ppbv and between ~1.9 and ~1.6 ppbv over a period of 4 hours. These are upper limits as in this study much of the NO_3 was titrated by NO. In any case, loss of O_3 through nocturnal gas-phase is predicted to be rather small compared to the total O_3 loss observed (~26 ppbv over 9 hours, see section 3.1.3 and Figure 4C in the main text).

Brown et al. (2003) show that in these scenarios, NO_3, N_2O_5, and NO_2 remain in equilibrium almost throughout; for completeness, the corresponding plot for these simulations is shown in Figure S-6.

As shown in equation (2) of the manuscript, the steady state lifetime is approximately equal to:

$$\frac{[N_2O_5]}{k_1[NO_2][O_3]} \approx \left(k_{N_2O_5} + \frac{k_{NO_3}}{K_2[NO_2]}\right)^{-1} \quad (2)$$

A comparison of these two expressions is shown in Figure S-7. The time when these two expressions are equal is equal to the time to steady state.

Table S-3. Reactions included in the box model to estimate the time for NO_3 and N_2O_5 to achieve steady state with respect to their production and loss

#	Reaction	Rate coefficient
R1	$NO_2 + O_3 \rightarrow NO_3 + O_2$	2.28×10^{-17} cm^3 molecule^{-1} s^{-1}
$R2_f$	$NO_3 + NO_2 \rightarrow N_2O_5$	1.35×10^{-12} cm^3 molecule^{-1} s^{-1}
$R2_r$	$N_2O_5 \rightarrow NO_3 + NO_2$	0.00923 s^{-1}
(R7)	$NO_3 \rightarrow$ products	$k_x = k_{NO3} = 0$ s^{-1}, 1×10^{-3} s^{-1} or 1×10^{-2} s^{-1}
(R5)	$N_2O_5 \rightarrow$ products	$k_y = k_{N2O5} = 1\times10^{-3}$ s^{-1}

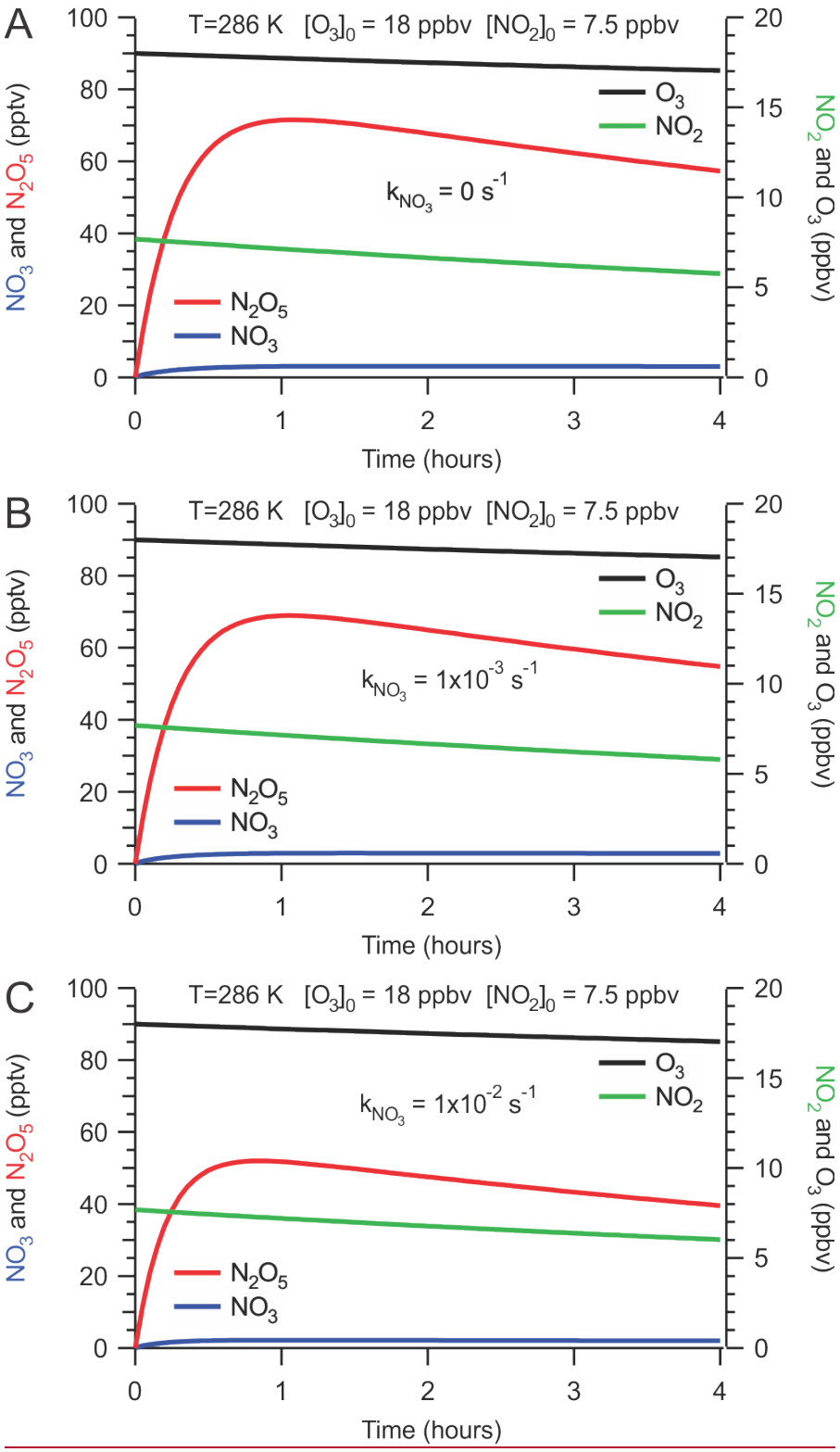

Figure S-5. Simulated temporal profiles of NO_3 and N_2O_5 (left axis) and O_3 and NO_2 (right axis). The subpanels A, B, and C are simulations with k_{NO3} = 0 s^{-1}, 1×10^{-3} s^{-1} or 1×10^{-2} s^{-1}, respectively.

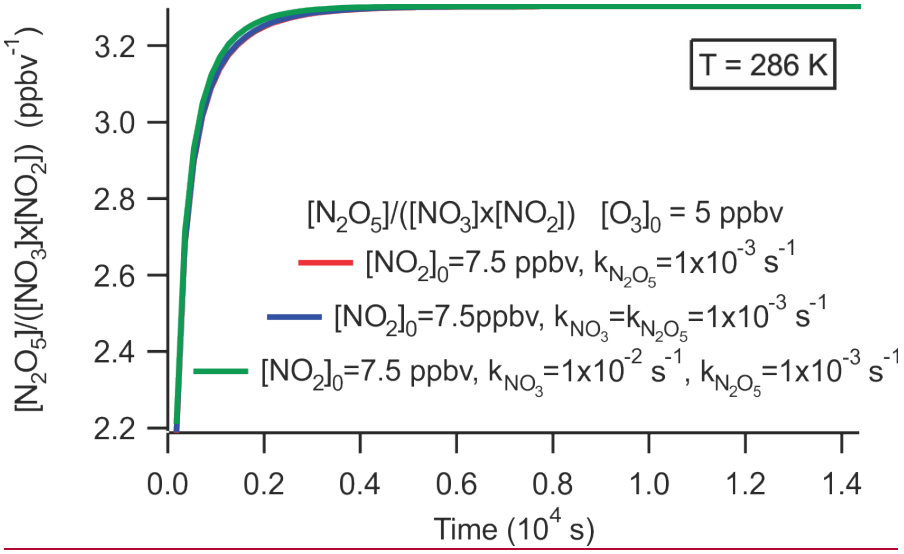

Figure S-6. Equilibrium constants for reaction (2) calculated for the three scenarios shown in Figure S-5.

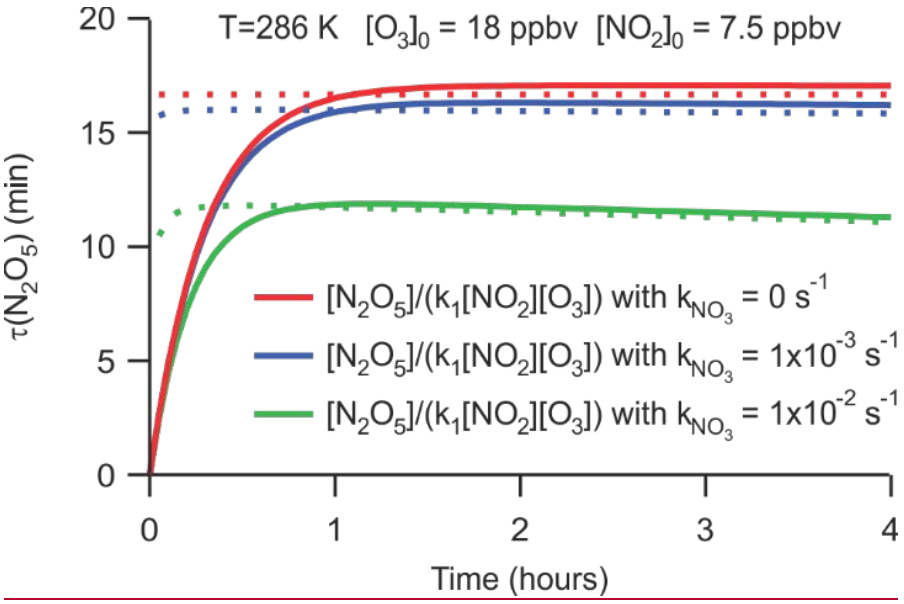

Figure S-7. Comparison of $\tau(N_2O_5)$ calculated using equation (2) of the main manuscript. with the dashed lines calculated using equation (11) of Brown et al. (2003).

References

Brown, S. S., Stark, H., and Ravishankara, A. R.: Applicability of the steady state approximation to the interpretation of atmospheric observations of NO_3 and N_2O_5, J. Geophys. Res., 108, 4539, doi: 4510.1029/2003JD003407, 2003.

Geyer, A., and Stutz, J.: Vertical profiles of NO_3, N_2O_5, O_3, and NO_x in the nocturnal boundary layer: 2. Model studies on the altitude dependence of composition and chemistry, J. Geophys. Res., 109, D12307, doi:12310.11029/12003JD004211, 2004.

Lin, C. H., Lai, C. H., Wu, Y. L., and Chen, M. J.: Simple model for estimating dry deposition velocity of ozone and its destruction in a polluted nocturnal boundary layer, Atmos. Environm., 44, 4364-4371, 10.1016/j.atmosenv.2010.07.053, 2010.

Pisano, J. T., McKendry, I., Steyn, D. G., and Hastie, D. R.: Vertical nitrogen dioxide and ozone concentrations measured from a tethered balloon in the Lower Fraser Valley, Atmos. Environm., 31, 2071-2078, 10.1016/S1352-2310(96)00146-X, 1997.

Seinfeld, J. H., and Pandis, S. N.: Atmospheric chemistry and physics: from air pollution to climate change, 2nd ed., Wiley, Hoboken, N.J., 2006.